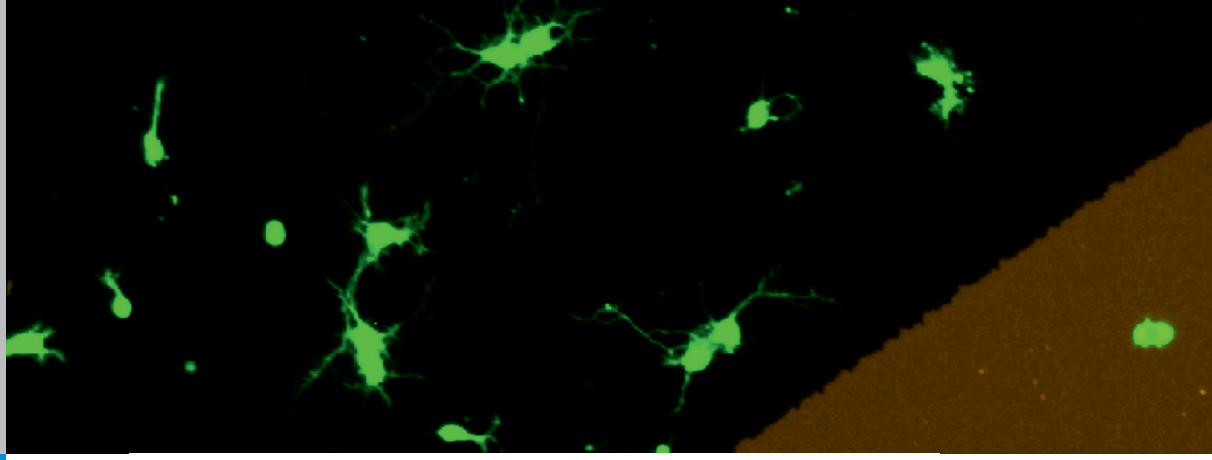

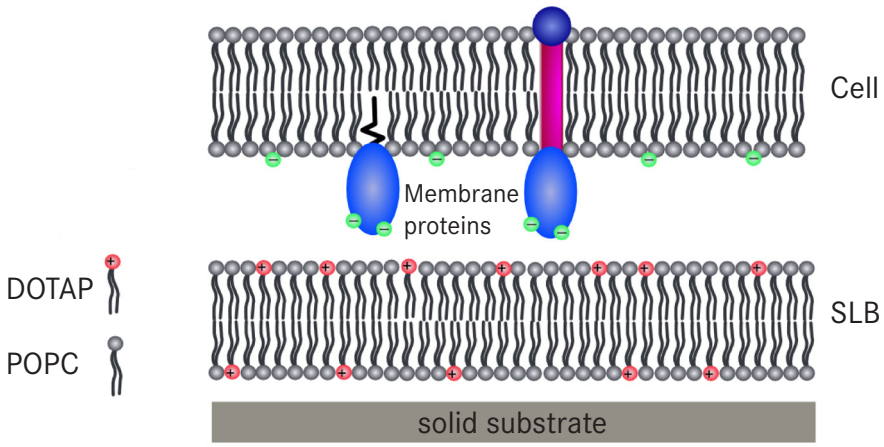

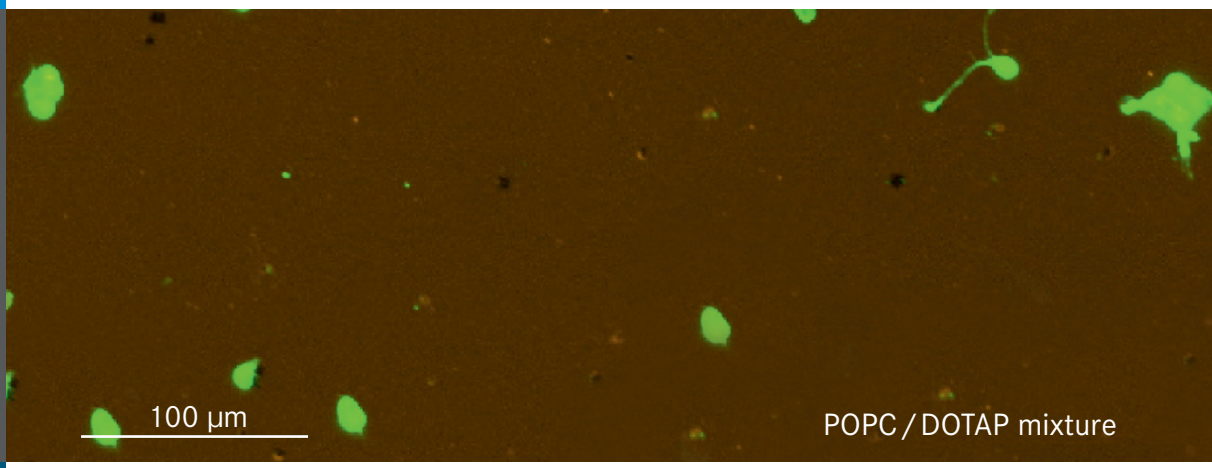

Supported lipid bilayer as a biomimetic platform for neuronal cell culture

Dzmitry Afanasenkau

JÜLICH
FORSCHUNGSZENTRUM

Member of the Helmholtz Association

Schriften des Forschungszentrums Jülich
Reihe Information / Information Band / Volume 26

Forschungszentrum Jülich GmbH
Peter Grünberg Institute / Institute of Complex Systems (PGI / ICS)
Bioelectronics (PGI-8 / ICS-8)

Supported lipid bilayer as a biomimetic platform for neuronal cell culture

Dzmitry Afanasenkau

Schriften des Forschungszentrums Jülich
Reihe Information / Information Band / Volume 26

ISSN 1866-1777 ISBN 978-3-89336-863-1

Bibliographic information published by the Deutsche Nationalbibliothek.
The Deutsche Nationalbibliothek lists this publication in the Deutsche Nationalbibliografie; detailed bibliographic data are available in the Internet at http://dnb.d-nb.de.

Publisher and Distributor: Forschungszentrum Jülich GmbH
Zentralbibliothek
52425 Jülich
Tel: +49 2461 61-5368
Fax: +49 2461 61-6103
Email: zb-publikation@fz-juelich.de
www.fz-juelich.de/zb

Cover Design: Grafische Medien, Forschungszentrum Jülich GmbH

Printer: Grafische Medien, Forschungszentrum Jülich GmbH

Schriften des Forschungszentrums Jülich
Reihe Information / Information, Band / Volume 26

D 82 (Diss., RWTH Aachen, Univ., 2012)

ISSN 1866-1777
ISBN 978-3-89336-863-1

The complete volume is freely available on the Internet on the Jülicher Open Access Server (JUWEL) at www.fz-juelich.de/zb/juwel

Contents

List of abbreviations

Ab	Antibody
AFM	Atomic force microscopy
AP	Action potentials
ATP	Adenosine-5'-triphosphate
BLM	Black lipid membranes
CAM	Cell adhesion molecules
DHPE	1,2-dihexadecanoyl-sn-glycero-3-phosphoethanolamine
DIV	Days in vitro
DNA	Deoxyribonucleic acid
DOTAP	1,2-dioleoyl-3-trimethylammonium-propane
ECM	Extracellular matrix
EPSP	Exitatory post synaptic potentials
FET	Field effect transistor
FRAP	Fluorescent recovery after photobleaching
GBSS	Gey's Balanced Salt Solution
GDP	Guanosine-5'-diphosphate
GPCR	G protein-coupled receptor
GPI	Glycosylphosphatidylinositol
GTP	Guanosine-5'-triphosphate
GUV	Giant unilamelar vesicles
HBSS	Hanks' Balanced Salt Solution
IgG	Immunoglobulin G
ITO	Indium tin oxide
LMV	Large multilamellar vesicles
MEA	Microelectrode array
NB	Neurobasal medium
NBD-PE	1-oleoyl-2-{6-[(7-nitro-2-1,3-benzoxadiazol-4 yl)amino] hexanoyl} -sn-glycero-3-phosphoethanolamine
NMR	Nuclear magnetic resonance
NW	Nano wire
OD	Optical density
PBS	Phosphate buffered saline
PC	Phosphatidylcholine
PDL	Poly-D-lysine
PDMS	Polydimethylsiloxane

PLL	Poly-L-lysine
POPC	1-palmitoyl-2-oleoyl-sn-glycero-3-phosphocholine
QCM-D	Quartz Crystal Microbalance with Dissipation Monitoring
RTK	Receptor tyrosine kinase
SAM	Sterile α-mottf
SDS	Sodium dodecyl sulfate
SLB	Supported Lipid Bilayer
SPR	Surface plasmon resonance
SUV	Small unilamelar vesicles
TIRF	Total internal reflection fluorescence microscope
VA-TIRF	Variable angle TIRF

List of figures

List of tables

Abstract

The lipid bilayer is the basis of the cell membrane. It serves as a barrier that separates the cell from the environment and provides platform for membrane proteins helping them to fulfill their functions. To advance studies of the cell membrane, membrane proteins and cell-cell interactions, it would be favourable to create an artificial platform which can mimic the cell membrane. It can help to exclude various factors influencing the experiments carried out on real cells and provide a possibility to focus on the phenomena interesting for researchers. It would allow many advanced methods of investigation which can not be applied for living cells. Such a platform can also help to use some advanced properties of the cell membrane in biosensors and medical applications.

Several systems that can mimic the cell membrane have been developed such as liposomes (lipid vesicles) or pore suspended lipid membranes (such as black lipid membranes – a classical membrane system). Although these systems have been used extensively for many years, they possess disadvantages which limit their applications.

Such a system as *supported lipid bilayer (SLB)* can mimic the cell membrane and provides high stability and accessibility for measurement techniques. The SLB consist of a lipid bilayer placed on a solid surface (such as glass, Si, mica) covered with aqueous solution and separated from the substrate by very thin (around 1 nm) hydration layer. It gives a possibility for incorporation of membrane proteins providing natural environment for them. It can be immobilized on the surface of a sensor - optical, electrical or mechanical. There are also ways of patterning of the SLB which enhance possibilities of integration with recording devices and is especially useful in experiments with guiding cells in culture or studying cell adhesion.

The SLB can provide a wide spectra of possibilities for studying cells in vitro. They include studying of cell adhesion, cell signaling, redistribution of molecules in the cell membrane. However, by now the SLB has been used for experiments with cells not very intensively. One reason for it is that lipid bilayers made of only natural lipids such as phosphatidylcholine are cell repellent: cells can not adhere to it. Thus, to maintain cells the SLB should be functionalized in a special way. There are many possibilities for it but they are mostly complicated and not well studied.

The aim of the present work is to study possibilities of using SLB as a platform for neuronal cell culture. To reach this aim several tasks were considered:

1. Development of methods to increase cell adhesion to the SLB
2. Utilizing proteins incorporated into the SLB for investigation of cell signaling processes.

3. Patterning of the SLB

For increasing adhesion of cells a simple approach was developed: bilayers contained *positively charged lipids* (DOTAP) were used. Such bilayers, which are very easy to prepare, were shown in this work to promote adhesion of neuronal cells most likely due to electrostatic interaction. A possibility for using these bilayers for long term experiments with neuronal cell was demonstrated.

Fluidic properties of the prepared SLB were monitored using *fluorescence recovery after photobleaching* (FRAP). A MatLab based software was developed to analyse FRAP images and calculate diffusion coefficient. The diffusion coefficient appeared to decrease with the increase of the concentration of positively charged lipid, but even the SLB consisted of only positively charged molecules was found to be fluid with the diffusion coefficient three time lower than for the bilayer made of phosphatidylcholine.

Possibilities of using the SLB for studying cell signalling processes were shown in this work. *Ephrin A5*, a synaptic adhesion protein, which performs also many signalling functions, was incorporated into the SLB. Patch clamp experiments showed that the probability for a neuronal cells growing on such bilayers to develop functional synapses is higher than for control cultures maintained on the usual cell-culture substrates such as poly-L-lysine.

For creating *patterned SLB* the idea of using giant unilamellar vesicles (GUV) was utilized. This method allowed to form patches of the SLBs of different type on a surface without risk of exposing the surface to air (which would destroy SLB) that exist in usually used methods such as droplet deposition.

In conclusion, this work demonstrates a possibility of using SLB as a platform for neuronal cell culture which can allow long term experiments directed into studying cell adhesion, cell signaling, and cell development processes.

Zusammenfassung

Die Lipiddoppelschicht ist die Basis der Zellmembran. Sie dient als Barriere, die die Zelle von der Umgebung trennt und stellt eine Plattform für Membranproteine dar, die diesen hilft ihre Funktionen auszuüben. Um Studien der Zellmembran, ihrer Protein sowie von Zell-Zell-Interaktionen voranzutreiben, ist eine künstliche Plattform, die die Funktionen der Zellmembran nachahmt, von Vorteil. Eine solche Plattform könnte dabei helfen, eine Vielzahl von Faktoren aususchließen, die Experiment mit biologischen Zellen beeinflussen. Sie könnte somit eine Möglichkeit bereitstellen, sich auf einige wissenschaftlich interessante Phänomene zu konzentrieren. Sie würde viele fortgeschrittene Untersuchungsmethoden erlauben, die mit lebenden Zellen nicht durchführbar sind. Ebenso könnte eine solche Plattform dabei helfen, einige interessante Eigenschaften der Zellmembran für Biosensoren und medizinischen Anwendungen zu nutzen.

Um die Funktion der Zellmembran nachzuahmen sind mehrere Systeme wie z. B. Liposome (Lipidvesikel) oder pore suspended lipid membranes (wie z. B. black lipid membranes – ein klassisches Membransystem) entwickelt worden. Obwohl diese Systeme seit vielen Jahren intensiv in Benutzung sind, besitzen sie Nachteile, welche ihre Anwendungen limitieren.

Ein System wie unterstützte Lipiddoppelschichten (supported lipid bilayer, SLB) ist in der Lage die Zellmembran zu imitieren und bietet gleichzeitig eine hohe Stabilität und Zugäng-lichkeit für verschiedene Messtechniken. SLBs bestehen aus einer Lipiddoppelschicht die auf eine feste Oberfläche (wie z. B. Glas, Si oder Mica) aufgebracht ist, von einer wässrigen Lösung bedeckt wird und durch eine sehr dünne Hydrationsschicht (ca. 1 nm) vom Substrat getrennt ist. Sie bieten die Möglichkeit zur Einbettung von Membranproteinen und stellen gleichzeitig eine natürliche Umgebung für diese dar. SLBs können auf der Oberfläche eines optischen, elektrischen oder auch mechanischen Sensors platziert werden. Ebenso bestehen Möglichkeiten SLBs lateral zu strukturieren, wodurch die Integration mit z. B. Mikroelektrodenarrays verbessert wird. Des Weiteren sind diese Techniken besonders nützlich um Zellen in Kultur zu strukturieren oder die Zelladhesion an sich zu untersuchen.

Die Möglichkeiten, die SLBs für in vitro Studien von Zellen bereitstellen können sind vielfältig. Unter Anderem zählen Studien der Zelladhesion, der Signalübertragung zwischen Zellen sowie der Neuverteilung von Molekülen in der Zellmembran dazu. Jedoch sind SLBs bisher nicht besonders intensiv für Zellexperimente angewandt worden. Ein Grund hierfür ist, dass Lipiddoppelschichten, die ausschließlich aus natürlichen Lipiden wie Phosphatidylcholin bestehen, zellabweisend sind: Zellen adherieren nicht auf

ihnen. Um somit als Substrat für Zellexperimente in Frage zu kommen, müssen die SLBs speziell funktionalisiert werden. Hierfür bestehen viele, zumeist komplizierte und wenig untersuchte, Möglichkeiten.

Ziel der vorliegenden Arbeit ist es, Möglichkeiten der Nutzung von SLBs als Plattform für neuronale Zellkultur zu untersuchen. Hierbei werden die folgenden Punkte eingeschlossen:

1. Verbesserung der Zelladhesion an die SLB
2. Untersuchung der Möglichkeit, in die SLB eingebettete Proteine zur Untersuchung zellulärer Signalübertragung zu nutzen
3. Laterale Strukturierung der SLB

Zur Verbesserung der Zelladhesion wurde ein einfacher Ansatz entwickelt: Es wurden Doppelschichten, die positiv geladene Lipide (DOTAP) enthalten, benutzt. Für solche Doppel-schichten, die sehr einfach herzustellen sind, wurde in dieser Arbeit gezeigt, dass sie die Ad-hesion neuronaler Zellen, höchstwahrscheinlich aufgrund elektrostatischer Wechselwirkungen, verbessern. Es wurde außerdem eine Möglichkeit demonstriert, diese Doppelschichten in Langzeitexperimenten mit neuronalen Zellen zu nutzen.

Die fluidischen Eigenschaften der preparierten SLBs wurden mittels fluorescence recovery after photobleaching (FRAP) untersucht. Zur Analyse der FRAP-Bilder und zur Berechnung des Diffusionskoeffizienten wurde eine MatLab-basierte Software entwickelt. Ein Abnehmen des Selbigen wurde unter Zunahme der Konzentration des positiv geladenen Lipids festgestellt. Jedoch wurden sogar ausschließlich aus positiv geladenen Lipiden bestehende SLBs als Fluid bestimmt und es wurde ein Diffusionskoeffizient gemessen, der dreimal niedriger als der einer reinen Phophatidylcholindoppelschicht ist.

Des Weiteren wurden in dieser Arbeit Möglichkeiten zur Nutzung von SLBs bei der Untersuchung zellulärer Signalweitergabe gezeigt. Ephrin A5, ein synaptisches Adhesions¬protein, welches zudem viele signalvermittelnde Funktionen ausübt, wurde in die SLB ein¬ge¬bettet. Patch-Clamp-Experimente zeigten, dass die Wahrscheinlichkeit zur Entwicklung funktionaler Synapsen für Neuronen, die auf derartigen Doppelschichten kultiviert wurden höher ist, als die von Kontrollkulturen, die auf üblichen Zellkultursubstraten, wie z. B. Poly-L-lysin, kultiviert wurden.

Um lateral strukturierte SLBs zu erzeugen, wurde der Ansatz großer unilamellarer Vesikel (giant unilamellar vesicles – GUV) genutzt. Diese Methode erlaubt es, Bereiche aus SLBs ver-schiedener Typen auf der Oberfläche herzustellen, ohne das Risiko, diese der Luft auszusetzen (wodurch die SLBs zerstört werden). Dieses Risiko besteht bei den üblicherweise genutzten Methoden wie z. B. Tröpfchendeposition.

Zusammenfassend zeigt die Arbeit Möglichkeiten auf, SLBs als Plattform for neuronale Zellkultur zu nutzen, die Langzeituntersuchungen im Hinblick auf die Untersuchung von Zell-adhesion, zellulärer Signalübertragung und des zellulären Entwicklungsprozesses erlaubt.

Chapter 1

Fundamentals

Think how many persons before you asked
the same question you want to ask now

Svetlana Borisova

1.1 The cell membrane

1.1.1 Cells and membranes

Very often the cell is called a smallest unit of life [1]. However, this is probably not true in the wide philosophical sense as a cell of an organism can not live alone outside of this organism and depends on the presence of other cells, biological fluids and properly running homeostasis. In the case of the single cell organism we speak already about the organism (although consisted of one single cell) not a cell. The cell can be defined as the basic structural and functional unit of all known living organisms (except viruses). The unity of the cell is provided in a high degree by *the cell membrane* which separates the interior of the cell from the environment. It also separates specialized compartments in the cell – cell organelles, providing a possibility for maintaining defined conditions in them, which is necessary for certain function to be performed. Except encapsulating and separating materials of the cell, the membrane play an important role in many other aspects of the cell life such as cell adhesion, cell signalling, transport of materials, generating electric potentials, etc. All this makes the cell membrane one of the most important structural and functional elements of the cell.

1.1.2 The structure of the cell membrane

The cell membrane is considered as a lipid bilayer in which proteins are incorporated (fig. 1.1). According to the well known fluid mosaic model of S.J. Singer and G.L. Nicolson (1972), it can be represented as a two-dimensional liquid in which all lipid and protein molecules diffuse more or less easily [2]. Lipids form a double layer in such a way that their polar heads are directed to

surrounding water and their hydrophobic tails - into the bilayer. The structure of the bilayer is maintained by hydrophobic interactions provided by amphiphilic nature of the lipid molecules. Proteins can penetrate the lipid bilayer, completely or only one leaflet, or be attached to the surface.

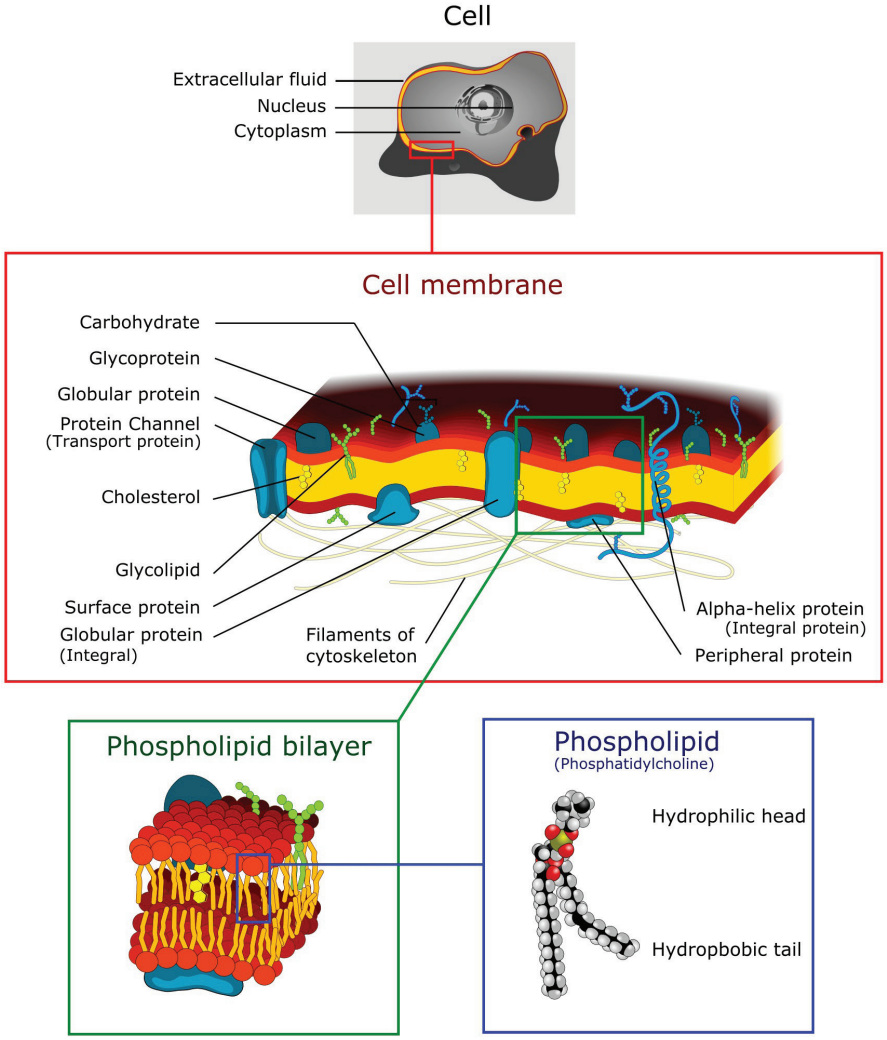

Figure 1.1: The structure of the cell membrane. Figure from [3].

In general, the cell membrane of an animal cell can be considered as more complicated structure consisting of three layers [4], the lipid bilayer with incorporated proteins being the central part of it (fig. 1.2). The outer part of the lipid-protein layer is covered by the glycocalyx: a macromolecular film formed by

the oligosaccharides of the glycolipid head groups and the branched polypeptide/oligosaccharide head groups of the glycoproteins. The glycocalyx plays an important role in cellular recognition processes, cell signalling and adhesion. The glycocalyx is usually connected to extracellular matrix (ECM) - a mesh of proteins and glycoproteins which plays an important role in providing support for the cell and separation of tissues [5].

At the intracellular side the lipid-protein layer is connected to the cytoskeleton consisted of microfilaments (made of actin), intermediate filaments (made of different proteins such as keratin, vimentin, lamin) and microtubules (made of tubulin) [6]. Among the functions of the cytoskeloton one can name mechanical support and adaptation of the shape of the cell, endo- and exocytosis, movement of the cell, intracellular transport.

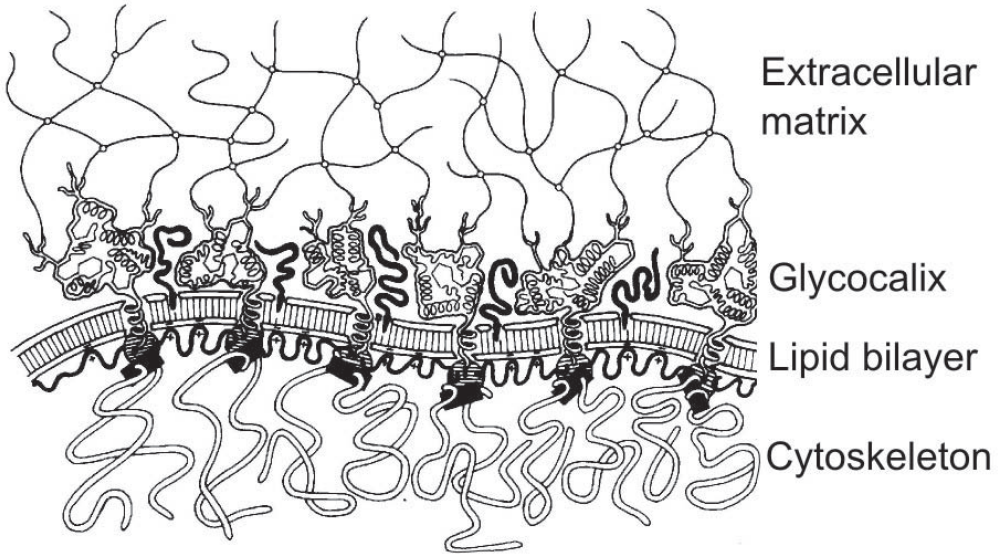

Figure 1.2: Structure of the animal cell membrane. Modified from [4].

Thus, the main components of the cell membrane are lipids and proteins. Lipids play mostly structural role and proteins perform most of the functions. The ratio of mass of lipids to the mass of proteins depends on the cell type and can vary from 4 in human myelin to 0.2 in Halobacterium halobium [7]. The mass of carbohydrates is considered to constitute around 10% of the mass of the membrane [8].

Lipids of the cell membrane

The cell membrane consists of the three main classes of lipids: phospholipids, glycolipids, and cholesterols (fig. 1.3). The phospholipids and glycolipids, in their turn, can be either glycerolipids or sphingolipids depending on which alcohol residue they are based on. All these types of lipids contain a

hydrophobic “tail” composed of residues of fatty acids (or part of sphingosine) and a polar “head”. In the case of phospholipids the “head” is made of a phosphate group, and a simple organic molecule (e.g. choline, in the case of phosphatidylcholine). The molecules of a glycolipid contain a carbohydrate in their “head”. There can be also glycophospholipids containing both the phosphate and a carbohydrate.

The fatty acid chains in phospholipids and glycolipids usually contain an even number of carbon atoms, typically between 16 and 20. Fatty acids may be saturated or unsaturated, with the configuration of the double bonds nearly always "cis". The length and the degree of saturation of fatty acid chains have a profound effect on membrane fluidity, as unsaturated lipids create a kink preventing the fatty acids from packing together tightly, thus decreasing the melting temperature (increasing the fluidity) of the membrane [3].

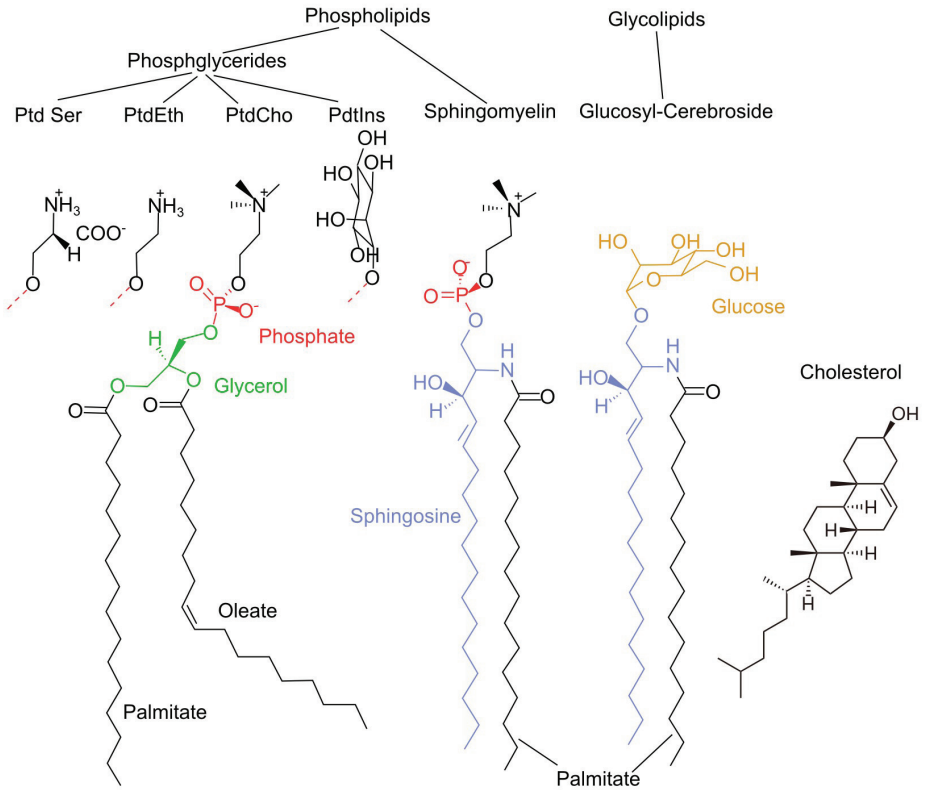

Figure 1.3: Examples of the major membrane lipids. Different molecular groups are marked with different colours. Modified from [3].

The main role of phospholipids and glycolipids is structural – their amphiphilic nature makes possible the formation of the bilayer due to hydrophobic interactions. Some lipids can perform signalling functions (e.g. glycosphingolipids of the membrane of the red blood cells carry antigen of the blood type[9]), cell adhesion [10] or play a role in maintaining functional state of enzymes.

Cholesterol has a different structure. It consists of small and stiff hydrophobic nucleus and a hydroxyl group playing a role of polar head. It modulates fluidity of the cell membrane. Occupying positions between hydrophobic tails and reducing their possibilities to bend, cholesterol makes the membrane stiffer. It can also influence passive permeability of the membrane and modulate activity of the membrane proteins [11].

Proteins of the cell membrane

Unlike lipids, which play mostly structural role, proteins are the main active components of the cell membrane. Depending on the way they connect to the membrane, two types of membrane proteins can be distinguished: *integral (transmembrane)* proteins that penetrate the membrane, and *peripheral* proteins that are placed at the surface of the membrane. Polypeptide chains of the integral proteins contain places enriched with hydrophobic aminoacids. These parts are preferably placed inside of the lipid bilayer so that the polypeptide chain penetrates the membrane one or several times. Peripheral proteins can be connected to the membrane by means of electrostatic interactions, attached to an integral protein, absorbed on the membrane, anchored to the bilayer by a short hydrophobic peptide segment or by covalent binding to a lipid residue (as in case of ephrine A5 – protein studied in this work). Different ways of connections of proteins to the cell membrane are shown in fig. 1.4.

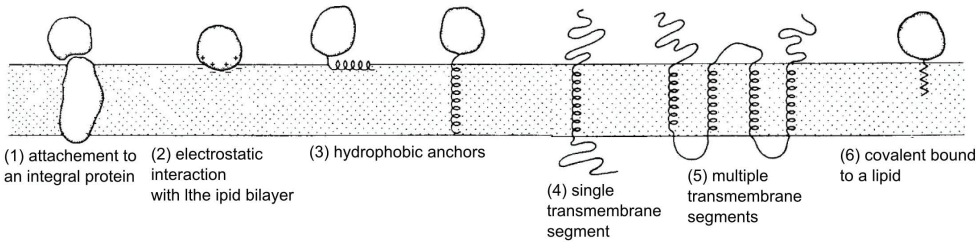

Figure 1.4: Different ways proteins connect to the cell membrane. Figure from [8].

Proteins of the membrane perform many functions. They can be receptors which start intracellular signalling cascades upon binding of ligands. They can be ionic channels or transporters providing transport of ions and other molecules through the lipid bilayer. Many membrane proteins are enzymes which require hydrophobic surrounding for proper functioning. Proteins of cytoskeloton provide the mechanical support for the bilayer.

1.1.3 Functions of the cell membrane

The cell membrane performs a lot vital for the cell functions. Most important of them are listed below.

- First of all it creates a ***barrier*** which separates the cell from the environment. It also creates barriers inside of the cell separating inner parts of the cell organelles from each other and from the cytoplasm.
- At the same time it provides possibilities for selective ***transport*** of substances inside and outside of the cell and the cell organelles. Transport can be active or passive. Passive transport takes place due to gradient of concentration of the substance across the membrane. Some non-polar substances such as gases can pass through the lipid bilayer. Passive transport of polar molecules and ions is provided through special channels formed by integral proteins. For active transport energy of ATP is consumed to move molecules across the forces created by the gradients of concentrations. It is done by special integral proteins – pumps and exchangers. Transport of big molecules, particles or volumes of liquid is done by endo- and exocytosis – engulfing of a particle by the membrane and forming a vesicle carrying it inside the cell (endocytosis) or fusion of the vesicle to the membrane and releasing the content to the surrounding medium (exocytosis).
- The membrane creates a ***matrix*** for membrane proteins to place them in the proper orientation and provide optimal conditions for their functioning. For example, the membrane contains enzymes that require hydrophobic environment to work properly.
- The membrane participates in ***energy transformation*** processes taking place in the cell, e.g. photosynthesis in chloroplasts or ATP production in mitochondria.
- ***Adhesion of cells*** is provided by special proteins of the cell membrane. These proteins touch their specific partners on the membrane of another cell providing a contact between the cells.
- The membrane provides not only transport of substances but also plays an important role in ***signal reception and transmission***. It contains receptors (they are usually special membrane proteins) which bind ligands at the extracellular part of the membrane and, by changing their conformation, start cascades of intracellular signalling processes. Receptors can be ionic channels that open upon ligand binding, providing a way for ions to flow inside the cell. Some cells contain antigens (usually glycoproteins) on their membranes which act as markers in the processes of cell recognition. Using these markers cells can recognize each other while forming organs. This also helps the immune system to find allogeneic bodies.

- ***Generation of electric potentials*** is another important function of the cell membrane. The lipid bilayer plays the role of a capacitor. Ionic pumps and exchangers can separate electric charges creating a potential difference across the membrane. Ionic channels provide a way for currents to flow across the membrane changing the potential. Functioning of voltage gated ionic channels produces fast reversible changes of the membrane potentials such as nerve pulses.

1.1.4 Membrane potential

The last function of the cell membrane mentioned in the previous section is generation of electric potentials. It is important for functioning of almost all cells because cells of almost all types maintain potential difference across their membranes. Potential inside the cell is usually negative with respect to media outside. For neurons it is usually around -70mV. This potential difference is created by the electric charge of ions, concentration of which is different inside and outside of the cell. The concentration of ions is maintained by ionic pumps and exchangers which spend the energy of ATP to pump ions across the forces of their electrochemical gradients.

The potential difference across a membrane permeable only for ions of one type can be calculated using the Nernst equation [12]:

$$\Delta\varphi = \frac{RT}{zF} \ln\left(\frac{c_o}{c_i}\right) \tag{1.1}$$

where $\Delta\varphi$ is the potential difference across the membrane, c_o and c_i are the concentration of the ion outside and inside the cell respectively, R is the universal gas constant, T is temperature, F is Faraday's constant, and z is the charge of the ion. The situation is more complicated when the membrane is permeable for ions of different type and the permeability is different for each of them as in the case of the cell membrane. In this case, the membrane potential can be calculated using the Goldman's equation [13]. Taking in to account only three ion species (Na^+, K^+ and Cl^-) which create highest currents across the cell membrane, the Goldman's equation can be written in the following way, giving the membrane potential:

$$\varphi_m = \frac{RT}{F} \ln\left(\frac{P_K[K]_o + P_{Na}[Na]_o + P_{Cl}[Cl]_i}{P_K[K]_i + P_{Na}[Na]_i + P_{Cl}[Cl]_o}\right) \tag{1.2}$$

where P_x is the permeability for the ion of the type X, $[X]_o$ and $[X]_i$ is the concentration of the ion of the type X outside and inside of the cell respectively (X is either Na, K or Cl).

Some cells, such as neurons, muscle or endocrine cells, generate pulses of transmembrane potentials from its resting value (usually around -70mV) to the

positive value around +50mV (fig. 1.5). This pulse is called the action potential. It can propagate along neurites or along muscle fibre. The action potential is created due to work of voltage gated ionic channels – mostly Na and K. At the resting potential these channels are mostly closed. Depolarization of the membrane increases the probability of opening of the sodium channels. This probability depends on the potential nonlinearly in such a way that, when the potential becomes higher than a certain threshold, large number of the sodium ion channels become opened allowing the entry of sodium ions into the cell. This is followed by the opening of potassium ion channels (after a delay) that permit the exit of potassium ions from the cell. The inward flow of sodium ions increases the concentration of positively charged cations in the cell and causes depolarization. The sodium channels close at the peak of the action potential while potassium continues to leave the cell. The efflux of potassium ions decreases the membrane potential or hyperpolarizes the cell [14]. After closing, sodium channels stay in the refractory state which means that they can not be opened for some time even at high potentials. This property of sodium channels is responsible for the refractory period when the cell can not generate an action potentials.

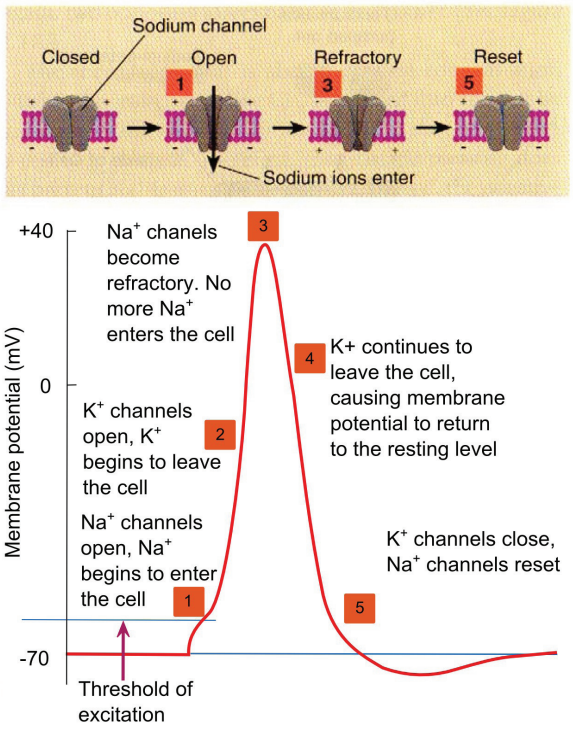

Figure 1.5: The action potential. The top shows the state of the sodium channels. The bottom represents the changes of the membrane potential. When the membrane potential is shifted higher than a certain threshold, the sodium channels open letting the sodium ions flow into the cell depolarizing it (1). Potassium channels open after a delay and potassium ions start to leave the cell (2). When the membrane potential reaches its maximum, sodium channels close and no more sodium can flow in (3). The potassium continues to flow outside through the still opened potassium channels leading to repolarization of the membrane (4). Then, the potassium channels close, and sodium channels reset to their resting state. Figure from [15].

1.1.5 Surface charge of the cell membrane

Although membrane potential is created by the charge of the ions, local electric field in the membrane can be affected by immobile electric charges on the surface of the membrane. This local field can influence activity of many membrane proteins, especially voltage-gated ion channels, pumps and exchangers. The surface charge is also important for adhesion of cells. It is especially interesting in the context of this thesis as adhesion of cells to the positively charged SLB was investigated.

The charge of the membrane is determined by the polar groups of the carbohydrates, proteins and lipids. The value and the magnitude of the charge depends on pH, but as cell survive only in the small range of the physiological pH, this factor can be omitted.

The overall magnitude of the electric charge density on the cell surface can be determined by measurement of the cell's electrophoretic mobility. Such a measurement provides an estimate of the average charge density over the entire cell membrane [16].

Summary of the literature data about electric charge of the cell membrane is presented in the work of Lakshminarayanaiah [17]. The value of electric charge is strongly varied for different preparations (from $1e^-$ per $43Å^2$ for crayfish axon [18] to $1e^-$ per $8000Å^2$ for squid axon [19]). Different methods also give different results for the same preparation. However, whole literature data suggest that the cell membrane is negatively charged.

1.1.6 Electrical double layer

Surface charge of the cell membrane leads to the formation of an electrical double layer which can influence many physiological processes. The distribution of the potential in the double layer can be calculated using the Boltzmann's distribution for ions in the electric field and the Poisson equation. In the one dimensional case the Boltzmann distribution is given by the formula:

$$c(x)=c_0\exp(-\frac{ze\varphi(x)}{kT}) \tag{1.3}$$

where *c(x)* is the concentration of an ion depending on the distance x from the surface, c_0 – is the concentration in the bulk solution, z – the valency of the ion, e – the elementary charge, k - the Boltzmann's constant, T – temperature, φ – electric potential.

The Poison's equation for the one dimension case can be written in the following way:

$$\frac{d}{dx}(\varepsilon(x)\frac{d\varphi}{dx})=-\frac{\rho(x)}{\varepsilon_0} \tag{1.4}$$

where ρ is the density of charge, ε - the relative permittivity of medium, ε_0 – the permittivity of free space.

For a solution containing positively and negatively charged univalent ions the concentrations of these ions at the surface can be calculated on the basis of the Boltzmann's distribution:

$$c^+ = c_0 \exp(-\frac{e\varphi}{kT}) \tag{1.5}$$

$$c^- = c_0 \exp(\frac{e\varphi}{kT}) \tag{1.6}$$

The charged surface is assumed to be placed at $x=0$. Potential $\varphi \to 0$ at $x \to \infty$.

The density of the total charge is equal to:

$$\rho = -e(c^- - c^+) = -ec_0(\exp(\frac{e\varphi}{kT}) - \exp(-\frac{e\varphi}{kT})) = -2ec_0 \sinh(\frac{e\varphi}{kT}) \tag{1.7}$$

Accepting that the medium is uniform ($\varepsilon=const$) and substituting ρ in the Poisson's equation one can get:

$$\frac{d^2\varphi}{dx^2} = -\frac{-2ec_0}{\varepsilon\varepsilon_0} \sinh(\frac{e\varphi}{kT}) \tag{1.8}$$

Introducing a new variable

$$y = \frac{e\varphi}{kT} \tag{1.9}$$

and a new constant

$$\chi^2 = \frac{2e^2 c_0}{\varepsilon\varepsilon_0 kT} \tag{1.10}$$

(χ is called Debye-Huckel's constant) one obtains:

$$\frac{d^2 y}{dx^2} = \chi^2 \sinh(y) \tag{1.11}$$

Making an approximation by accepting that $sinh(y) = y$ (which is true when $y \to 0$) one can simplify the equation to the following form:

$$\frac{d^2 y}{dx^2} = \chi^2 y \tag{1.12}$$

This linear differential equation can be easily integrated giving the dependence of φ on the coordinate:

$$\varphi = \varphi_0 \exp(-\chi x) \tag{1.13}$$

φ_0 is the potential at the surface. It can be used to calculate the surface density of the charge. The Debye length, defined as

$$\lambda_D = \frac{1}{\chi}, \tag{1.14}$$

serves as a measure of distance of distribution of the electric field created by the surface into the medium.

According to the principle of charge conservation, the total charge in the medium per area unit is equal to the surface charge density:

$$\sigma = -\int_0^\infty \rho(x)\,dx = \int_0^\infty \varepsilon\varepsilon_0 \frac{d^2\varphi}{dx^2} dx = -\varepsilon\varepsilon_0 \chi \varphi_0 \tag{1.15}$$

Thus, the potential in the double layer can be expressed via surface charge density:

$$\varphi = \frac{\sigma}{\varepsilon\varepsilon_0 \chi} \exp(-\chi x) \tag{1.16}$$

1.2 Physics of the lipid bilayer

1.2.1 Hydrophobic interactions

Lipids form the bilayer by a self-assembly process. The main physical basis of it is the hydrophobic effect. The hydrophobic forces have the entropic origin. They result from the entire system's statistical tendency to increase its entropy, rather than from a particular underlying microscopic force [20]. Although, complete physical explanation of these forces is complicated, the general idea can be easily understood on the principle of the minimization of energy. All tends to minimize free energy. Bonds (e.g. chemical) reduce energy. Water is electrically polarized and is able to form hydrogen bonds internally which leads to minimization of energy. Since hydrophobic molecules are not electrically polarized they are not able to form hydrogen bonds. Thus, when a hydrophobic molecule comes into water, water repels it in favour of making bonds with itself and to minimize its energy. In this way, hydrophobic tails of lipid molecules appear to be oriented to each other and hydrophilic heads to water. This effect leads to formation not only lipid bilayer but also a variety of other lipid-water structures discussed in the next section.

1.2.2 Lipid polymorphism

Being mixed with water lipids can form not only double layers but can exist in a variety phases depending on the lipid-water ratio, temperature, pressure, ionic strengths and pH. Lipid molecules can form cylinders with their polar heads

making the surface of the cylinder or being directed into the centre. The centres of such cylinders form hexagonal structures giving the name for the phase. There can be also cubic, rectangular, tetragonal and other structures. Various lamelar phases different from each other in a way the hydrophobic tails are packed in the lipid bilayer can also exist. Several most commonly considered phases in which lipids can exist are shown in the fig. 1.6.

Different phases can be identified by a number of methods most useful of which is X-ray scattering [21], [22]. Nuclear magnetic resonance (NMR) [23–25] and differential scanning calorimetry are also used [26].

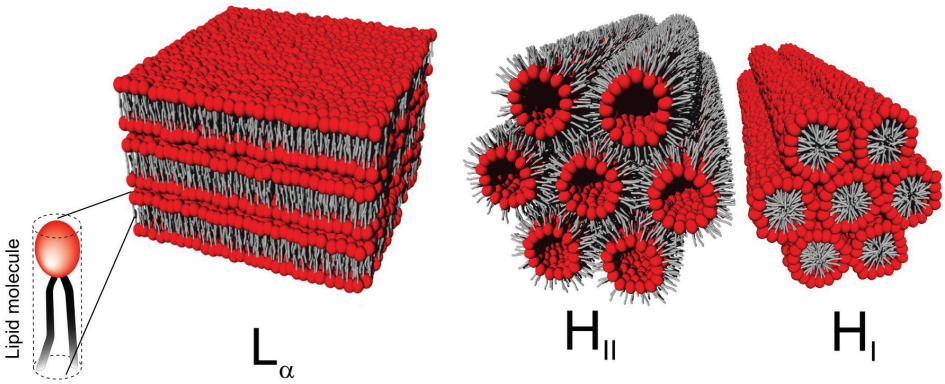

Figure 1.6: Examples of lipid phases: Lamellar phase L_α, inverted hexagonal (H_{II}) and hexagonal (H_I) phases. Modified from [27].

The most widely used nomenclature for lyotropic phases was proposed by Luzzati [22]. The lattice type is denoted by a capital letter, e.g., L for lamellar, H for hexagonal and Q for cubic. Subscripts I and II are used to denote normal (oil in water) or reversed (water in oil) topology phases. A Greek subscript is used to denote the chain conformation: c for crystalline, β for ordered gel-like, α for liquid-like, αβ for coexisting gel- and liquid-like regions, and δ for a helically coiled chain conformation [28]. A prime after the Greek letter is used to denote phases with tilted lipid tails. A list of well established phases is given in the Table 1.1 [28]. Most of lipids in biological membranes are considered to be in L_α - fluid lamellar phase. At lower temperatures this phase can be transformed to gel phases L_β or $L_{\beta'}$ sometimes passing through the rippled gel phase $P_{\beta'}$.

Table 1.1: List of well established lyotropic phases

Phase	Description	Reference
L_c	3D lamellar crystals	[33]
$L^{2D}{}_c$	Lamellar stack of 2D crystalline bilayers	[34]
L_β	Lamellar gel (untitled)	[29]
$L_{\beta'}$	Lamellar gel (tilted)	[29]
$L_{\beta I}$	Interdigitated gel	[35]
$L_{\alpha\beta}$	Partial gel	[22]
L_δ	Lamellar phase of square-packed, helically-coiled (δ) chains	[29]
$P_{\beta'}$	Rippled gel phase	[29]
P_δ	Ribbon phase with -packed chains	[29]
L_α	Fluid lamellar phase	[22]
H	Hexagonal	[30]
H^c	Hexagonal, complex	[22]
R	Rectangular	[31]
M	Oblique	[31]
Q	Cubic	[32]
T	Tetragonal	[22]
Rh	Rhombohedral	[22]

1.2.3 Lipid movements in the bilayer

As any other molecule, lipid molecules in the lipid bilayer experience haotic motion. Due to special structure of the bilayer and the structure of lipid molecules there can be several types of molecular movements (fig. 1.7).

Rotation of molecules. Lipid molecules can spin around their "axis". The time of this rotation is around 10^{-9} s. Average energy required for the activation of this process is around 5-15kJ/mol which is of the same order of magnitude as the thermal energy defined usually as kT which is equal to 2.4 kJ/mol for the room temperature (k – is the Boltzmann's constant).

Rotation of molecular segments. This is an internal rotation of segments in the lipid molecule. It can be considered as a transition between different isomeric forms of the molecule. The energy of activation of this movement is different for different bonds and molecular groups. For a single bond in the carbon chain it is around 15 kJ/mol. For double bound between carbon atoms this energy is around 140 kcal/mol [36], which is much higher than the value of kT and makes the probability of this rotation very low.

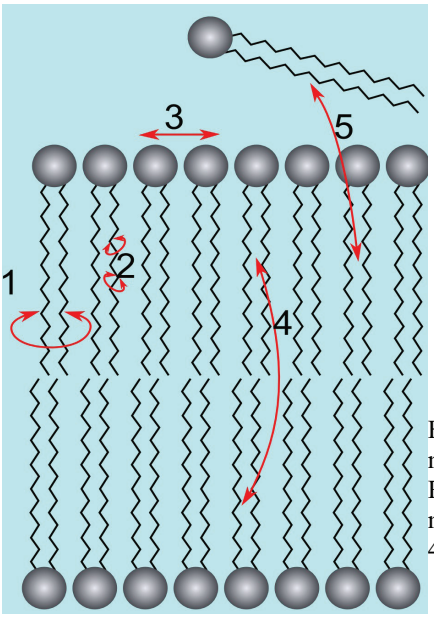

Figure 1.7: Schematics of the types lipid molecule movements in the bilayer. 1) Rotation of molecules, 2) Rotation of molecular segments, 3) Lateral diffusion, 4) Flop-flop, 5) Molecular exchange

Lateral diffusion. The lipid molecules can float in the plane of the lipid bilayer. The diffusion coefficient for the lipid bilayer made of phosphatidylcholine is around 1 um^2/s. This process can be studied in living cells and, even easier, in artificial systems such as supported lipid bilayers (SLB) using fluorescent recovery after photobleaching (FRAP). This method is described in details in Chapter 3.

Lateral diffusion plays an important role in the cell membrane. Proteins floating in the lipid bilayer can come to the area where they are required. The same is true for lipids because a special type of lipids can be required at specific places in the membrane. Rotation of proteins together with their lateral movement helps to adjust a ligand in one membrane to it's receptor in the membrane of another cell.

Diffusion is described mathematically by the second Fick's law:

$$\frac{\partial c}{\partial t} = \nabla (D \nabla c) \tag{1.17}$$

where c is the concentration (it is a function of coordinates and time), D – the diffusion coefficient (can be a function of coordinates), t – time.

In the case of the lipid bilayer the diffusion can occur only in two dimensions and the diffusion coefficient is constant. Thus, the equation (1.1) for the bilayer can be written in the following form:

$$\frac{\partial c}{\partial t} = D\left(\frac{\partial^2 c}{\partial x^2} + \frac{\partial^2 c}{\partial y^2}\right) \tag{1.18}$$

where x and y are spatial coordinates.

Flop-flop. This is a jump of a lipid molecule from one side of the bilayer to another. This process is very slow as it requires transition of the polar head of the lipid molecule through the hydrophobic interior of the bilayer. Half transition time of this process is considered to be from hours to days in model membranes [37]. In natural membranes the rate of this process can be increased by special membrane proteins: translocases and flippases [38].

Molecular exchange. This is a process of exchange of the lipid molecules between two lipid bilayers or the lipid bilayer and another lipid reservoir. This process is also slow as it requires transfer of the hydrophobic tail out of the bilayer.

1.3 Artificial lipid membrane systems

The lipid bilayer is probably the most interesting lipid structure as it comprises the basis of the cell membrane Thus, being reproduced artificially it provides possibilities for studying many properties of the cell membrane. Many different lipid membrane systems have been developed over years of research in order to study the structure of the cell membrane, its electric properties, function of ionic channels and transporters, membrane enzymes, processes of cell adhesion and signalling, etc. Some of these systems are described below.

1.3.1 Lipid vesicles

A lipid vesicle (or a liposome) is a bubble, often having spherical shape, the wall of which is made of the lipid bilayer (fig. 1.8A). This is probably the simplest one among the artificial lipid membrane systems. Liposomes can be easily produced by reconstitution of dry lipids in aqueous solution (although, to reach definite size and lamelarity special conditions may be required). The size of the lipid vesicles ranges from several nanometers in the case of small unilamellar vesicles (SUV), to hundreds of micrometers, for example, in the case of giant unilamellar vesicles (GUV, shown in the fig 1.8).

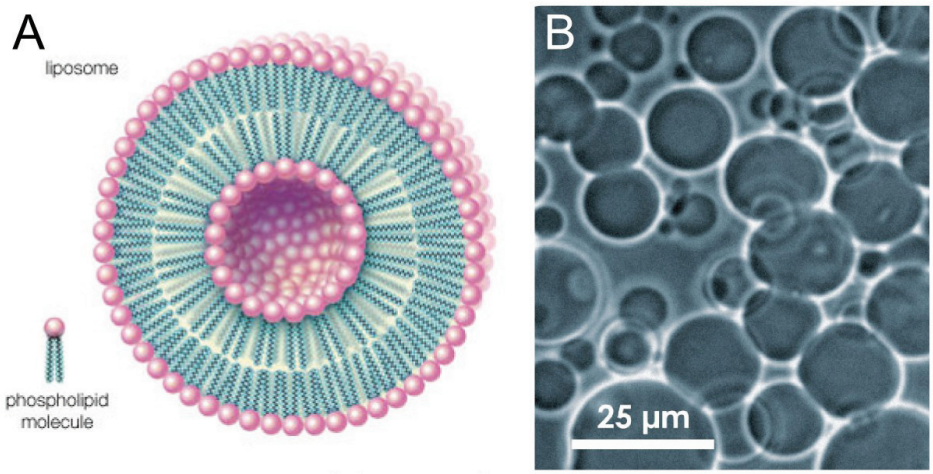

Figure 1.8: (A) Schematic representation of the liposome [40], (B) a micrograph of giant unilamellar vesicles GUV [39].

Vesicles are easy to use and store as they do not require any support or special conditions – they exist in suspension. Many methods of bulk material studies such as light scattering [41], turbidity measurements [41], chromatography [42], electrophoresis [43], NRM [44], x-ray scattering [45], differential scanning calorimetry [46], [47], etc., can be used to characterize vesicles giving information about size, shape, lamellarity, composition, etc. Vesicles can be used to study ionic channels using patch-clamp method [48]. Liposomes with incorporated adhesion proteins and receptors can be used for studying cell adhesion and signalling. Except scientific applications there are many applications in medicine [49] (e.g. for drug delivery [50]) and industry (reviewed in [51], [52]). Vesicles can be produced not only from dry lipids but also derived from living cells [53]. It gives the possibility to study real structures of the cell membrane (but, of course, makes the system more complicated). A general overview of analysis of liposomes and their applications is given in several review papers [54], [55]. In many cases vesicles are an intermediate step for producing other lipid systems such as supported lipid bilayers.

1.3.2 Langmuir monolayers

Langmuir monolayer is a one-molecule thick layer of an insoluble organic material spread onto an aqueous phase (fig. 1.9) [56]. In the case of the lipid film this monolayer can serve as a model of the cell membrane. It is not suitable for studying transmembrane processes as it contains only half of the lipid bilayer but it can be used for studying phenomena taking place on the surface of the membrane.

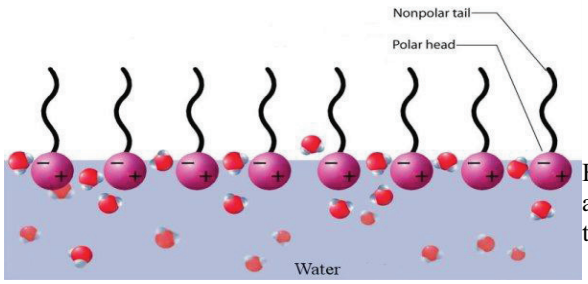

Figure 1.9: A monolayer of amphiphilic molecules arranged on the air-water interface [57].

1.3.3 Suspended lipid bilayers

This class of membrane systems originates from one of the earliest lipid bilayer model - black lipid membranes (BLM) - first described by Mueller et al. [58], [59]. It is also called the "painted" bilayer because it is usually made by putting a drop of lipids dissolved in organic solvent with a brush onto an aperture in hydrophobic material such as Teflon. The lipid molecules starts to move along the Teflon surface, the drop becomes thinner and the bilayer is finally produced across the aperture (fig. 1.10). The term "black" refers to the fact that this bilayer looks black due to destructive interference of light reflected from the back and front surface of the bilayer (because the bilayer is only several nanometers thick).

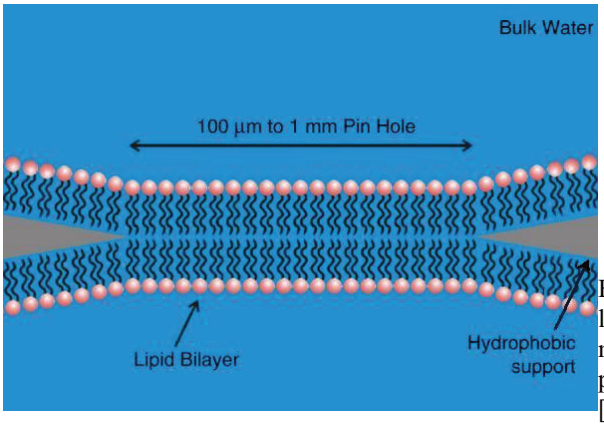

Figure 1.10: Illustration of a black lipid membrane. The phospholipid membrane spans a 100 µm–1 mm pin hole in a hydrophobic support [60].

Although BLM were successfully used for studying membrane proteins (e.g. ionic channels [61–64]) they possess a number of drawbacks making their use difficult. Firstly, they are relatively fragile, can be destroyed easily thus making long term experiments almost impossible. Secondly, organic solvent can be trapped between the lipid layers which can affect incorporated transmembrane proteins.

Suspended membranes similar to BLM can be formed on the tip of patch-pipette [65]. In this case no organic solvent can be trapped in the bilayer as it is formed by vesicle fusion. The same bilayer can be formed on the tip of a pipette with the opening of nanometer size [66]. The small size makes the system more stable but limits the area of applications. Suspended membranes can be also formed over an array of nanopores produced e.g. by alumina anodization [67], [68] or by focused ion beam [69]. In this case bilayer occupies large area which allows to use surface analysis techniques but at the same time due to presence of pores the system becomes more fragile.

1.3.4 Supported lipid bilayers (SLB)

The lipid bilayer can be formed on a solid substrate. Firstly it was done by Tamm and McConnell in early 1980s [70] and since that time this membrane system has been widely used as a model for fundamental studies of the cellular membrane and membrane proteins [71–74] as well as for developing biosensors [75–78].

In its basic configuration SLB consist of lipid bilayer placed on a solid surface (such as glass, Si, mica), covered with aqueous solution and separated from the substrate by a very thin (around 1 nm) hydration layer as shown is the fig. 1.11 (see reviews [60], [79], [80]). This system provides large plane lipid bilayer being at the same time more stable than BLM. Good stability makes it possible to carry out long term experiments. Large plain area covered with the bilayer provides the possibility to use advanced methods designed for surface analysis such as ellipsometry, SPR, QCM-D, TIRF, and AFM. Also, the SLB is an interesting system for studying cell adhesion on an artificial substrate due to the structural similarity with the cell membrane.

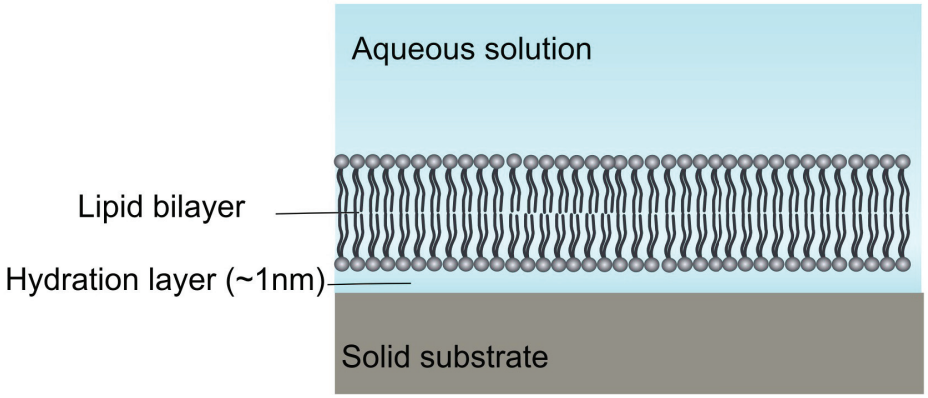

Figure 1.11: Supported lipid bilayer is a double layer of lipid molecules formed on a solid surface, separated from it by a thin aqueous layer and covered by aqueous solution.

During the past decades many modifications of the basic supported bilayer system has been developed to expand the application area. Among them one can name polymer-cushioned lipid bilayer, hybrid bilayer, tethered bilayer, suspended lipid bilayer, supported vesicle layer (fig. 1.12).

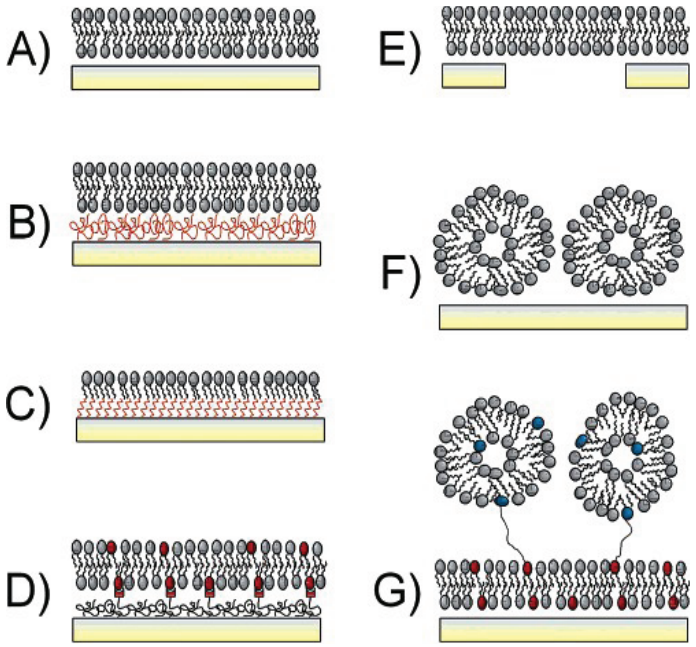

Figure 1.12: Surface-confined membrane models: (A) solid-supported lipid bilayer; (B) polymer-cushioned lipid bilayer; (C) hybrid bilayer, consisting of a self-assembled monolayer (e.g., thiols on Au or silanes on glass or silica) and a lipid monolayer; (D) tethered lipid bilayer; (E) freely suspended lipid bilayer; (F-G) supported vesicular layers [79].

There are many ways of the SLB preparation (fig. 1.13). It can be made by subsequent deposition of two Langmuir monolayers on the surface [70]. The bilayer can be achieved by spreading from a lipid reservoir as described in [81]. It can be produced by assembly of lipids onto the substrate directly from a detergent solution [82]. But the simplest, effective and most widely used way of producing SLB is vesicle deposition: being deposited onto hydrophilic surface lipid vesicles rupture and fuse with each other forming lipid bilayer. This method was used in the present work and is described in details in Chapter 3.

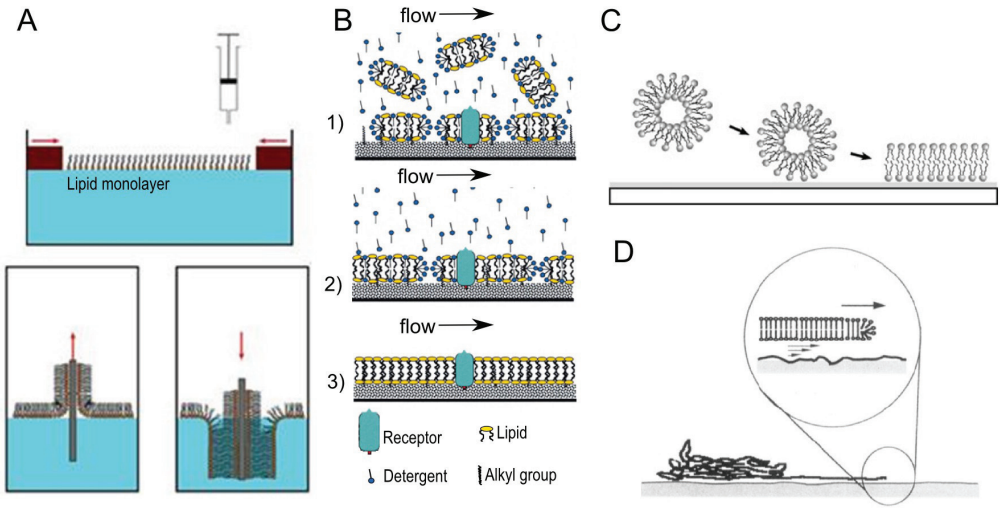

Figure1.13: Methods of SLB preparation: (A) Langmuir-Blodgett technique [83], (B) deposition from detergent solution [82], (C) vesicle deposition, (D) spreading from a lipid reservoir [81].

1.4 Cell adhesion and signalling

1.4.1 Membrane receptors

Many membrane proteins have extracellular domains which can be contacted by molecules from extracellular space. This contact can lead to changes in the conformation of the protein which can be transmitted through the cell membrane giving the origin to a cascade of the secondary signalling processes inside the cell such as enzymatic chemical reactions, release or production of certain substances (second messengers), etc. These signals can go deep inside the cell influencing protein production and gene expression. Such proteins in the cell membrane are called receptors. The signalling molecules which activate receptors are called ligands.

There are three main types of receptors: ion channel linked receptors, enzyme-linked receptors and G protein-coupled receptors [84]. Ion channel linked receptors are ion-channels themselves and constitute a large family of multipass transmembrane proteins. They are involved in rapid signalling events most generally found in electrically excitable cells such as neurons and are also called ligand-gated ion channels.

Enzyme-linked receptors are either enzymes themselves, or are directly associated with the enzymes that they activate. The majority of enzyme-linked

receptors are protein kinases, or receptors associate with protein kinases.

G protein-coupled receptors (GPCR) are integral membrane proteins which possess seven membrane-spanning domains or transmembrane helices [85]. When a ligand binds to the GPCR it causes a conformational change that may involve disruption of a strong ionic interaction between the third and sixth transmembrane helices, which facilitates activation of the G-protein heterotrimer. Depending on the type of G protein to which the receptor is coupled, a variety of downstream signalling pathways can be activated [86].

1.4.2 Signalling via adhesion molecules

Another function of the extracellular domains of the proteins is to provide adhesion. They can be specifically connected to other proteins on the surface of the membrane of another cell providing a connection between two cells. There are also proteins that can provide adhesion to the extracellular matrix (or to the surface in vitro).

Adhesion between cells, which involves the binding of cell adhesion molecules (CAMs) to adjacent cells, regulates fundamental processes such as cell differentiation, contact inhibition of cell growth and apoptosis. These processes ensure correct tissue organization during development, and tissue regeneration in the adult. Interactions between CAMs mediate mechanical adhesion among cells, but also, importantly, CAMs are able to propagate intracellular signals. This last function is due to their connections to the major signalling networks that control most the cellular responses. Therefore, these adhesive proteins not only maintain tissue integrity but also may serve as sensors that modulate cell behaviour in response to the surrounding microenvironment. Such an important adhesion molecules as cadherins are linked to a large variety of intracellular partners that mediate intracellular signalling and modulate the organization of the actin cytoskeleton to provide the dynamic forces necessary for correct tissue morphogenesis [87] .

Signalling via adhesion molecules plays important role in axon guidance and development of neuronal synapse because an axon has to find its target and stop growing after touching it. Such adhesion molecules as cadherins, protocadherins, sidekick are important for target recognition and initiation of the synapse growth. Many other adhesion molecules such as SynCAM, N-cadherin, Neuroligin-Neuroxin pair and Eph-ephrin pair are important for synapse formation, maturation and synaptic plasticity. The types and roles of synaptic adhesion molecular have been described in several review papers and books [88–93].

1.4.3 Eph-ephrin signaling

One example of signalling via adhesion molecules, important for the present work, is Eph-ephrin signalling. Last years a lot of attention has been devoted to investigation of Eph receptor protein kinase and it's ligand ephrin because of many important functions this pair performs during development of the organism and in adulthood including vascular development, formation of tissue-border, cell migration and axon guidance and synapse formation [94–98].

Interesting feature of Eph-ephrin signalling system is it's bidirectionality: ephrin is not only a ligand for Eph receptor but sometimes can play the role of receptor, transmitting signals in its host cell.

An excellent review of the Eph-ephrine signalling is presented in the work of Kullander and Klein [99]. Eph- receptor belongs to the receptor tyrosine kinase type (RTK). Of all the RTKs that are found in the human genome, the Eph-receptor family—which has 13 members — constitutes the largest one. Their ligands, the ephrins, are divided into two subclasses, the A-subclass (ephrinAl-ephrinA5), which is tethered to the cell membrane by a glycosylphosphatidylinositol (GPI) anchor, and the B-subclass (ephrinBl-ephrinB3), members of which has a transmembrane domain that is followed by a short cytoplasmic region (fig. 1.14).

The receptors are divided on the basis of sequence similarity and ligand affinity into an A-subclass, which contains eight members (EphAl-EphA8), and a B-subdass, which in mammals contains five members (EphBl-EphB4, EphB6). A-type receptors typically bind to most or all A-type ligands, and B- type receptors bind to most or all B-type ligands, with the exception of EphA4, which can bind both A-type and most B-type ligands.

The Eph-receptor extracellular domain is composed of the ligand-binding globular domain, a cysteine-rich region and two fibronectin type III repeats. The cytoplasmic part of Eph receptors can be divided into four functional units; the juxtamembrane domain that contains two conserved tyrosine residues, a classical protein tyrosine kinase domain, a sterile α-mottf (SAM) and a PDZ-domain binding motif. The solved structure of the SAM domain (~70 amino adds) indicates that it could form dimers and oligomers. The PDZ-binding motif—located in the carboxy-terminal 4-5 amino-acid residues — contains a consensus binding sequence that includes a hydrophobic residue (usually valine or isoleudne) at the very carboxyl terminus.

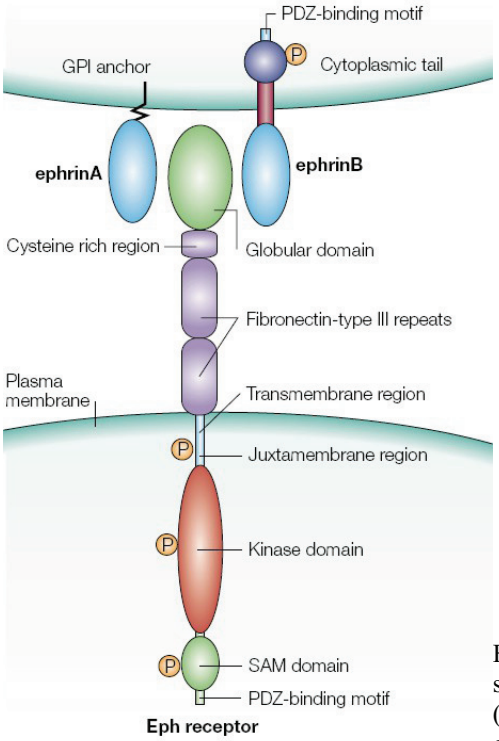

Figure 1.14: A schematic diagram showing an ephrin-expressing cell (top) interacting with Eph-expressing cell (bottom) [99].

In contrast to most other RTK, Eph receptor is activated when it is connected to clustered membrane attached ephrin ligands. This requirement for the membrane clustering of the ligand indicates that the contact between cells that express Eph receptor and cells that express ephrin is needed [99]. This phenomenon creates difficulties for studying Eph-ephrin signaling because ephrin simply dissolved in medium can not form necessary clusters. For such experiments ephrin should be incorporated into lipid bilayer where it can stay in the proper conformation and freely float having the possibility to form clusters. SBL represents an excellent platform for such experiments providing not only a possibility for ephrin incorporation but also stability and possibilities for applying many advanced methods of surface research.

Chapter 2

Motivation and goals

-Why don't you use the dish washer to wash your plates after lunch?
-We don't use plates when we eat.

From a conversation of students

2.1 Interfaces in nature and technology

Basic interfaces between living matter and surrounding are created by means of the cell membrane. As one could see from the previous Chapter membranes not only separate the cell from the outer world but also provide possibilities for material, energy and information exchange. By means of incorporated proteins the cell membrane provides the possibility to sense chemicals selectively, transmit and amplify signals, interact with other cells, facilitate chemical reactions, generate electric potentials. Biological interfaces are adjustable to the environmental conditions, self tunable, self controllable.

Many technological applications in biosensing or medicine as well as fundamental research in life sciences require interfaces with similar functionality. Biosensors would require selectivity and sensitivity similar to the receptors of the cell membrane. Implants would need higher biocompatability and provide effective and stable information and material exchange with biological tissues. This would be especially relevant in a rapidly growing field of cell-electronic and neuro-electronic interfaces [100–102].

Although, big progress in development of materials and structures (e.g nanostructures) suitable for such applications has been achieved there still exist many problems with biocompatability, adhesion properties or stiffness of such surfaces. Instead of developing new artificial materials one could directly mimic the cell membrane to use at least some advantages of this biological system. There are many ways to mimic the cell membrane; some of them were discussed in the previous chapter. They all have both advantages and disadvantages. This work is focused on one of them – the SLB. The reasons for this choice are discussed in the following section.

2.2 Why SLB?

2.2.1 Advantages of the SLB

What makes the SLB so interesting for applications? There are several reasons:

1. It is a biomimetic system. It reproduces many properties of the lipid bilayer of the cell membrane. It creates natural environment for proteins: enzymes, receptors, ion channels, making them to work properly. Many proteins require a hydrophobic surrounding, at least at some parts of them, to maintain their three-dimensional structure and perform their function. Immobilization of proteins on the surface (covalently, tethering, printing) in many cases does not produce the same effect as they lose their conformation and, as a result, properties (fig. 2.1).
2. It provides possibility for proteins to move in the plane of the SLB in such a way that they can be collected in the place where they are required. Possibility of free movement and rotation also increases the probability to bind the ligand as the conformation of the receptor can be adjusted.

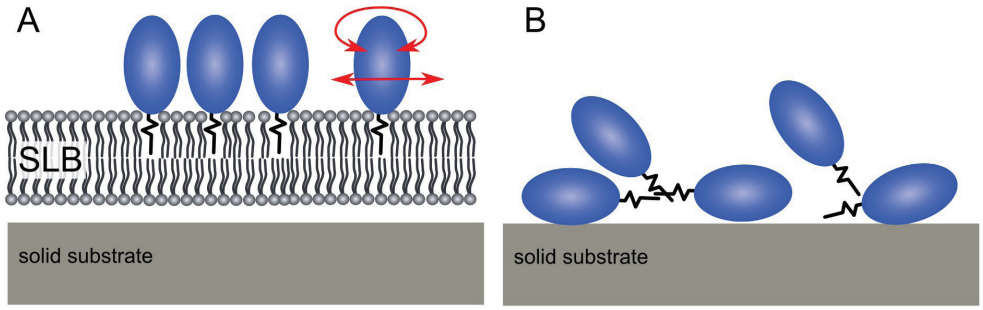

Figure 2.1: (A) Proteins incorporated in the SLB. They have the correct position and conformation. They are also mobile and rotatable as in the cell membrane. (B) Proteins printed on the surface are immobile and nonoriented.

3. The SLB is more stable than suspended lipid bilayers providing possibilities for long term measurements. At the same time, unlike vesicles, it is localized on the surface. This makes it possible to build a bilayer on a signal transducer such as electrode, transistor, optical fiber, etc.
4. The SLB is a good insulator which makes it a good platform for sensors that require electrical measurement reducing leak currents. It is useful e.g.

for applications with incorporated ion channels or electron transport proteins.

5. Lipid bilayers, at least made of phosphocholine, are protein repellent – proteins from solution do not adhere to it. It creates possibility to provide high selectivity of adsorbed material - if one have incorporated receptor, only its ligand can be adsorbed and measured.
6. It creates a way of immobilizing proteins on the surface, that is in some cases easier than other methods. Sometimes this method is the only possible one.
7. As a plane surface can be covered with the SLB. Thus, many advanced methods designed for surface analysis such as ellipsometry, SPR, QCM-D, TIRF, and AFM can be used to study it or to serve as transducers in the case of using the SLB for biosensors.
8. Large plane area that can be covered with the SLB provides a possibility to use it as a platform for cell culture. The required number of cells can be plated on it which makes it easier to maintain the culture and increase statistics. The SLB with incorporated proteins can be used for studying cell adhesion and signalling. Biomimetic properties can provide perfect environment for cells to improve their viability.
9. The patterned SLB can be created providing possibilities for cell guiding and wider possibilities for integration with electronic devices.

2.2.2 Applications of the SLB

Several areas of applications can be distinguished:

1. Fundamental research of the membrane structure, functions and properties of membrane proteins
2. Biosensors
3. Platform for cells

For the first application SLBs have been extensively utilized for several decades. There are many papers devoted to using SLBs for fundamental studies of the cellular membrane and membrane proteins [71–74]. There were also many attempts of using the SLB for developing biosensors [75–78], [103]. But using the SLB as a platform for cells is no so common now.

2.2.3 SLB for cell culture

Using the SLB as a platform for cell culture can enhance possibilities for

studying cell adhesion and cell signaling. However, the number of experiments using the SLB for studying cells is not very high. This is, perhaps, due to the fact that the SLB made of natural lipids, such as phosphatidylcholines (PC), is protein and cell repellent – cells can not adhere to it. This effect was shown for the SLB prepared by a vesicle fusion method [104–106] and earlier for lipid films prepared by spincoating [107], [108].

To use SLBs as a platform for cell culture one has to functionalize it with special molecules that can provide adhesion. These functional molecules can be membrane proteins responsible for adhesion between cells *in vivo*. However, the protein incorporation step makes the whole procedure to prepare the functionalized SLB more complicated. Nevertheless, a few attempts have been made to use SLBs as a platform for cell culture. Among papers describing the use of SLBs for studying cells, several recent ones can be mentioned. Thid et al. [109] used IKVAV peptide to promote adhesion of neural progenitor cells on SLBs. Ananthanrayanan et al. [110] functionalized SLBs with RGD peptides to study neural stem cells. Huang et al. [111] used collagen functionalized SLBs as a platform for smooth muscle cells. Pautot et al. [112] used Glycosylphosphatidylinositol (GPI) anchored neuroligin to promote adhesion between the SLB and HEK cells expressing neuroxin. Furthermore, Baksh et al. [113] produced silicon microspheres covered with neuroligin doped bilayers and showed that adding them to neuronal cell culture could promote synapse formation. Another example is formation of immunological synapses between T cells and a SLB [114].

Although, some steps were done in the direction of using the SLB as a platform for cells, many aspects of this idea should be investigated and ways of applications of the SLB need to be developed.

2.3 The aim and directions of work

2.3.1 The aim

Providing all the advantages, discussed above, that the lipid bilayer can provide for supporting and studying cells, and not a very high number of research made in this direction ***the aim of the present work is to study possibilities of using the SLB as a platform for neuronal cell culture.***

To reach this aim the work pursued several directions.

1. Increasing cell adhesion to the SLB
2. Studying possibilities of utilizing proteins incorporated into SLB for cell signalling.
3. Patterning of the SLB

2.3.2 Increasing of cell adhesion to the SLB

The most natural way of increasing adhesion of cells to the SLB would be incorporation of adhesion proteins. This way, however, is quite complicated because of difficulties of work with proteins. If no specific adhesion or signalling is required it would be better to find simpler ways of enhancing cell adhesion. While adhesion proteins bind specifically to their partners on the membrane of another cell, adhesion can be provided by nonspecific interactions, such as electrostatic interaction. As the cell membrane is negatively charged (as discussed in the Chapter 1), positive charge incorporated into the SLB can provide adhesion. To introduce positive charge into the SLB positively charged lipids can be used (fig. 2.2). This way is much easier than incorporation of proteins or covalent binding of the other functional molecules to the SLB, as the positively charged lipids can be simply mixed with the main lipids from which the bilayer is prepared.

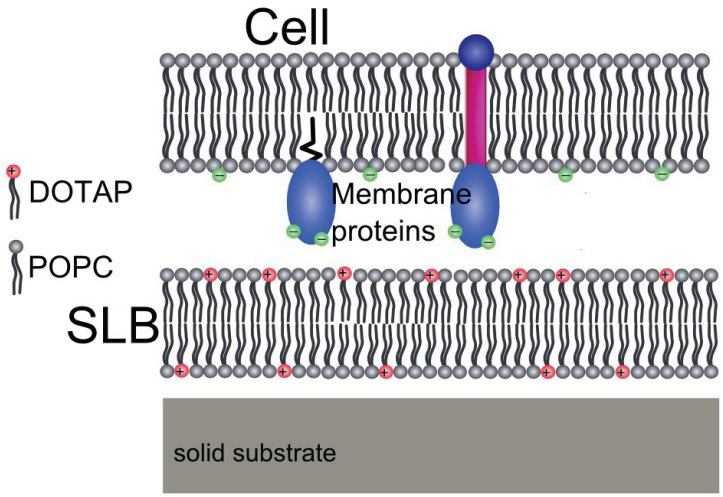

Figure 2.2: Illustration of the principle of providing cell adhesion to the SLB by electrostatic interaction. Positively charged lipid (DOTAP) is added to the SLB made of zwitterionic lipid (POPC). Cell membrane is negatively charged due to surface carbohydrates, proteins and some lipids. Interaction of these charges with the positive charge of the SLB can provide cell adhesion.

2.3.3 SLB with incorporated ephrin A5

Positively charged SLB can be used to provide cell adhesion. But if an application requires signalling function of the membrane proteins or specific adhesion of cells of a certain type or adhesion of a certain part of the cell (neurites, axons, etc), adhesion proteins should be used. By now, not every protein can be used in SLB. First of all, because membrane proteins are difficult to extract and

purify. Procedures of incorporation of proteins into the SLB are sometimes complicated and are suitable not for every protein.

One of the important signalling and adhesion proteins that performs many functions (some of them are described in the previous chapter) is ephrin which interacts with the Eph receptor tyrosine kinase. Many of the functions are relatively well characterized which makes ephrin a good candidate for testing it in an SLB based platform for cells.

Two subclasses of this protein are different in their structure: natural ephrin A is linked to the membrane by means of a simple GPI anchor while ephrin B has the transmembrane part and the small cytoplasmic domain.

It was shown in literature that Eph receptor is activated when it is connected to clustered membrane attached ephrin ligands [99]. This requirement makes it important to use ephrine incorporated into a lipid bilayer for *in vitro* studies of Eph-ephrin signalling. As protein molecules can float in the SLB, they can gather together and form clusters, occupy required position relative to the receptor and have a proper conformation. Thus, ephrin can be used to show the usefulness and importance of the SLB based systems.

2.3.4 Preparation of patterned SLB using the GUV

Patterning of substrates is necessary for many branches of research using cell culture. Patterning can be used for creating cell adhesive and cell repellent areas (e.g. on planar micro-electrodes arrays (MEA) [115], [116] to increase probability of cell-electrode contact), neurites guiding (creating neuronal networks with predefined geometry) or studying redistribution of membrane proteins during adhesion process. As using of the lipid bilayer is desirable for some applications, development of approaches of creating patterned SLB is required.

Several methods of patterning the SLB are known [117–119]. Most of them just create separated areas of the SLB of the same type. These methods that can provide possibility of creating areas of different SLBs are usually based on an approach that requires deposition of small droplets of SUV suspension on the surface [119]. They have disadvantages connected with the evaporation of liquid during patterning process which can lead to destruction of the SLB [120].

In the present work the idea of using the GUV for creating patterned SLB is utilized. When a giant vesicle touches the surface, it breaks and form a patch of the lipid bilayer up to hundreds of micrometers in diameter. If there are barriers on the surface, dividing it into areas, the patches can be confined in these areas and patches of the SLB of different types can be produced in different places of the surface. The GUV can be moved by a micro pipette (although it was not done in the present work) and positioned precisely on desired place. At the same time the whole system always stays under liquid. Thus, the GUV can provide a new method for SLB patterning.

Chapter 3

Materials and methods

Glass is cheap, our time is expensive

Kristin Michael

3.1 Preparation of the supported lipid bilayers

3.1.1 Overview of the preparation procedure

Several methods of preparation of the SLB are known including deposition of the Langmuir–Blodgett films in the solid substrates [70], deposition from detergent solution [82], spreading from a lipid reservoir [81], and fusion of vesicles on the solid surface [121]. In this work, the method of vesicle fusion was used because it is relatively simple, comparing with other methods, and gives pure SLBs without residues of the organic solvents. This method requires several stages of preparation: cleaning of substrates, preparation of small unilamelar vesicles (SUV), deposition of the vesicles. The whole procedure is schematically shown in fig. 3.1. In the following sections each step is considered in details.

3.1.2 Substrate preparation

The SLB were formed on the surface of the glass cover-slips. The cover-slips were washed extensively in 2% Hellmanex in an ultrasonic bath until the surface was clean as indicated by a uniformly spread very thin film of liquid, on which lines of interference of light could be seen. Afterwards, glass was rinsed extensively with Milli-Q water and dried at 60°C. Glass slides were activated by oxygen plasma in Plasma system PICO (5 min, at 0.4 mbar, 40% power of the generator) right before bilayer preparation. Oxygen plasma removes possible residues of organic contamination and makes the surface hydrophylic by producing hydrophylic molecular groups, most likely hydroxyl groups [122].

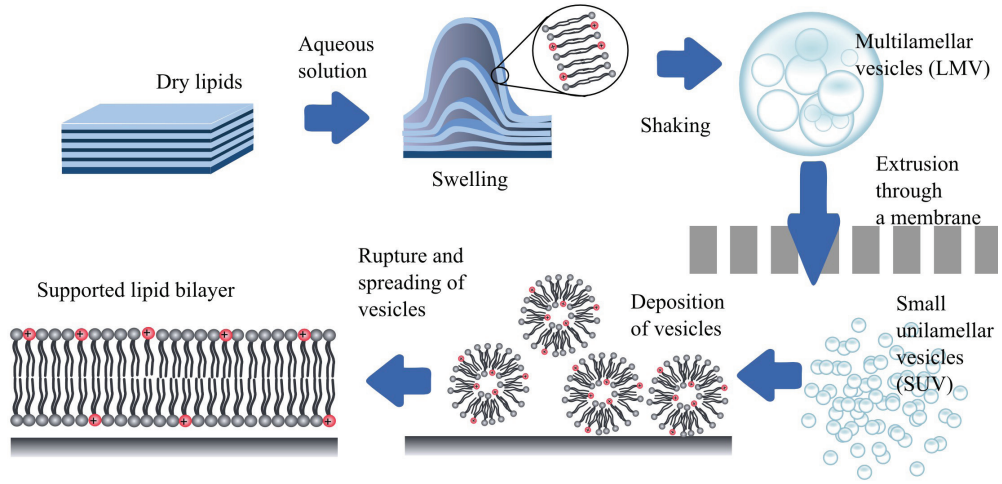

Figure 3.1: A schematic representation of the SLB preparation process including reconstitution of dry lipids in aqueous solution, formation of LMV, production of SUV by extrusion, vesicle deposition on the surface, their fusion and the SLB formation. Lipids of different types can be used. Positively charged lipids are marked by red colour. Zwitterionic lipids are grey.

3.1.3 Preparation of small unilamellar vesicles (SUV)

For producing of the SUV, lipids, dissolved in chloroform, are mixed in desired concentrations, dried on the walls of a glass flask under a stream of nitrogen and then left in vacuum for 1h to remove residues of solvent. Dry lipids forms layers on glass. After addition of aqueous solution these layers swell and, after shaking, large multilamellar vesicles (LMV) are produced. These vesicles have size of tens to hundreds of micrometers (the scattering of sizes is quite high) and consist of many shells made of lipid bilayers. LMV were extruded 11 times through a 100 nm poly-carbonate membrane using Avanti mini extruder (fig. 3.2) to produce small unilamellar vesicles.

Figure 3.2: Avanti mini extruder used for production of SUV

3.1.4 Formation of supported lipid bilayers

SLBs were prepared in wells made of PDMS that were attached to clean glass slides (fig. 3.3). The size of one well was 9mm x 9 mm. An array of four wells was mounted on each slide. These wells were used for two purposes: 1) to create a pattern for producing the SLB of different types in the same Petri dish and 2) to allow solution exchange without the danger of exposing the surface to air (as the SLB are destroyed immediately after exposing them to air). Suspension of SUV was applied to these wells and incubated at room temperature more than 20 min to allow vesicle to adsorb, rupture, fuse and form the SLB. After that, the samples were rinsed with phosphate buffer saline (PBS) using a syringe (20ml of PBS per well) to remove excess of vesicles that usually stay on the SLB. After the preparation quality of the SLB can be checked using fluorescent microscopy as described in section 3.3 . The bilayers can be kept in aqueous solution for several days. For the experiments with cells, the bilayers were usually prepared day before cell preparation and left overnight at 4°C in Petri dishes filled with PBS.

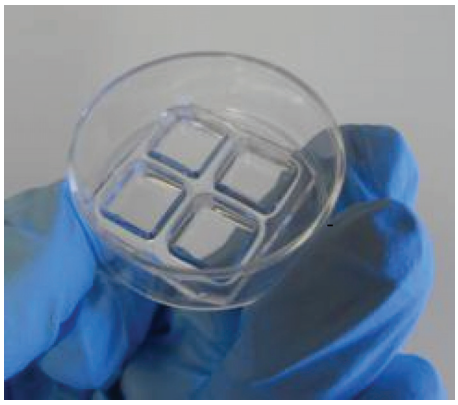

Figure 3.3: PDMS wells on glass slides used for the supported lipid bilayer (SLB) preparation.

3.1.5 Lipids

Several types of lipids were used in this work for SLBs preparation and labelling. Their structures are shown in fig. 3.4. The main lipid used as a basis for most of preparation was 1-palmitoyl-2-oleoyl-sn-glycero-3-phosphocholine (POPC). It is a zwiterionic lipid: it contains both negative charge (in phosphate group) and positive charge (in choline group). This lipid was chosen because it is similar to natural phosphatidylcholine. Also, its temperature of gel-liquid phase transition is -2°C [123] which is quite low and assures that at the room temperature and at physiological conditions (37°C) the SLB is in liquid state.

To introduce positive charge into the SLB 1,2-dioleoyl-3-trimethylammonium-propane (DOTAP) was used. This lipid has only positive charge group in its polar “head”.

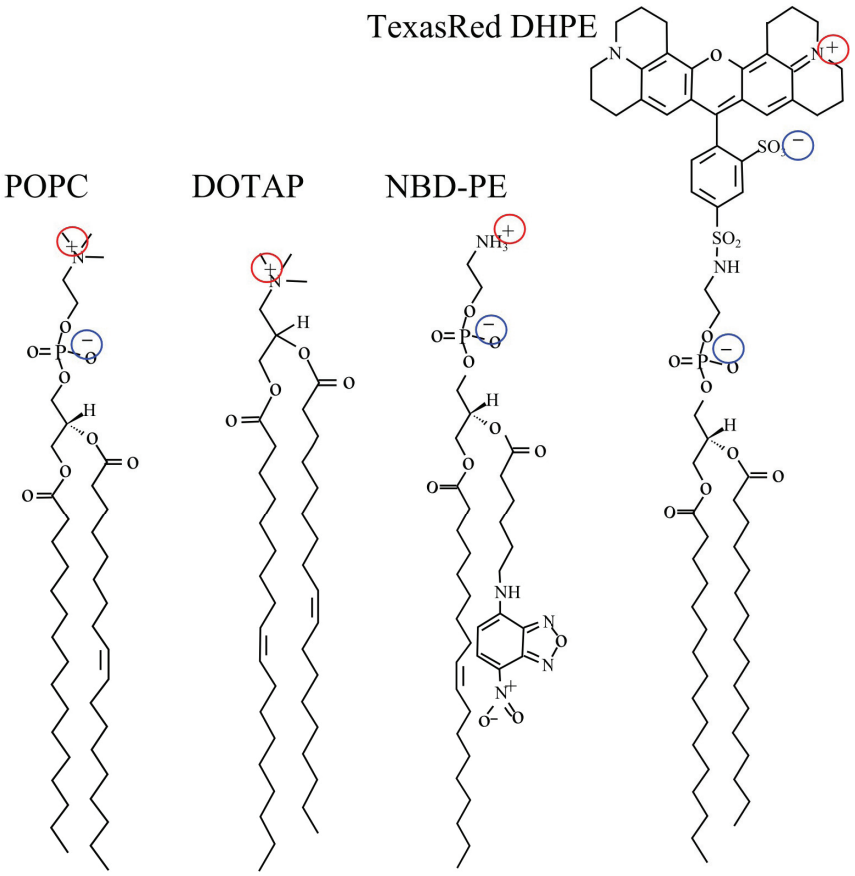

Figure 3.4: Structure of the lipids used for the SLB preparation and labelling. Positive charges of the lipids heads are labelled with red circles, negative – with blue ones.

To visualize the SLB by fluorescent microscopy two labeled lipids were used. One of them is 1-oleoyl-2-{6-[(7-nitro-2-1,3-benzoxadiazol-4-yl)amino] hexanoyl}-sn-glycero-3-phosphoethanolamine (NBD-PE). NBD label emits light in the green range of the spectrum. This dye was used mostly for bleaching experiments (see section 3.3.2), because the wave length of the available laser fits to it's absorption spectrum. However, this label can be bleached very easily even by day light which makes it complicated to work with it. Because of this reason, for most of experiments with cells another labelled lipid, Texas Red® 1,2-dihexadecanoyl-sn-glycero-3-phosphoethanolamine, triethylammonium salt (Texas Red DHPE) was used. Texas Red is more resistant to bleaching and is more suitable for long term experiments.

3.2 Incorporation of proteins into the SLB

3.2.1 Overview of the protein incorporation procedure

One of the most common method for protein incorporation into the lipid bilayers is reconstitution from detergent solution [124–126]. In this procedure proteins are mixed with detergent and lipid vesicles in defined concentrations. Small amphiphilic molecules of detergent can easily go into the lipid bilayer, disturb its structure and facilitate protein incorporation. Detergent also increases solubility of membrane proteins, that are usually poorly soluble in water, and prevent formation of protein aggregates. After certain time of incubation in such solution at least some of the protein molecules appeared to be inserted into lipid bilayers of the liposomes – proteoliposomes are formed. After that, detergent is removed by dialysis, adsorption on polystyrene microbeads, chromatography or simply by dilution. The procedure of protein incorporation is schematically shown in fig. 3.5. Proteoliposomes can be applied to the solid surface to form the SLB.

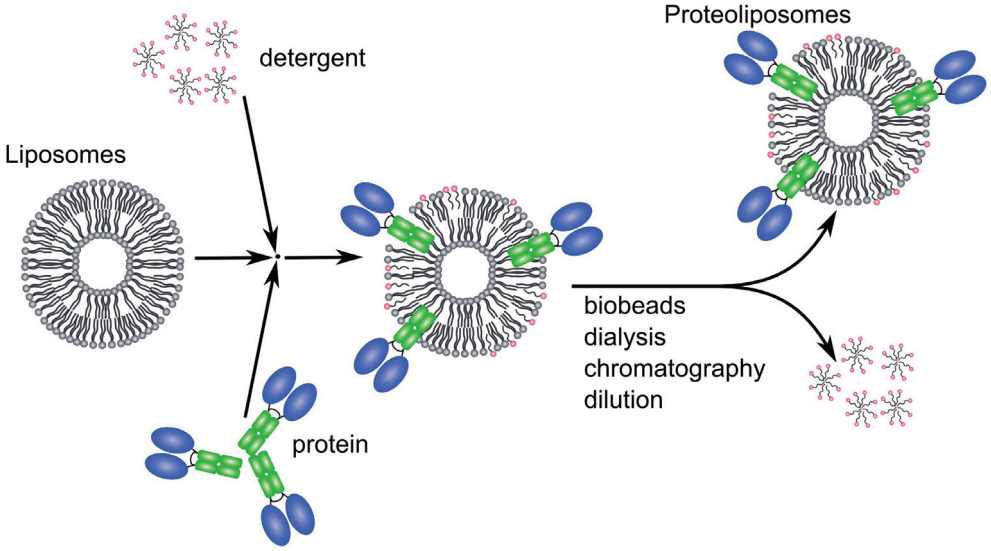

Figure 3.5: A schematic representation of the generally used method to reconstitute proteins into liposomes from detergent solution.

In the present work a similar method was used for incorporation of ephrin A5 into SLB . The recombinant human ephrin-A5 Fc chimera, CF from R&D systems was used. It consists of two ephrine molecules connected to the Fc antibody domain (like proteins shown in fig. 3.5). It was shown in literature that the hydrophobic Fc fragment of IgG, most likely, can be embedded into the lipid bilayer providing a preferential orientation of the IgG molecules in the supported bilayer structure [127]. Thus, ephrin-A5 Fc chimera seems to be a reasonable replacement of the natural molecule.

There were several differences in the reconstitution process utilized in the present work comparing with the standard method. First, detergent (*n*-octyl-β-D-glucoside was used) and protein were added not to SUV but to dry lipids on the stage of LMV formation. This was done because ephrin A5 Fc chimera (as well as natural ephrin A5) is not transmembrane protein and penetrates only one leaflet of the SLB. Providing this, there is a big probability that the protein can be accumulated only on the outer surface of the SUV. After deposition and rupturing of these vesicles it could be found only in the lower leaflet of the SLB as shown in fig. 3.6(A). Addition of detergent and protein to the dry lipids assures that the protein appear on the both sides of the walls of LMV and, after extrusion, both in the inner and outer part of SUV. After formation of the SLB from such vesicles at least half of the protein molecules should be faced into solution (fig. 3.6(B)).

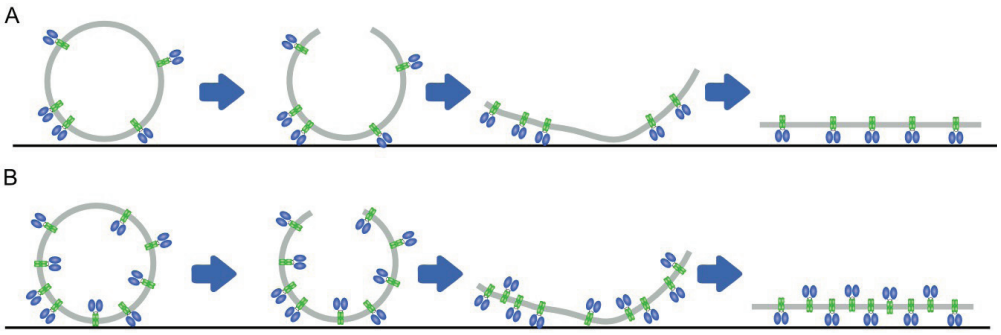

Figure 3.6: Most probable mechanisms of the liposome rupturing: (A) proteoliposomes prepared from SUV treated in detergent solution with ephrin A5. (B) Proteoliposomes prepared by adding detergent and protein to dry lipids at the stage of LMV formation.

After proteoliposomes were formed, dialysis, or any other way of detergent removal was not used. Suspension of these liposomes were diluted (see protocol in the Appendix B) and applied to clean substrates. There are two reasons for not using dialysis (or another detergent removal technique). Firstly, the detergent is presented not only in surrounding solution but also inside of the liposomes. This detergent is difficult to remove. Secondly, as experiments showed (see Chapter 5) vesicles could rupture at the surface and fuse, forming the SLB, even in the solution containing detergent. Thus, one can simplify the whole procedure avoiding detergent removal steps.

When the SLB is formed, detergent that stays in the bilayer is removed during the washing step. In this case, washing is similar to dilution technique, because total amount of the solution passed through the sample is much higher than the initial amount of the solution with detergent. Thus, detergent molecules, that sometimes come out of the bilayer due to Brownian motion are washed out

with the stream of buffer. After washing the SLB was left for some time in the big amount of buffer. The rest of detergent, which could probably stay in the bilayer, could go out. After that, the solution in the well was changed again.

Summing up, the whole procedure of preparation of the SLB with proteins can be represented schematically as shown in fig. 3.7.

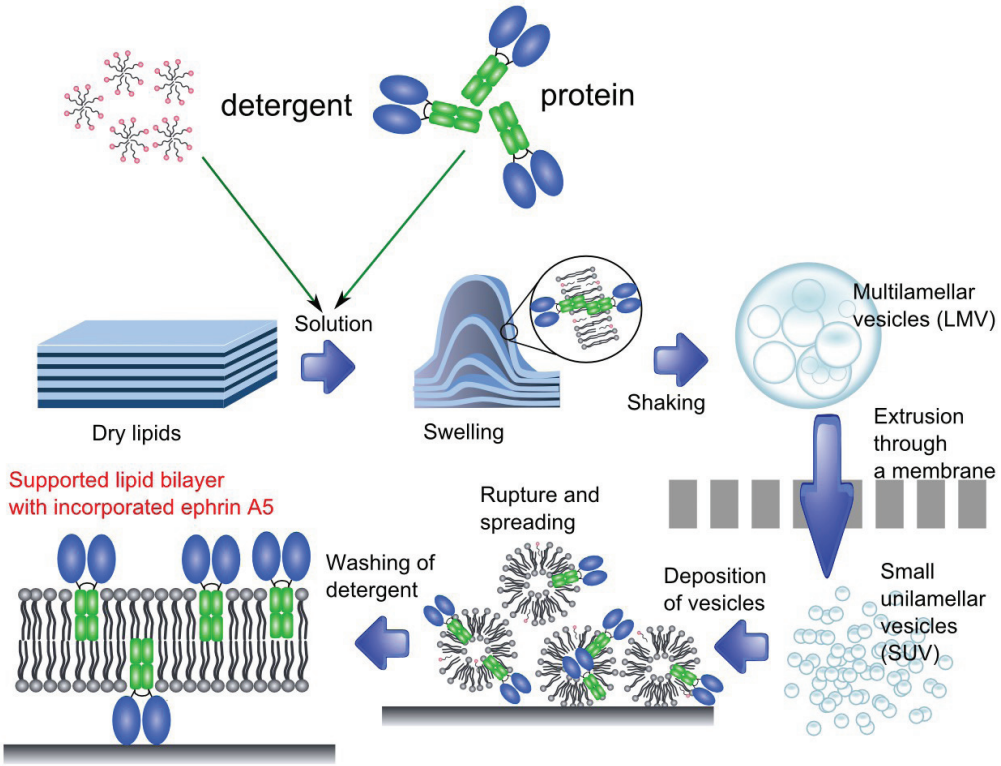

Figure 3.7: A schematic representation of preparation of the SLB with incorporated protein

3.2.2 Determination of the concentration of detergent

For successful reconstitution of protein from detergent solution one should define the concentration of detergent precisely. Too low concentration can not facilitate protein insertion into the liposomes, while too high concentration of detergent can lead to liposomes solubilization and micelle formation. Increase of the amount of detergent in the bilayer of the liposomes leads to change of light scattering properties of suspension. These changes can be measured by spectrophotometer as increase of optical density (OD). In the present work a PerkinElmer Lambda 900 spectrophotometer from PerkinElmer, Inc was used and OD at 500 nm was measured (see Appendix B for the details). When the concentration of detergent reaches a certain level, liposomes start to dissolve and the solution becomes more transparent, giving decrease of the OD. The described

dependence of the OD on concentration of the detergent is schematically shown in fig. 3.8. A peak of optical density is seen. This peak indicates the concentration of the detergent at which liposomes are saturated with detergent molecules. This concentration is chosen for protein incorporation.

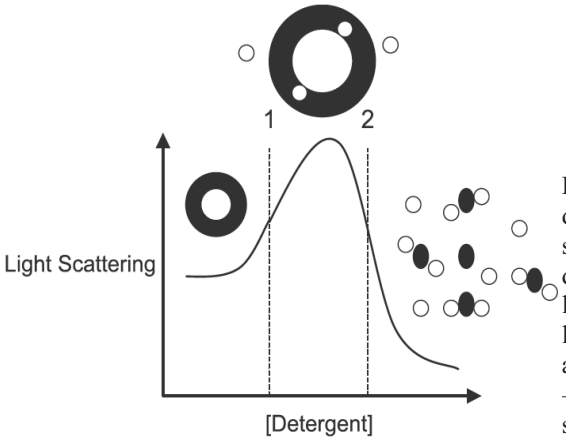

Figure 3.8: A diagram showing the dependence of light scattering in liposome suspensions on the concentration of detergent. The region between the dotted lines 1 and 2 estimate transition between liposomes and micelles. The liposomes are shown as thick black circles, micelles – as black dots, detergent molecules – as small white circles. Figure from Seddon et al. [126].

3.3 Optical methods

3.3.1 Microscopy

In the present work optical observation of lipid bilayers and cells where done. The cells where pictured using phase contrast microscopy and, after staining, using fluorescent microscopy. Lipid bilayers, stained with fluorescently labelled lipids were also observed using fluorescent microscopy. Several microscopes were used: Axiovert, Axio Scope and Apotome from Carl Zeiss GmbH. Axiovert is an inverted microscope – was used in the phase contrast mode for observations and making pictures of cells during their growth, as it allows observation from the bottom of the cell culture dish without necessity of insertion of the objective into cell culture medium which would introduce contamination. Axio Scope - an upright microscope - was used mostly for fluorescent observations of bilayers and bleaching experiments, as it is coupled with 473 nm laser (Rapp OptoElectronics). Apotome was used for high quality imaging of fluoresently labelled cells and bilayers.

3.3.2 Fluorescence recovery after photobleaching (FRAP)

Fluorescence recovery after photobleaching (FRAP) is a method of observing and quantifying diffusion [128], [129]. It is usually used for two dimensional systems such as molecular layers, SLB or cell membranes of living

cells [130–132]. The idea of this method is presented in fig. 3.9.

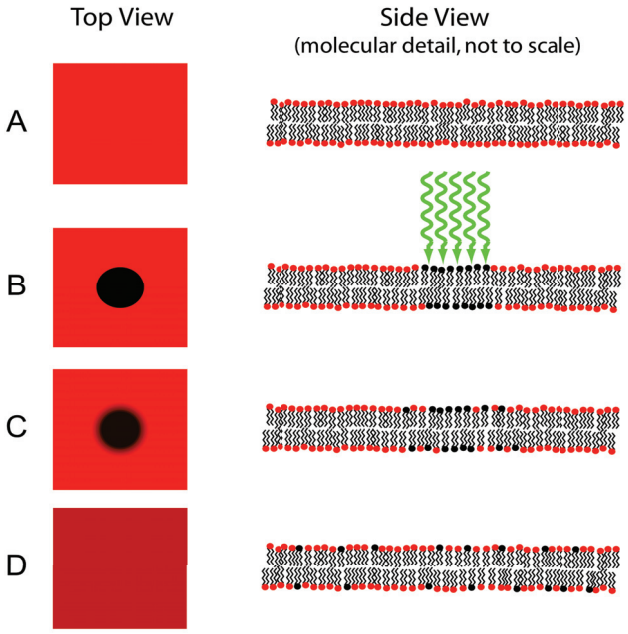

Figure 3.9: A schematic representation of FRAP in the lipid bilayer. Initially, fluorescently labelled lipid molecules are distributed uniformly (A). A spot is bleached by laser light(B). Due to diffusion bleached molecules move outside of the bleached area, while emitting light molecules move inside (C). Uniform distribution of bright and bleached molecules is set and the dark spot disappears (D). Figure from [133]

Fluorescently labelled molecules have to be presented in the system. A spot is usually bleached in the sample by laser or by switching to a higher magnification objective. The fluorophores in the area of this spot are bleached and produce no more fluorescence. Due to Brownian motion in the plane of the sample the bleached molecules move out of the bleached area while light emitting molecules move into the bleached spot. This process makes the edges of the spot less sharp and finally leads to disappearing of the spot.

Observing these changes one can calculate the diffusion coefficient of the labelled molecules. Classical approach was introduced in the pioneering work of Axelrod [128]. It is based on several assumptions. Firstly, no diffusion is assumed during the bleaching process. Secondly, an assumption about the shape of the intensity profile of the bleached spot is done. Usually, a circular bleached area with the Gaussian profile for the fluorescence intensity is assumed (as the intensity in the laser beam usually has Gaussian distribution). Under these conditions fluorescence recovery in the centre of the spot is described by the formula [129]:

$$f(t)=\sum_{n=1}^{\infty}\frac{-k^n}{n!}\frac{1}{1+n(1+\frac{2t}{\tau_D})} \tag{3.1}$$

where *f(t)* is normalized fluorescence intensity, *k* is the bleached constant which is the measure of the amount of fluorescent molecules that are bleached, τ_D is the characteristic diffusion time that is related to the diffusion coefficient by:

$$\tau_D=\frac{w^2}{4D} \tag{3.2}$$

where *w* is defined as a half of the width of the Gaussian intensity profile determined at e^{-2} times the height of the profile, *D* is the diffusion coefficient. Thus, measuring *f(t)* and calculating τ_D from the formula (3.1), one can find the diffusion coefficient using formula (3.2).

Although this approach is widely used, the assumption it requires are not always valid. At least, special experimental conditions should be provided ensuring special shape of the initial intensity profile. To avoid these difficulties other methods of analysis of the FRAP data were introduced based on numerical simulations of the diffusion process [134]. Numerical methods allow high flexibility of experimental conditions as almost any shape of the bleached spot and any intensity profile can be analyzed. At the same time, numerical methods require higher computational power and sophisticated algorithms.

Meanwhile, analytical analysis of the recovery after photobleaching is possible even without assuming Gaussian or any other special form of initial profile of the fluorescence intensity. Solution of the Dirichlet problem based on Fick's second law (equations (1.16) or (1.17)) is possible using, for example, Hankel's transform [135]. The only requirement is the circular symmetry of the bleached spot. Similar approach was utilized in the present work, although the differential equation was solved by the variable separation method [136]. First, the image taken before the bleaching procedure was subtracted from all subsequent images to compensate uneven illumination. The equation for the Fick's second law (1.17) was rewritten in the polar coordinate system. A Dirichlet problem then was set up using intensity profile of the first image as the initial condition and intensity on the border of the area under consideration as the boundary condition, such that:

$$\begin{aligned}&\frac{\partial u}{\partial t}=D\left(\frac{\partial^2 u}{\partial r^2}+\frac{1}{r}\frac{\partial u}{\partial r}\right)\\&u_{t=0}=u_{expl}(r)\\&u_{r=r_0}=1\end{aligned} \tag{3.3}$$

where *u* is normalized intensity, *D* – diffusion coefficient, *r* – distance from the centre, r_0 – radius of the area under consideration, *t* – time, u_{expl} – experimental

profile of intensity at the first point of time. Using the method of separation of variables one can find analytical solution for this problem:

$$u(r,t)=\sum_{m=1}^{\infty} C_m J_0\left(\frac{\mu_m^{(0)}}{r_0} r\right) e^{-D\left(\frac{\mu_m^{(0)}}{r_0}\right)^2 t} \tag{3.4}$$

where C_m is defined as:

$$C_m=\frac{2\int_0^{r_0} u_{exp1}(r) J_0\left(\frac{\mu_m^{(0)}}{r_0} r\right) r dr}{r_0^2 J_1(\mu_m^{(0)})^2} \tag{3.5}$$

where J_0 is the zero order Bessels function, J_1 – first order Bessel function, $\mu_m^{(0)}$ – nulls of the zero order Bessel function.

A fitting procedure similar to the one described in [134] was used to find such a value of the diffusion coefficient that the analytically calculated curves fit the experimental ones. Generally, this procedure is the least squares method based on the minimization of the sum of squared residuals:

$$S=\sum_{i=1}^{m}\sum_{j=1}^{n}(u_{\exp i,j}-u_{i,j})^2 \tag{3.6}$$

where $u_{i,j}$ is the value of normalized intensity analytically calculated using the formula (3.4), $u_{exp\ i,j}$ is the experimental value, i and j are the indexes for time and the spatial coordinate. A guess about the value of the diffusion coefficient is made. This value is used to calculate the distribution of intensity and then S. Then, a minimization algorithm was used to find the value of D corresponding to the minimum S. Initial value was chosen around 1 um^2/s according to literature data [109], [137].

Data processing was performed by custom developed Matlab based software. The code can be found in Appendix C.

3.4 Cell culture

3.4.1 Preparation and plating of neurons

Primarily neuronal cell culture was used in this study. Although primarily culture is considered to be more difficult to run than cell lines, it has also some advantages. The cells of the primarily culture are more natural as they were not modified in a process of "immortalization". Another advantage is that neurons, as used in this work, do not proliferate and the number of cells do not increase. Generally, they are less active and the probability that these cells destroy a soft substrate, like the SLB, is lower.

Rat embryonic cortical neurons were prepared as described in [138]. The

exact protocol can be found in Appendix B. Briefly, embryos were recovered from pregnant Wistar rats at 18 days gestation (E18). Cortices were dissected from the embryonic brains; cells were mechanically dissociated in cold HBSS− (without $Ca2^{+}$ and $Mg2^{+}$) with a fire polished, silanized, glass pipette.

One volume of cold HBSS+ (with $Ca2^{+}$ and $Mg2^{+}$) was added to the dispersed cells. Non-dispersed tissue was allowed to settle for 3 minutes, then the supernatant was centrifuged at 200g for 2 minutes. The pellet was resuspended in neurobasal medium containing 1% B27, 0.5 mM L-glutamine and 50 ug/ml gentomicin.

An aliquot was diluted: 1 part of cell suspension, 2 parts of neurobasal medium and 1 part of trypan blue. Dye-excluding cells were counted in a Neubauer counting chamber. The remaining cells were diluted in neurobasal medium with the above supplements and plated onto the substrates. Half of the medium was changed 4 hours after preparation and subsequently every 3–4 days.

3.4.2 Preparation of poly-L-lysine coated glass

Polylysine surface coating is widely used for cell culture to increase adhesion of cells. Polylysine is a small natural homopolymer of the essential amino acid lysine (the structure of the molecule is shown in fig. 3.10). This molecule possesses positive charge which is probably the reason for cell to adhere to polylysine coated surface. There are two forms of polylysine: poly-L-lysine (PLL) and poly-D-lysine (PDL). PDL is considered to be more stable as it consists of D-form of lysine, which is not natural and can not be consumed by cells. However, PLL also appeared to be stable enough to maintain cell culture for many weeks. In this work PLL was used.

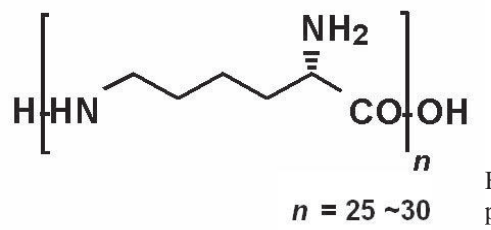

Figure 3.10: Chemical structure of the poly-L-lysine

Coating of the substrates was done by application of PLL dissolved in Gay's phosphate buffer saline (GBSS). After incubation, the samples were washed in GBSS and kept at 4°C overnight. The exact protocol can be found in Appendix B.

3.4.3 Cell counting and staining

Cells were counted on images made using phase contrast or fluorescent microscopes. Counting was done using ImageJ software with CellCounting plug in. This software provides the way of manual counting of objects on images by clicking them. Automatic counting seems to be difficult (or even not possible)

All available programs for automatic counting didn't show reliable results.

Although for most cases it was easy to distinguish live and dead cells on phase contrast images, to be sure that only live cells were counted, and to clearly visualize neurites, the live-dead staining procedure was performed. Live cells were stained with calcein-AM, ans dead cells – with ethidium homodimer. Calcein-AM is an acetomethoxy derivative of a fluorescent dye calcein (also known as fluorexon, fluorescein complex). The acetomethoxy group blocks binding of Ca^{2+}, Mg^{2+} and other ions which are necessary for fluorescence of calcein. When it passes through the cell membrane, acetomethoxy group is removed by intracellular esterases, giving rise to greed fluorescence (fig. 3.11). As dead cells does not contain esterases, calcein-AM does not emit light in them.

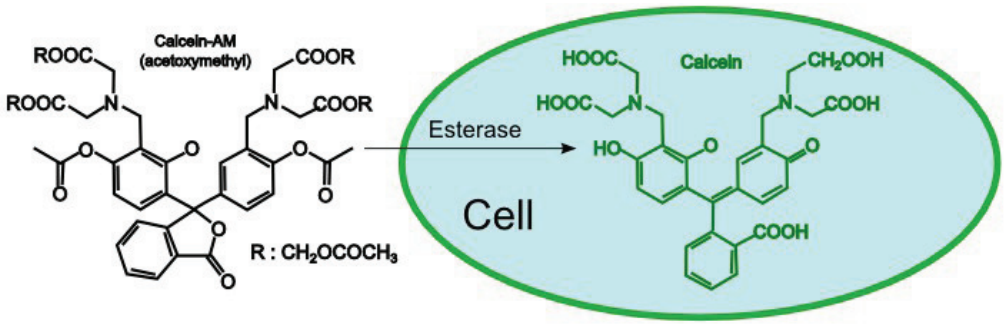

Figure 3.11: The chemical structure of calcein-AM as produced (left) and in the cell after the activity of intracellular esterases (right).

Ethidium homodimer is a membrane-impermeable fluorescent dye which binds to DNA. The membranes of dead cells are damaged, thus, ethidium homodimer can access DNA of these cells and emit light upon excitation. An example of live-dead staining is shown in fig. 3.12.

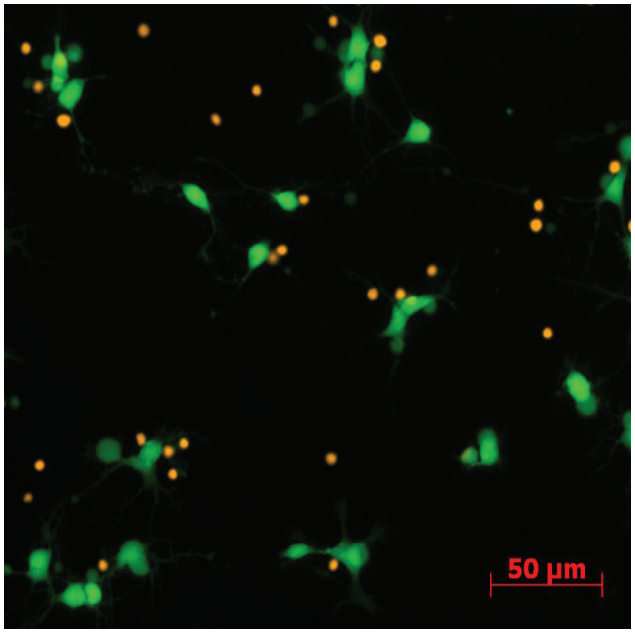

Figure 3.12: An example of staining of live cells with calcein-AM (green fluorescence) and dead cells with ethidium homodimer (red fluorescence). Neurons of DIV1 are shown.

3.5 QCM-D

The quartz crystal microbalance (QCM) is a nanogram sensitive technique that utilizes acoustic waves generated by oscillating a piezoelectric, single crystal quartz plate to measure mass [139]. The basis of QCM operation relates to quartz's inherent property of piezoelectricity. By applying alternating electric fields to quartz, an alternating expansion and contraction of the crystal lattice is induced. In today's most common QCMs a circular piece of quartz is sandwiched between two metal electrodes (fig. 3.13(A)). Resonance is excited when a sufficient AC voltage is applied with a frequency close to the resonant frequency (f_0) of the particular crystal (fig. 3.13(B)). The resonant condition of the QCM occurs when the standing wave produced by the alternating expansion and contraction is an odd integer of the thickness of the quartz plate. Resonant frequencies of typical QCMs are on the order of MHz and the tradeoff between the frequency (relating to sensitivity) and the thickness (relating to usability) of QCMs is that the higher the resonant frequency, the thinner the crystal. The common frequency (f_0) of 5 MHz has a corresponding thickness of ~ 330 um. QCMs became widely used as mass balances only after the theory and experiments, relating a frequency change of the oscillating crystal to the mass adsorbed on the surface, was demonstrated by

Sauerbrey in 1959 [140]. This linear relationship between frequency change (Δf) and mass adsorbed (Δm) is given by:

$$\Delta m = \frac{C}{n} \Delta f \tag{3.7}$$

where n is the harmonic number and

$$C = \frac{t_q \rho_q}{f_0} \tag{3.8}$$

with t_q being the thickness of quartz, and ρ_q being the density of quartz and equals ~ –17.7ng/(Hz cm^2) for a 5-MHz crystal.

There are three assumptions that must be fulfilled for the Sauerbrey relationship to hold. First, the adsorbed mass must be small relative to the mass of the quartz crystal; second, the mass adsorbed is rigidly adsorbed; and third, the mass adsorbed is evenly distributed over the active area of the crystal. This frequency/mass relationship was, in the early days of QCM, almost exclusively used in vacuum or gas phase for monitoring of metal plating in vacuum deposition systems. Liquid application of QCM technology expanded the number of potential applications, dramatically including biotechnology applications and in particular biosensor applications. The drawback of applying the QCM to many liquid applications was that the liquid phase often incorporated viscous and elastic contributions to the frequency change and thus violated the assumption of the Sauerbrey relation stating that the mass adsorbed must be rigidly adsorbed. This prompted new approaches for characterizing mass deposits with frictional dissipative losses due to their viscoelastic character. This approach, QCM with dissipation monitoring (QCM-D), fits the voltage of oscillatory decay after a driving power is switched off in such a way as to ensure that the quartz decays close to the series resonant mode. The amplitude decays over time depending on the properties of the oscillator and the contact medium (fig. 3.13(C)). The decay voltage, i.e., the output voltage amplitude as a function of time, with a frequency given by the resonant frequency of the quartz crystal (f_0), is mixed with a reference frequency (f_R) and filtered with a low pass band filter. This gives an output

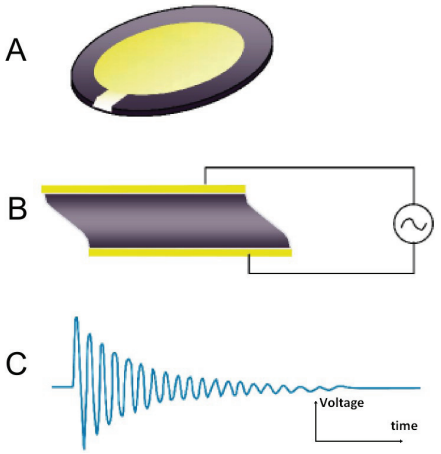

Figure 3.13: (A) A circular piece of quartz is sandwiched between two metal electrodes used for QCM-D. (B) A schematic representation of mechanical oscillations in the quartz crystal by application of variable voltage. (C) The decay of the amplitude of the oscillations over time after switching of voltage.

frequency (f) based on the difference between f_R and f_0. This difference frequency is fit to an exponentially damped sinusoidal, A(t), according to:

$$A(t)=A_0 e^{t/\tau}\sin(2\pi f t+\alpha) \tag{3.9}$$

where $f = f_0 - f_R$. The dissipation parameter is given by

$$D=\frac{1}{\pi f \tau} \tag{3.10}$$

and is dimensionless, defined as

$$D=\frac{1}{Q}=\frac{E_{dissipated}}{2\pi E_{stored}} \tag{3.11}$$

with Q being the quality factor, $E_{dissipated}$ being the energy dissipated during one oscillatory cycle and E_{stored} being the energy stored in the oscillating system.

A typical response of frequency and dissipation on protein adsorption (human serum albumin), antibody binding to it and it's further redistribution after washing is shown in fig. 3.14.

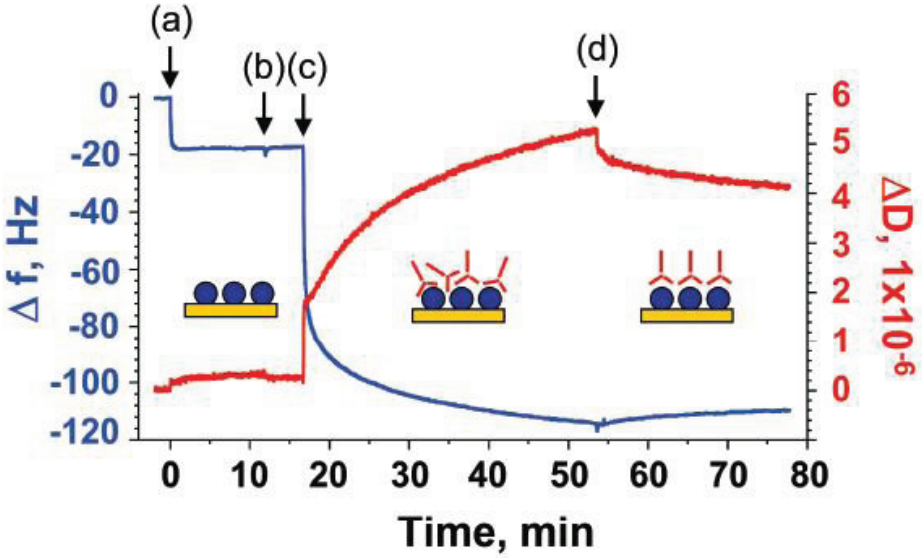

Figure 3.14: The adsorption of human serum albumin (a) and an antibody for human serum albumin (c). Steps b and d correspond to buffer rinses. Frequency changes (Δf) are shown in blue, and dissipation changes (ΔD) are shown in red. The frequency change of step (a) and lack of dissipation change indicating the rigid characteristics of the human serum albumin film as it adsorbs on the surface. In contrast, the adsorption of the antibody at (c) gives a large frequency and dissipation change, indicating both mass adsorbed and increased viscoelastic characteristics due to the incorporation of water [139].

In the present work QCM-D was used for characterization of the SLB and testing the conditions of the blayer formation such as time of incubation of the liposomes on the SiO_2 surface. Q-Sense E4 device was used [141]. Measurements

were carried out at the Department of biological physics, Chalmers university of technology, Göteborg, Sweden.

3.6 Nanoparticle Tracking Analysis

Nanoparticle Tracking Analysis is a method to detect and visualize populations of nanoparticles in liquids and to measure the size of each particle from direct observations of diffusion. This particle-by-particle methodology goes beyond traditional light scattering and other ensemble techniques in providing high-resolution particle size distributions [142].

Usually a conventional microscope is used and particles in suspension are illuminated by a laser (fig. 3.15). The average distance each particle moves in x and y in the image is calculated. From this value the particle diffusion coefficient, D_t, can be obtained. Knowing the sample temperature T, and solvent viscosity η, the particle hydrodynamic diameter d can be identified. Three dimensional Brownian movement is tracked only in 2 dimensions (x and y) and accommodated by use of the following variation of the Stokes-Einstein equation:

$$\overline{(x,y)}^2 = D_t = \frac{kT}{3\pi\eta d} \tag{3.12}$$

where k is Boltzmann's constant. Simple review of the technology can be found in [143].

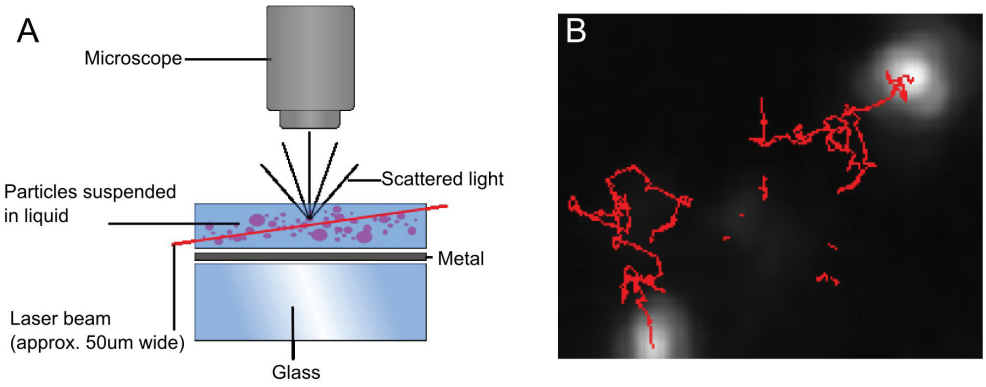

Figure 3.15: (A) A schematic representation of the set up for Nanoparticle Tracking Analysis [142]. (B)An enlarged image of typical tracks of particles moving under Brownian motion. Note: the particles are not being imaged, structural information, such as shape of the particle is below the resolving power of the optical microscope used [143].

In this work the nanoparticle tracking analysis method was utilized to measure the size of the SUV. For this purpose a Nanosigh LM10 instrument from Nanosight,Ltd was used. This device is based on a conventional optical microscope and uses a laser light source to illuminate nano-scale particles within a

0.3 ml sample introduced to the viewing unit with a disposable syringe. Enhanced by a near perfect black background, particles appear individually as point-scatterers moving under Brownian motion [142]. Measurements were carried out at the Department of biological physics, Chalmers university of technology, Göteborg, Sweden.

3.7 Patch-clamp

Electrophysiological recordings from neurons in culture were carried out in this work using patch-clamp technique. This technique allows to record current through the whole cell membrane or patches of it, as well as potential in the cell. It was introduced by Sackmann and Neher in 1970th for measurements of single channel currents [144] and later developed by Hamill [145]. Since that time patch-clamp is considered to be one of the most powerful techniques of single cell electrophysiology. This method has been described in a number of books [146–148].

A glass micro pipette filled with electrolyte solution with the diameter of the opening of around 1-2 um is used for recordings (fig. 3.16(A) shows the tip of a patch-clamp pipette). Such an electrode usually has resistance around 4-10MOhm. This pipette is brought to the vicinity of the cell using the micromanipulator which can provide motion with submicrometer steps. Positive pressure is applied through the pipette to avoid clogging of the tip while moving the pipette in the solution.

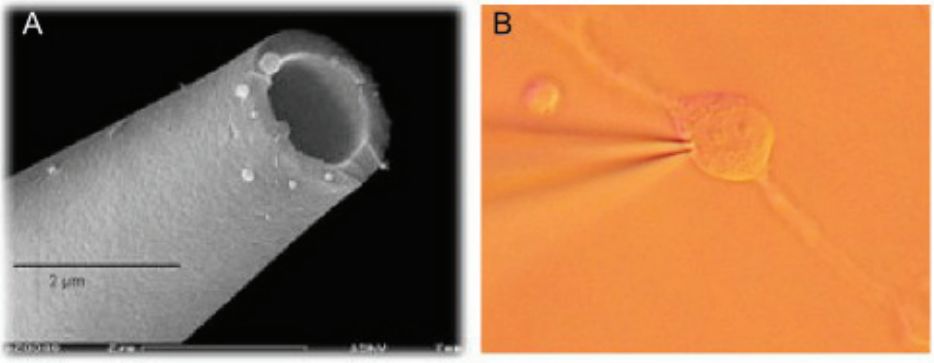

Figure 3.16: (A) An electron microscopy image of the tip of a glass micropipette used for patch-clamp [149]. (B) A micropipette touching a cell during a patch-clamp experiment

As soon as the tip of the pipette touches the cell membrane, (fig. 3.16(B)) which is indicated by a slight drop of the measured resistance, positive pressure is released and slight suction is applied. This usually leads to formation of a sealed

contact between the tip and the cell membrane which has leak resistance in gigaohm range. This is one of recording modes of patch-clamp called the *cell-attached* mode (fig. 3.17(A)). In this mode currents through a single ionic channel (or a group of channels) trapped in the tip of the pipette can be measured. From this mode all the other modes are archived. If one apply brief and strong suction through the pipette, the membrane patch in the tip can be broken and the connection between the pipette and the interior of the cell can be established. This is the *whole-cell* mode (fig. 3.17(B)). It can be used for recording currents through the whole membrane of the cell while clamping potential inside the cell or for measuring intracellular potential while clamping current through the membrane. This mode is most commonly used in electrophysiological experiments. It has many advantages as it is relatively easy to archive, recorded currents are high (in the range of hundreds of pA) and the whole cell is used for the recordings allowing to study not only ionic channels of the cell membrane but also influence of some intracellular processes on them. At the same time there are also problems, such as difficulties with clamping potentials in big or long cells (space clamp problem). Another problem is washing out of intracellular components (organelles, etc) through the pipette. This problem is solved by using so called *perforated patch*. It is achieved from cell-attached mode by adding special ionic transporters or channels (gramicidin, amphothericin-B, nystatin) in the pipette. These channels incorporate in the membrane area clamped in the tip creating electrical contact between the pipette and interior of the cell. At the same time the membrane stays impermeable for big intracellular components.

From the cell-attached mode another mode, called *inside-out*, can be achieved (fig. 3.17(D)). To establish this mode the pipette is moved away from the cell while keeping contact with the membrane. A patch of the membrane is detached usually forming a vesicle on the tip. After exposure to air this vesicle is broken giving a possibility to record the current through the channels trapped in the tip. As the inner part of the membrane is now exposed to extracellular medium this mode is called inside-out. If the pipette is puled away from the cell being in the whole-cell mode, a patch of the membrane which is detached from the cell is placed in such a way that its outer side is faced to the extracellular solution. This mode is called *outside-out* (fig. 3.17(C)). Inside-out and outside out modes are used for single channel recordings and allow to control medium composition at the inner or outer parts of the membrane.

In the present work patch clamp was used for testing electrophysiological activity of neurons growing on positively charged SLBs (Chapter 4) and on SLBs with incorporated ephrin A5 (Chapter 5) . The recordings were done in the whole-cell mode using HEKA EPC9 amplifier. Both currents through the membrane (while clamping potential across the membrane) and transmembrane potentials (while clamping currents) were recorded.

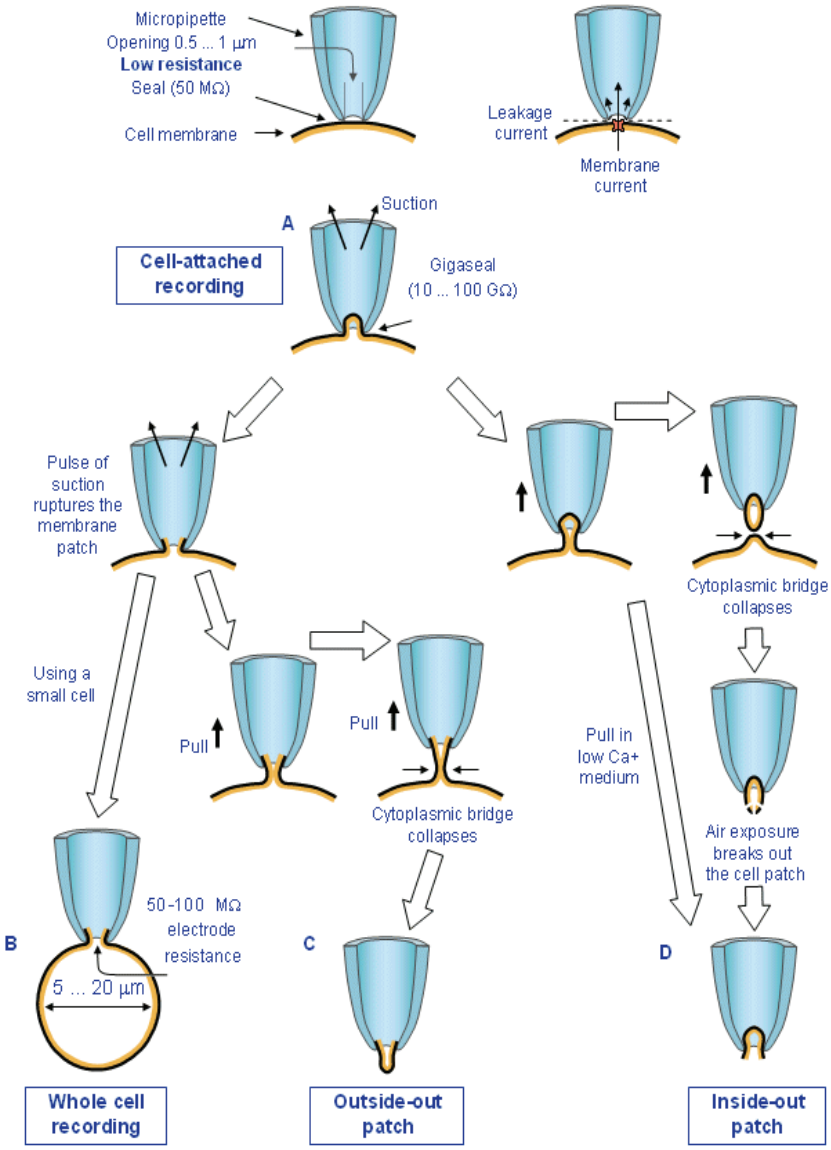

Figure 3.17: Modes of patch-clamp. See details in the text. Modified from [148].

3.8 Immunofluorescence of the lipid bilayers

The purpose of immunofluorescence is to detect the location and relative abundance of any protein for which an antibody is available [150]. This technique uses the specificity of antibodies to their antigen to target fluorescent dyes to specific biomolecule targets, and therefore allows visualisation of the distribution of the target molecule through the sample [151].

There are two classes of immunofluorescence techniques: primary (or direct) and secondary (or indirect). Primary immunofluorescence uses a single antibody that is chemically linked to a fluorophore. Secondary, immunofluorescence uses two antibodies; the unlabeled primary antibody specifically binds to the target molecule, and the secondary antibody, which carries the fluorophore, recognizes the primary antibody and binds to it (fig. 3.18). Multiple secondary antibodies can bind a single primary antibody. This provides signal amplification by increasing the number of fluorophore molecules per antigen. This protocol is more complex and time consuming than the primary (or direct) protocol, but it allows more flexibility because a variety of different secondary antibodies and detection techniques can be used for a given primary antibody [151].

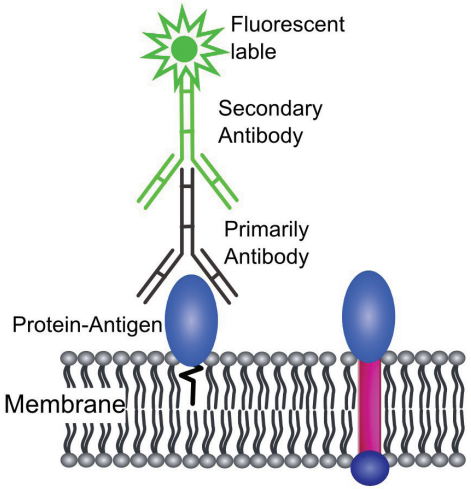

Figure 3.18: Representation of secondary (indirect) immunofluorescence. Unlabeled primarily antibody binds to its target protein. Then, a secondary antibody, which is specific for the primarily one, attaches to it. The secondary antibody carries a fluorescent label, which allows visualization of the distribution of the target molecule.

In this work secondary immunofluorescence was used. The primarily antibody was ephrin Ab-Goat IgG. It was dissolved in PBS and applied to the SLB with ephrin A5. Blocking of nonspecific binding sites by bovine serum albumin (or another protein) is usually used before application of the primarily antibody. But in the case of the SLB made of POPC this step appeared to be not necessary as such type of the SLB was protein repellent. Staining procedures with and without blocking were carried out and no differences were found. The sample was rinsed

gently with PBS after 1h of incubation at room temperature. Secondary antibodies (Alexa Fluor® 488 donkey anti-goat IgG (H+L)) were applied and incubated for 1h at room temperature. After that, the sample was gently rinsed again with PBS and used for fluorescent microscopy. The exact protocol of the staining procedure can be found in Appendix B.

3.9 Preparation of GUV

Giant unilamellar vesicles (GUV) are lipid vesicles that have size 10-100um. They are big enough to easily see them in an optical microscope and to move them with micromanipulators using micropipettes. The are many methods of producing GUV such as gentle hydration [152–155], freeze-and-thaw [156], [157], solvent evaporation [158], [159], emulsion based methods [160] or using hydrogels [161]. In the present work the method of electroswelling [162] was used. This method provides fast and stable way for producing GUV. Usually this method involves drying of lipids on the surface of plates made of conductive material (platinum, indium tin oxide (ITO), etc.). These plates are then placed opposite to each other and the gap between them is filled with an aqueous solution. Solution is usually not electrolyte solution but solution of sugars such as sorbitol or glucose. Glucose solution was used in this study. Alternative voltage is applied to the plates which promotes swelling of lipid sheets and formation of vesicles.

The Vesicle Prep Pro device from Nanion technologies was used. The device provides possibilities to easily vary electroswelling protocol parameters such as the amplitude and the frequency of the applied alternative voltage, temperature, duration of the procedure, rise time and fall time of the amplitude, of the voltage to achieve the best output of the GUV(s) of the desired size. Two ITO covered glass slides were used as electrodes. The transparent electrodes provide the possibility to observe the process of electroformation using optical microscope. Lipids were dried on the surface of one of the slides, a rubber ring was placed around dry lipids and filled with sugar solution. Then the second slide was put on the top. The slides were mounted into the device and alternating voltage was applied (fig. 3.19).

Base protocol of the device was modified by increasing the rise and fall time of the voltage as well as the duration of the whole procedure. This was done to make the procedure more stable as sudden changes can lead to destruction of the GUV(s). The exact protocol can be found in Appendix B.

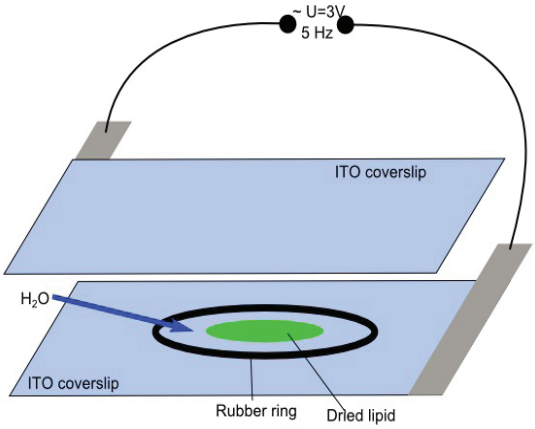

Figure 3.19: A schematic representation of the set up for GUV electroformation. Lipids are dried on the surface of an ITO coated glass slide. Aqueous solution is added inside the rubber ring used to seal the system. The second ITO slide is mounted on the top and alternative voltage is applied to the slides.

3.10 Protein microcontact printing

Microcontact printing is a technique for producing micropatterns on a surface by printing using stamps [163–165]. The stamps are usually produced form a polymer, such as PDMS, by moulding in a solid template (master mould). The master mould is usually produced from Si, SiO2, glass, metals by photolithography (electron beam lithography, etc.). Inks are put on the polymer stamp, dried and then the stamp is applied to the surface leaving inks in some places defined by the structure of the stamp (fig. 3.20(A)). Alternatively, inks can be put onto the flat surface of polymer and the master stamp is applied to it. After lifting off the polymer, a pattern of ink stays on it. This pattern can be then transferred onto the surface (fig. 3.20(B)).

Microcontact printing is widely used in the area of the lifescience for creating patterns of proteins, self-assembly monolayers, DNA, other biologically relevant molecules. This technique can be applied, e.g., to patterned substrates for cell culture or for axon guidance [115], [166], [167].

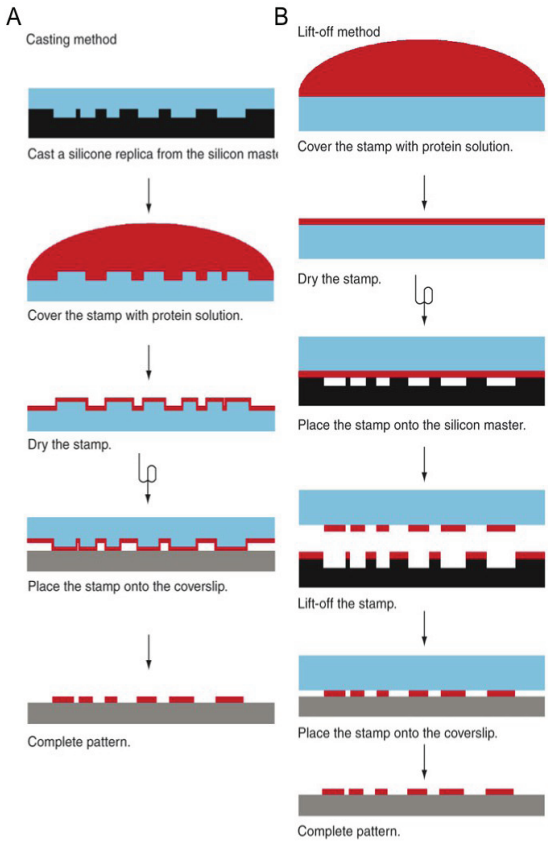

Figure 3.20: Two methods of micro contact printing [182]. (A) The casting method. A stamp is made by casting a silicon replica and then covered by ink. After drying the ink, the stamp is placed onto the substrate. (B) The lift-off method. Ink is dried on the surface of a polymer plate. Then the plate is placed on the silicon replica and after lift-off a pattern stays on the polymer. Then this pattern is transferred onto the substrate.

In the present work microcontact printing was used to create a grid on the glass surface. This grid was made of PLL and was used to create patterned SLB. The master stamp was made of Si by photolithography. It consisted of squares with diagonals. The size of the square was 100 um. The master stamp was silanized (Trichloro(1H,1H,2H,2H-perfluorooctyl) silane was used in the present work) before casting to ensure removal of the polymer stamp. PDMS was used as a material for the stamps. It was poured onto the master wafer and left overnight at 60°C to polymerize. Before applying protein ink the stamps were treated in SDS solution to create a sacrificial layer on the surface and facilitate detachment of the protein. PLL at the concentration of 10 ug/ml was applied to the stamps and dried. Then the stamps were carefully placed onto the substrate and a weight of around 10g was put on it for 3-5 min. Precautions were made while removing stamps to prevent smashing of the printed lines. The exact protocol of the printing procedure can be found in Appendix B.

Chapter 4

Characterization of liposomes and SLBs

Measure seven times before cutting once

A Russian proverb

4.1 Characterization of liposomes

Lipid vesicles were prepared using the extrusion through a polycarbonate membrane with the pore size 100 nm. Size of lipid vesicles was measured using nanoparticle tracking method which implies tracking of individual particles in the suspension and calculation their size using the Stokes-Einstein equation (equation 3.12, Section 3.6). Totally 2653 tracks of vesicles were analyzed using the software provided by Nanosight, Ltd. The distribution of size appeared to be relatively wide (fig. 4.1). Maximum of the peak of the distribution lies around 200 nm. Most of the vesicles were lager than 100 nm (92% of total amount). The biggest found vesicles were around 500 nm, the smallest – around 50 nm. This reflects the soft nature of the liposomes: they can be stretched or distorted, change their shape to pass through a hole smaller than their size. The size of the prepared vesicles appeared to be larger than the size of the vesicles produced by sonication (15-50 nm) [168]. But, as can be seen from the following sections, achieved size is small enough for vesicles to rupture and fuse on the surface forming uniform bilayer.

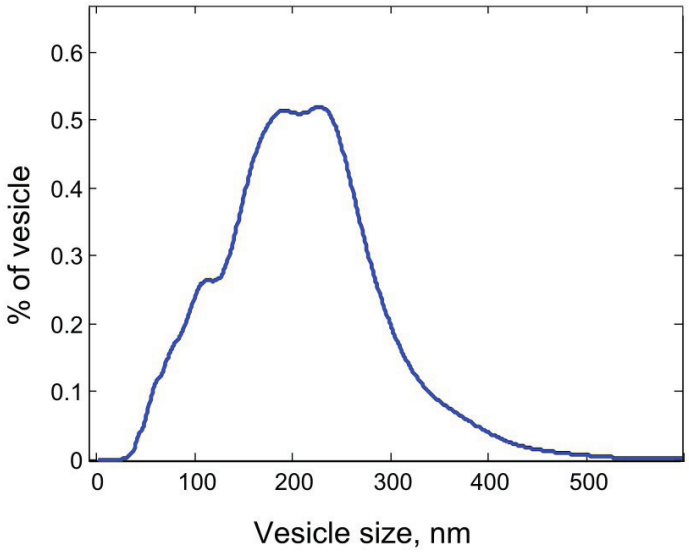

Figure 4.1: Distribution of size of POPC vesicles produced by extrusion through 100 nm membrane as measured by particle tracking analysis. Total number of measured vesicles was 2653.

4.2 Characterization of the SLB

4.2.1 QCM-D measurements

QCM-D is an advanced technique which allows to monitor adsorption of vesicles on the surface, their rupturing and SLB formation. It provides possibility not only to measure adsorbed mass (which is indicated by change of the resonance frequency) but also to investigate rigidity of the layer (by monitoring dissipation).

Typical changes of the resonant frequency and dissipation during formation of the SLB monitored by QCM-D is shown in fig. 4.2. The vesicles were prepared of POPC and extruded though 100 nm membrane and then, additionally through 30 nm membrane. After addition of liposomes frequency initially decreased as the vesicles are accumulated on the surface. Dissipation becomes higher indicating formation of a soft layer. After some time a critical concentration of vesicles is achieved and they start to rupture and fuse building the SLB. The frequency decreased because of the water release from the vesicles and the decrease adsorbed mass. The value of dissipation also decreased because the thickness of the formed the SLB became lower than the thickness of a layer of adsorbed liposomes.

In fig. 4.2A, B frequency and dissipation changes respectively are shown

during the SLB formation under the flow conditions (vesicle suspension is constantly pumped at the rate of 100 ul/min through the QCM-D chamber). In this case formation of the SLB takes around 3 minutes. When the flow is stopped this process takes much longer time – around 15 minutes (fig. 4.2C, D). At this condition there is no constant supply of vesicles but the number of liposomes contained in the volume of the chamber (around 100 ul) appeared to be enough to reach the critical concentration on the surface which promotes vesicles rupturing and bilayer formation. Thus in the case of preparing the SLB in the Petri dish, as was done in the present work for testing SLBs with neuronal cell culture, incubation times longer than 15 minutes should be used.

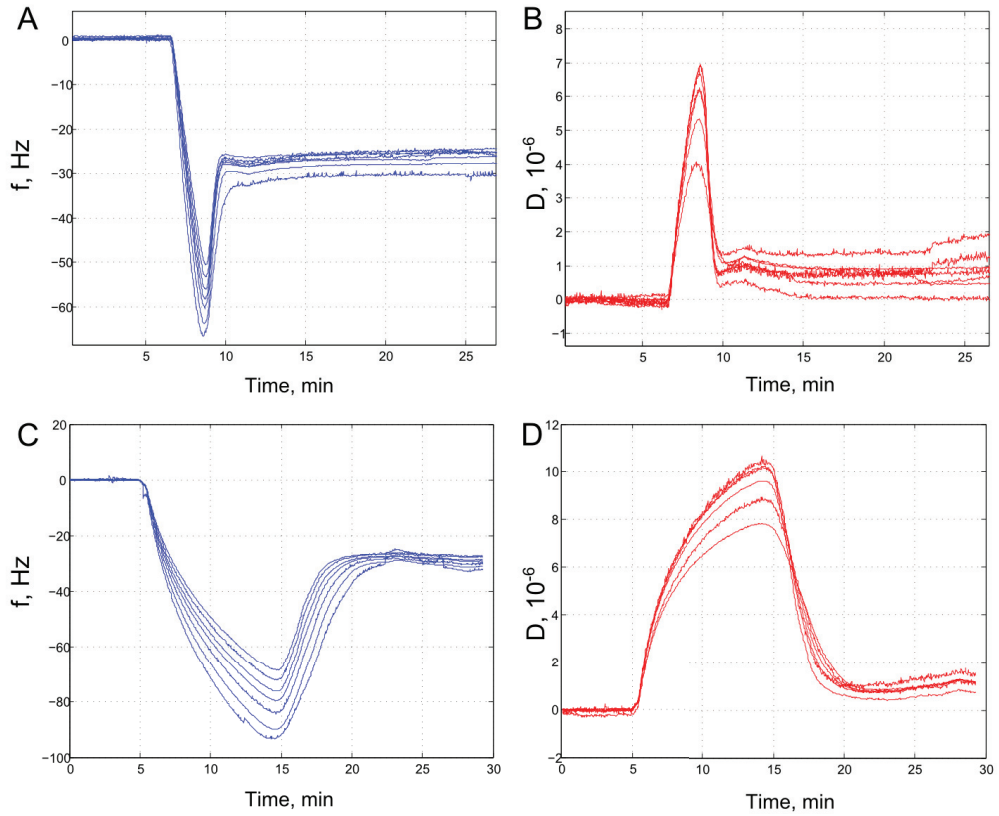

Figure 4.2: Changes of frequency (A, C) and dissipation (B, D) measured by QCM-D during deposition of POPC liposomes and following formation of the SLB. The multiple curves in each graph are responses measured for different overtones of the resonant frequency. The graphs A and B were recorded when the constant flow of liposome suspension through the measurement chamber was provided. The graphs C and D were recorded with no flow.

The final value of frequency change caused by formation of the bilayer was

almost the same in the both cases (with and without flow) and equals 27 Hz, which was in good agreement with literature data [169]. The same is true for dissipation, the final value of which appeared to be around $1 \cdot 10^{-6}$.

4.2.2 Observations using fluorescent microscopy

SLB(s) were prepared as described in chapter 3 (details can be found in appendix B). They contained fluorescently labeled lipids which provided a possibility to visualize them using fluorescent microscope. A typical image of a the SLB is shown in fig. 4.3. The bright area is the SLB, made of pure POPC and stained with NBD-PE. The dark area is glass. This area without the SLB appeared after exposure of it to air which destroys the SLB. The uniform fluorescence in the SLB indicates presence of the uniform layer on the surface. Bright dots, that are seen on the SLB, represent lipid vesicles that were not washed during washing procedure.

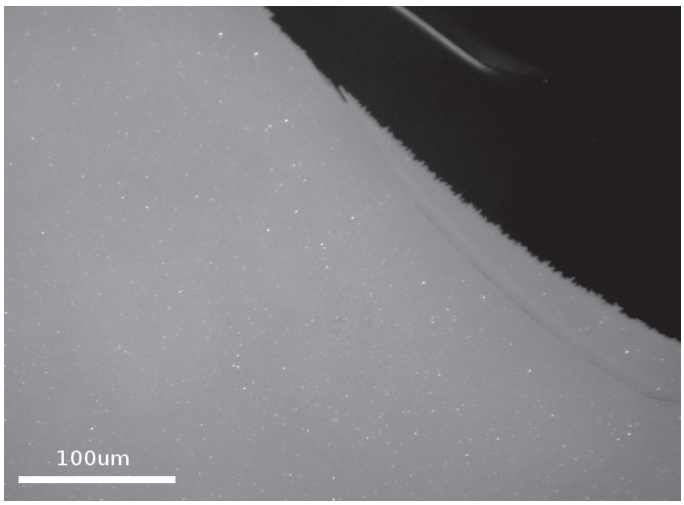

Figure 4.3: Fluorescent image of a SLB made of POPC and stained with NDB-PE.

4.2.3 FRAP

To check 2D fluidity of the prepared SLB, and to compare bilayers of different types, FRAP measurements were performed and the diffusion coefficients were calculated. A laser was used to bleach a small area of the bilayer and the recovery of the fluorescence was observed. The process of recovery is shown in fig. 5.6 for SLB(s) of different types. The bleached spots became blurred with time

and dissipated almost completely after several minutes for all SLB types.

The recovery, which is due to diffusion, was analyzed using Fick's second law (the method is described in chapter 3). The profiles of intensity at different time points were extracted from the images (fig. 4.5(A), blue curves) and the corresponding Dirichlet problem (eq. 3.2) was solved. The parameters of this solution were fit in such a way that the calculated curves match the experimental ones (fig. 4.5(A), red curves).

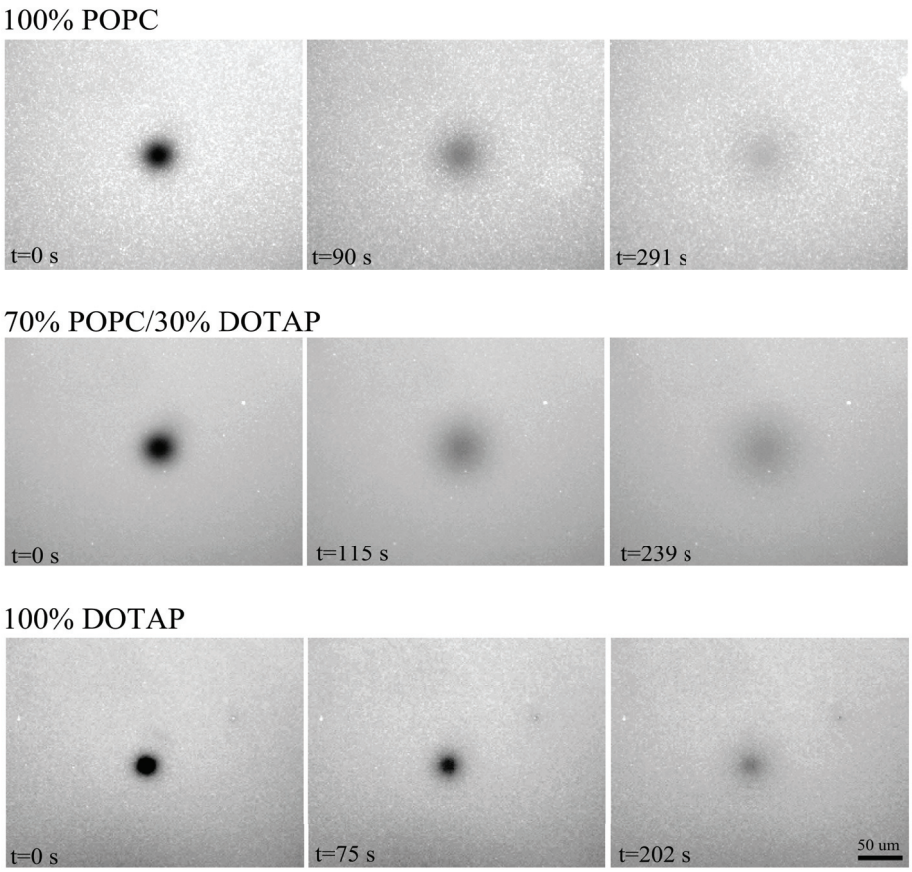

Figure 4.4: Time series of micrographs showing fluorescence recovery after photobleaching (FRAP) for a spot bleached in SLBs of different types. The scale bar is identical for all images.

The determination coefficient (R^2, the measure of the quality of a fit [170]) for most of the fits was higher than 0.90. Good fits prove that recovery was

mostly due to diffusion. The diffusion coefficient given by the fitting procedure for a pure POPC bilayer was 1.8 um^2/s, which is in good agreement with data from literature (for example 1.88 um^2/s [109]).

The diffusion coefficient was calculated for the SLB(s) containing different ratios of POPC and DOTAP. A decrease in the diffusion coefficient was observed with the increase in concentration of DOTAP. As shown in fig. 4.5(B), the diffusion coefficient decreases with increasing amounts of DOTAP in the mixed bilayer and reaches a value of 0.6 um^2/s for pure DOTAP bilayers, which is 3 times smaller than the value we determined for the SLB made of POPC only.

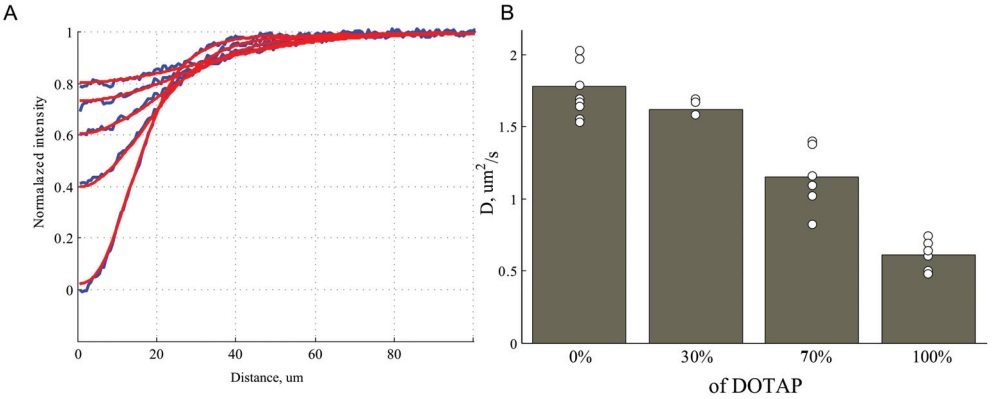

Figure 4.5: (A) Experimentally determined intensity profiles (blue curves) and a fit to analytical solutions of the diffusion equation (red) for the SLB made of 70%POPC/30%DOTAP. (B) Dependence of the diffusion coefficient on the concentration of DOTAP in the POPC/DOTAP mixed bilayers. The bars represent the average for each concentration. The circles represent single measurements.

Several explanations of this effect can be proposed: 1) This effect may arise from electrostatic interaction of the labeled lipids with positively charged lipid molecules which suppresses their mobility. 2) Another explanation of this dependence may be the increase in density of the lipid bilayer due to interaction of positively charged heads of DOTAP molecules with zwiterionic POPC molecules as described in literature [171]. Although, this effect may play a role only in the case of mixed SLB when positive charge of DOTAP can influence polar heads of POPC making them to be packed denser (fig. 4.6)

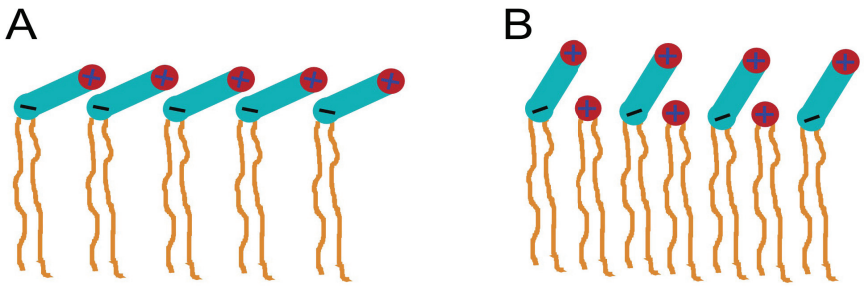

Figure 4.6: (A) The SLB made of zwitterionic lipids and (B) the SLB made of mixture of zwitterionic and positively charged lipids. Positively charged lipid molecules make the heads of the zwiterionic molecules stand vertically and occupy less space in the bilayer. This leads to denser packaging of the molecules. Modified from Zhang et al. [171]

3) It is also possible that positively charged lipids have stronger interactions with the negatively charged surface on which the bilayer is formed, making mobility lower. The Debye length, that can be calculated using formulas (1.14) and (1.10) (accepting an approximation of a symmetric monovalent electrolyte with the concentration 150mM), is equal to 0.8 nm which is in the order of magnitude of the thickness of the hydration layer between the surface and the bilayer (around 1 nm). Thus, electric field produced by the positive charges of the bilayer is not completely reduced by electrolyte at such low distance and can reach the surface. It makes the molecules to interact with the surface and can make their movement slower. 4) The structure of the fatty acid chains of DOTAP is different from that of POPC which can affect mobility of the labelled molecules. All these effects may act simultaneously.

Scattering of the magnitudes of the diffusion coefficient may be due to defects in the SLB(s) that introduce inhomogeneities, which could confound the computational approach based on the assumption of the uniform bilayer. Another reason for such scattering of results can be incomplete washing of liposomes that stay on the top of the bilayer and may locally slow down movement of the lipid molecules. The scattering is similar for all bilayer types which implies that if there are defects, they are similar for all types of the SLB.

Chapter 5

Positively charged SLB for neuronal cell culture

Seed the cells – crop the results

Alexey Yakushenko

5.1 Adhesion of neurons to charged SLB

5.1.1 Observations of neurons on charged SLB

SLBs made of different mixtures of POPC and DOTAP were prepared to test influence of positive charge on cell adhesion. SLBs were prepared within the PDMS wells as described in Chapter 3 (fig. 3.3). This method allows the preparation of different bilayers on one glass slide (usually complemented with one region covered by PLL as a control, which also ensures the right amount of growth factors excreted from cells in case the neuronal growth on SLBs was very limited). In addition, one can compare the effect of different surface coatings within one dish. The wells were removed just before cell plating. The PDMS well leaves a residue on the glass [122] that may be cell repulsive. Therefore, to create substrates with areas of glass and areas of the SLB within a single well one side of the bilayer was exposed to air to destroy it just before plating cells.

The cells were observed starting from the first day *in vitro* for up to 10 days. The bilayers made of pure POPC appeared to be cell resistant, as was previously reported in literature [104]. Only a small amount of cells adhering to and growing on the POPC was found. In fig. 5.1(A) one can see the POPC bilayer covered area (orange colour) that is almost cell free - while neurons are growing on areas uncovered by the bilayer. In contrast, charged bilayers support adhesion and growth of neurons. In fig. 5.1(B) one can see positively charged SLB made of 70% of POPC and 30% of DOTAP. The cells appear to grow both on glass and on the bilayer. Both figures show neurons after 1 day *in vitro* (DIV1).

The image shown in fig. 5.2 was made with higher resolution. It shows neurites growing on the SLB made of pure DOTAP. The neurites prefered to grow on positively charged SLB: they didn't cross the border between SLB and glass, following the edge of the bilayer. This is typical behaviour of the neurites, which were observed for many cases of neurons growing on positively charged bilayers prepared with different ratios of POPC and DOTAP. Holes of different size can be seen in the SLB. The possible reasons for their appearance are discussed further (section 5.3).

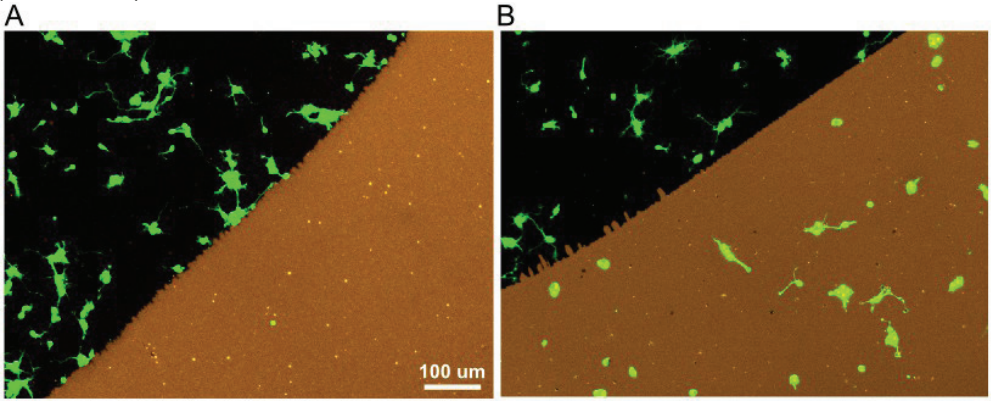

Figure 5.1: Fluorescence micrographs of neurons on the supported lipid bilayers made of POPC (A) and 70%POPC/30%DOTAP mixture (B) on DIV 1. The biayers are stained with TexasRed-PE (orange). Live cells are stained by calcein-AM (green). The black area is glass. The scale bar is identical for both images.

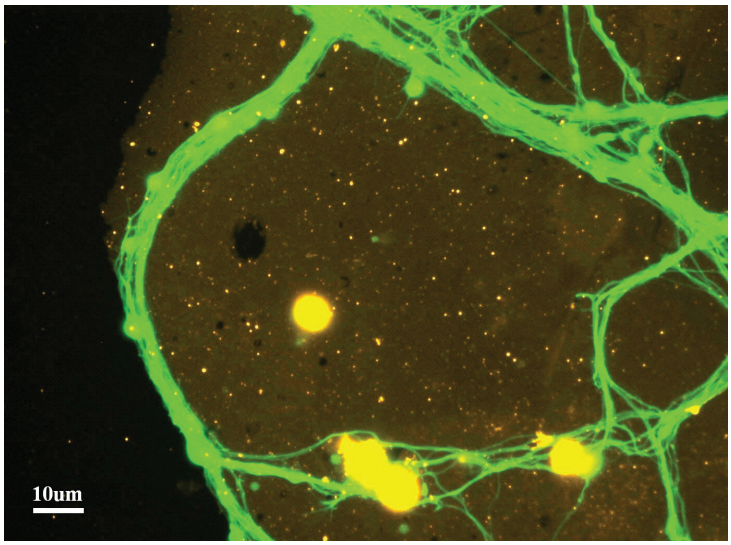

Figure 5.2: Fluorescence micrographs of neurtes on the supported lipid bilayers made of DOTAP. The biayer is stained with TexasRed-PE (orange). Live cells are stained by calcein AM (green).

5.1.2 Dependence of cell adhesion and growth on charge density

The influence of DOTAP concentration in the SLB on the adhesion and outgrowth of neurons was studied. fig. 5.3 shows bar plots representing the number of live cells on bilayers containing different concentrations of DOTAP and on uncoated glass. All data are normalized to the number of live cells on PLL coated glass. The number of live cells on positively charged SLBs after 1 day was high and comparable with cells grown on PLL, while the number of neurons growing on pure DOTAP bilayers was even higher than on the PLL-control. Increasing the amount of DOTAP leads to an improved adhesion and outgrowth on the bilayer, which can be attributed to the increased amount of positive charge. The spread of the experimental data is quite broad due to the various factors, affecting cell adhesion, as discussed below. A few cells were found on the pure POPC bilayer. However, one cannot rule out that they might adhere due to rare defects in the SLB.

Investigation of some phenomena of cell physiology (such as electric activity or synapse formation) may require long term cell culture. For this reason, cells on the SLB were studied for up to 10 days. Micrographs of cells on DIV4 and DIV10 are shown in fig. 5.4 and 5.5. After 4 days the neurons on all surfaces except the POPC bilayer showed good growth and development of neurites. After 10 days the cells on the positively charged SLBs formed a dense network although some neurospheres were observed. In comparison, on PLL the cells formed denser networks with a large number of highly branched processes. Those cells growing on glass without any coating showed a very different morphology from those ones grown on PLL or positively charged lipids on DIV 10. The neurons on glass formed many clumps connected to each other by a few bundles of neurites.

The longest time the culture on positively charged SLBs were observed was DIV 16. At this age the culture looked healthy. The were many clumps of cells, but the networks of neurites were highly branched and dense (fig. 5.6). Thus, these experiments showed the possibility to maintain healthy neuronal culture on the SLB for more than 2 weeks.

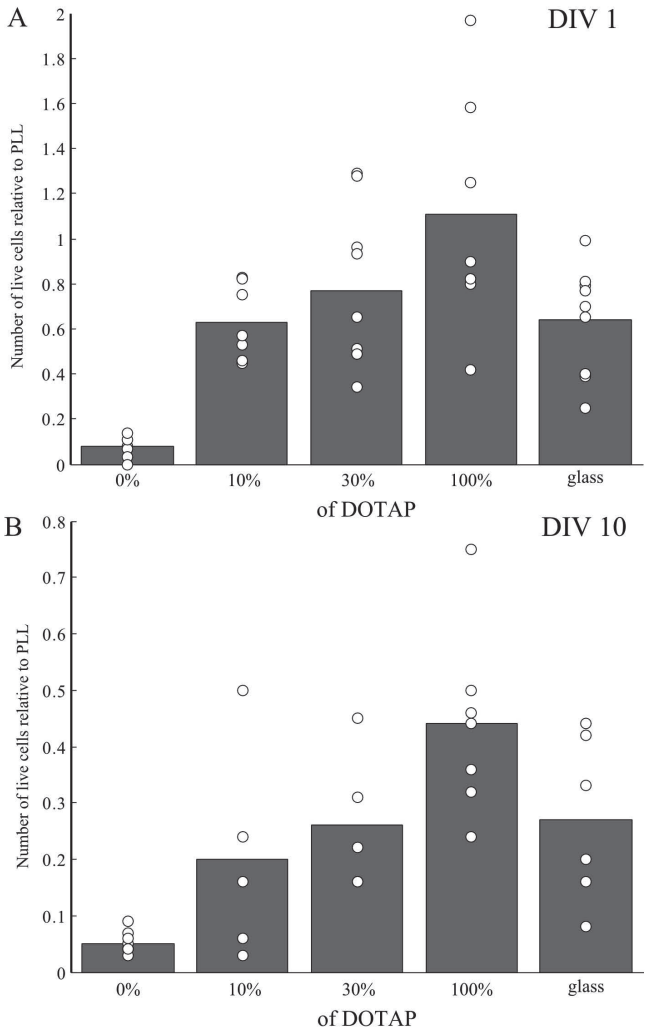

Figure 5.3: Number of live neurons growing on mixtures of POPC and DOTAP, as well as on uncoated glass for DIV1 (A) and DIV10 (B). The number of cells is normalized to the number of cells on PLL. The bars represent the average for each concentration. The circles are single measurements.

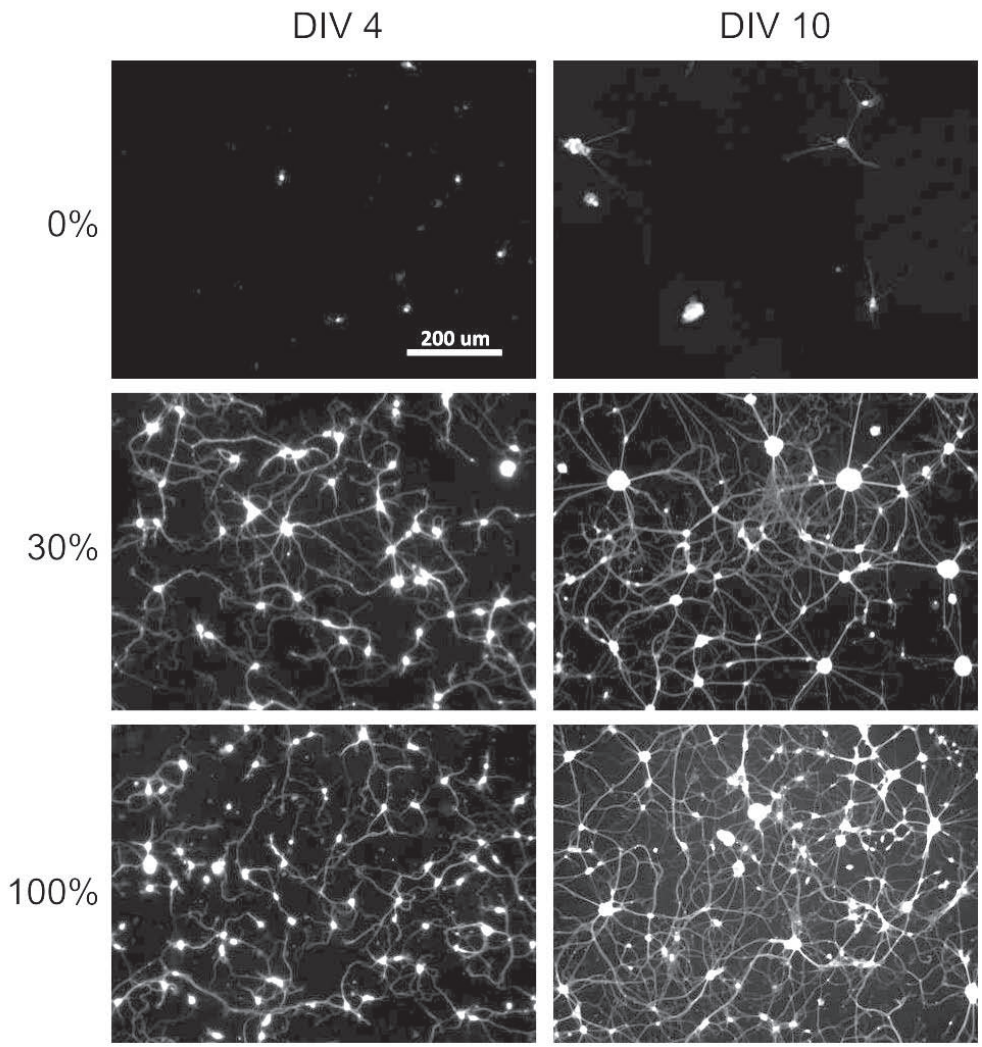

Figure 5.4: Microscopy images of DIV 4 and DIV 10 neurons growing on the SLBs made of different mixtures of POPC and DOTAP (the percentage of DOTAP in the mixture is indicated at the left side of the picture). Live cells were stained by calcein-AM. The scale bar is the same for all images.

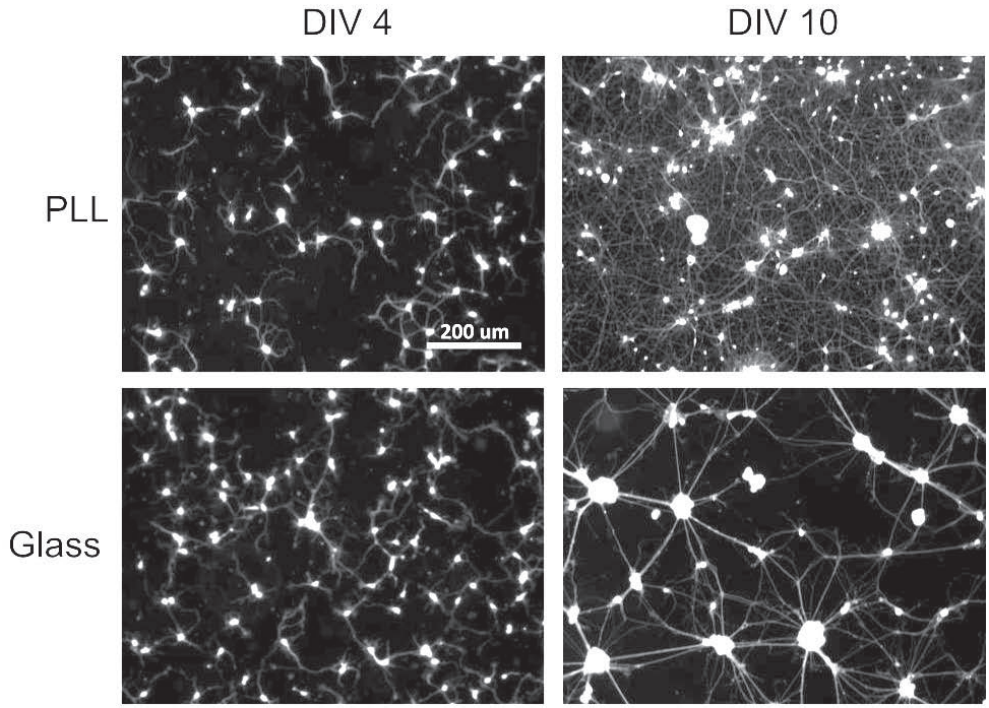

Figure 5.5: Microscopy images of DIV 4 and DIV 10 neurons growing on glass and PLL. Live cells were stained by calcein-AM. The scale bar is the same for all images.

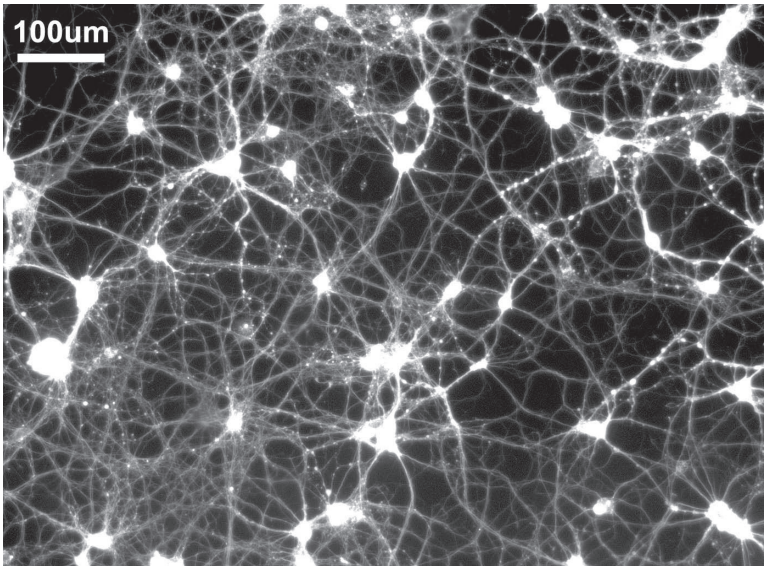

Figure 5.6: Neurons on the DOTAP SLB on DIV 16. Live cells were stained by calcein-AM.

5.1.3 Discussion of adhesion and growth of neurons on SLBs

Lipid surfaces made of pure phosphocholine are cell resistant as was previously shown in several papers [104], [105], [107], [108]. There are several hypothesis proposed in literature to explain this phenomenon [104]: 1)diminished electrostatic interaction between cells and the bilayer 2)formation of a comparatively strongly bound water layer associated with phosphocholine 3)fluidity of the SLB.

The results obtained in the present work show that two parameters of the SLB are changed with change of concentration of DOTAP: surface charge and fluidity of the SLB. The effect of positive surface charge of the SLB seems to be the main reason for adhesion of cells, as the outer surface of cellular membrane is usually negatively charged. Thus, it is very likely that cells adhere to positively charged SLBs due to electrostatic interaction. At the same time fluidity can be also important for adhesion as was shown by Oliver et al [106]. They found out that lipid monolayers built on hydrophobic polymers were not fluid but allowed cell adhesion. Bilayers made of the same lipids being fluid are cell repellent. This effect can contribute to increase the number of cells on the SLBs made of DOTAP (fig. 5.3) as the fluidity of the SLB decreases with the increase of DOTAP concentration (fig. 4.5(B)).

The average number of cells on positively charged bilayers after the first day in culture was 6-10 times higher than on POPC bilayer. At the same time fluidity for the SLB containing 10% and 30% DOTAP was not considerably changed comparing with pure POPC. This implies that positive charge is the main reason

for adhesion. For the bilayer made of pure DOTAP the effect of fluidity on cell adhesion can be taken to consideration.

The same two factors, charge and fluidity of the SLB, can influence morphology of neurons. Morphology of neurons on charged SLB, PLL and glass is quite similar after 4 days *in vitro* as can be seen in fig. 5.4 and 5.5. After 10 days in culture, the cell morphology differs between the various surfaces. Neurons on glass tend to form clumps, which indicate poor adhesion of the cells to the surface compared to cell-cell interactions. The number of clumps on SLBs was lower than on glass. On the SLBs with low concentration of DOTAP this number increased slightly, which was probably due to degradation of the SLB and appearance of areas of uncovered glass to which cells adhered poorly. The neurons on the SLB made of pure DOTAP generally didn't form clumps. Although the number of cells is around 2 times lower then on PLL, the neurons form dense networks. This indicated stronger adhesion of cell to such bilayers and their better stability.

5.2 Electrophysiology of cells on positively charged SLB

Positive charge of the SLB enhances the adhesion of cells, but at the same time can influence some physiological characteristics. Proteins of the cell membrane, that are negatively charged could be accumulated at the bottom of the cell due to interaction with the positively charged SLB. If the distance between the SLB and these proteins is short enough, positive charge of the SLB could affect their functions. In particular, one can imagine that electrophysiologycal characteristics of the cells growing on the positively charged SLB could be changed due to influence of positive charge onto functioning of the voltage gated ion channels.

To check if neurons growing on positively charged bilayers possessed normal electrophyological activity, patch-clamp experiments were carried out. Neurons of DIV10 growing on bilayers made of POPC with 30%DOTAP were patched and electric activity was observed. fig. 5.7 shows recordings done in the current clamp mode. The steps of current were injected into the cell, the amplitude of which were gradually increased. At a certain value of this current action potentials (AP) started to appear (fig. 5.7(A)). The rate of the action potentials increased with the increase of the injecting current as would be in normal tissue. A single action potential shown in fig. 5.7(B) is also similar to usually recorded ones [172]. It has slowly increasing phase of passive recharge of the membrane (1), fast depolarization due to opening of the sodium channels (2), a little bit slower repolarization due to the potassium channels (3), and hyperpolarization phase (4) when the membrane can not be exited.

At the low injected currents the action potentials were not generated but small temporal increase of potentials were observed that represented excitatory post synaptic potentials (EPSP) (fig. 5.7(C)) [173]. The presence of these potentials proves existence of mature synapses in the neurons that possess spontaneous activity. Small fast spikes seen in all recordings are due to electromagnetic pick up. The control experiments carried out on neurons of the same age growing on PLL showed similar results (data not shown). Taking into account also the data from literature [172], one can conclude that positive charge of the SLB does not influence electrophysiological properties of neurons.

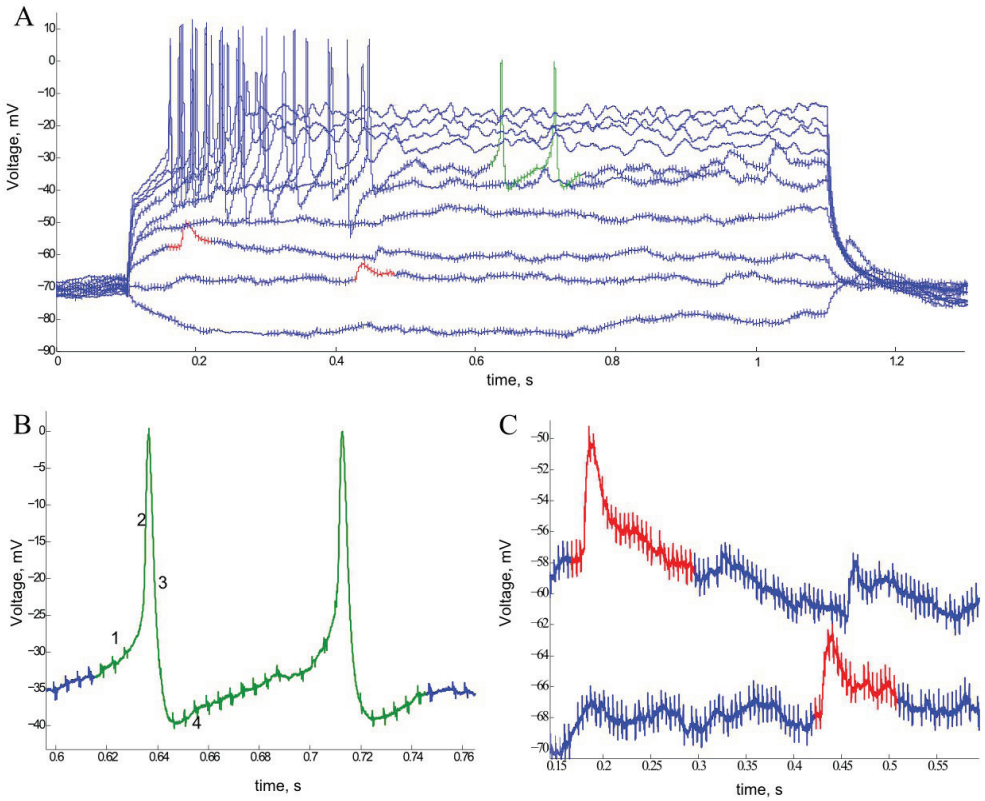

Figure 5.7: Patch-clamp recordings from neurons grown on 30%-70% DOTAP-POPC SLB on DIV10. (A) Current-clamp recording showing APs (green colour) and EPSPs (red colour). (B) Zoomed in APs. The numbers mark different phases of AP (details are in the text). (C) Zoomed in EPSPs.

5.3 Stability of the SLB

Stability of the SLB is an important issue for using it as a platform for cell culture. If the SLB degrades before cells become mature enough to express a phenomenon, one want to study all advantages of using the SLB disappear. The aim of this section is to show that the SLB is stable for enough time to allow studying at least some phenomena in neuronal cell culture.

5.3.1 Stability of the SLB in solution

In all experiments made in the frame of the present work holes appeared to be formed in the SLBs some time after preparetion. This effect was observed both for the SLBs made of pure POPC and for POPC-DOTAP mixtures. For some samples holes appeared only after several days, while for the others holes were observed almost immediately after preparation, especially at the edges of the SLB. This effect was observed not only in cell culture medium but in PBS and in Milli-Q water which implied that there were no biological reasons for it (although cells or proteins in cell culture medium could probably facilitate the process of the SLB destruction).

Images of several samples of the SLB taken on different age are shown in fig. 5.8 and 5.9 . Scratches in the SLBs (thick black lines seen in the images) were done by a needle to make a mark that could help to find and observe the same place of the sample (although it was not always possible). As one can see, for some samples holes appeared after already 2 days, while for some others even after 7 days there were no holes seen. There also seemed to be no dependence on the constitution of the SLB. The holes had irregular shape and became bigger with time. The number of holes also increased.

Despite of formation of holes, the SLB itself maintains its structure and saves fluidic properties. This was proved by FRAP experiments, an example of which is shown in fig. 5.10. A spot bleached in a POPC SLB after 7 days in cell culture medium without B27 supplement disappeared after some time.

The formation of holes in the SLB was previously described by Tamm et al. [70] for SLBs made by the Langmuir-Blodget technique. This effect was explained by stretching of the SLB. The effect was also dependent on the temperature since the surface pressure of the SLB was temperature dependent. The same effect could also take place in the SLB studied in the present work, as the samples didn't have any border to prevent its stretching. Defects on the surface of the glass slides or small impurities might facilitate this effect, as in the case of stretching lipid molecules tended to move to places where their interaction with the surface was stronger. Thus, a hole would appear in the place of a surface defect and become bigger with time due to stretching.

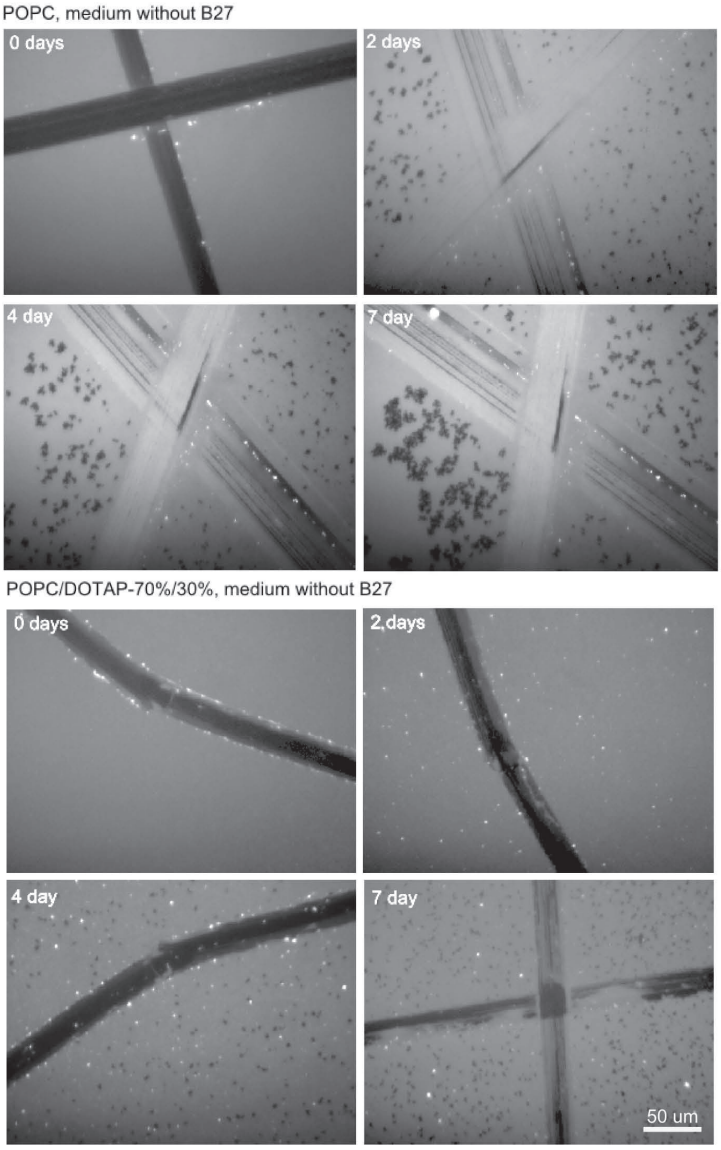

Figure 5.8: Formation of holes in SLBs kept in cell culture medium. Series of images taken on different days for SLB made of pure POPC and 70%-30% POPC-DOTAP mixture. The scale bar is the same for all images.

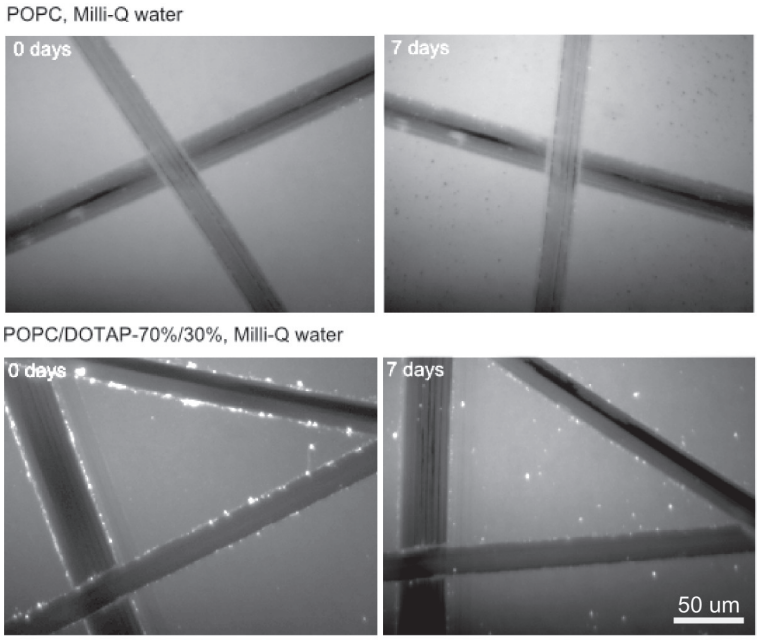

Figure 5.9: Formation of holes in SLBs kept in Milli-Q water. Series of images taken just after preparation and on day 7 for the SLB made of pure POPC and 70%-30% POPC-DOTAP mixture. The scale bar is the same for all images.

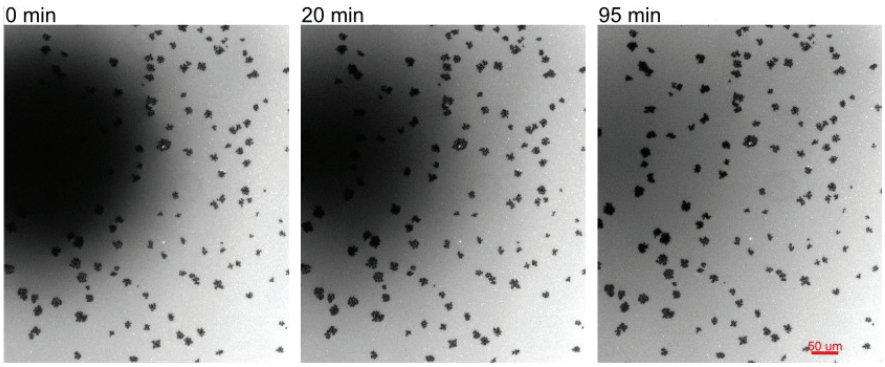

Figure 5.10: A FRAP experiment showing the recovery of fluorescence in the POPC SLB of 7 days old kept in cell culture medium without B27 supplement. The scale bar is the same for all images.

5.3.2 Influence of cell culture on SLB stability

Defects appear in the SLB most likely due to it's stretching. At the same time cells growing on the bilayer can produce additional influences on it and facilitate its degradation. This can be due to mechanical forces which the cells apply to the surface or chemical factors which the cells excrete. The cells could also consume lipids of the SLB as building material for their membranes. Among chemical factors one can mention phospholipases - enzymes that hydrolyse phospholipids into fatty acids and other lipophilic substances. These enzymes were shown to destroy lipid bilayers [174].

The SLBs tested in the present study were less stable in the presence of neurons than in solution or water. The area of destroyed SLB appeared to be bigger. fig. 5.11(A) shows a SLB made of POPC with 30% DOTAP after 16 days in neuronal cell culture. Large areas are not covered with the SLB but the rest of it is still uniform and, even after 16 days, seems to provide proper support for nerouns. Another SLB made of pure POPC was also destroyed a lot even without cells on it (fig. 5.11(B)). There are no cells on POPC SLB as they do not adhere to it but neurons were presented in that particular dish in the other areas (see Chapter 3 for description of the substrates). Thus, chemical factors excreted by neurons can influence the SLB. Although, the collected data are not enough to make a conclusion about real influence of neurons on degradation of the SLB, one can see that the SLB provides a platform for the cells for as long as 16 days which is enough to study many phenomena of cell growth, development and signalling.

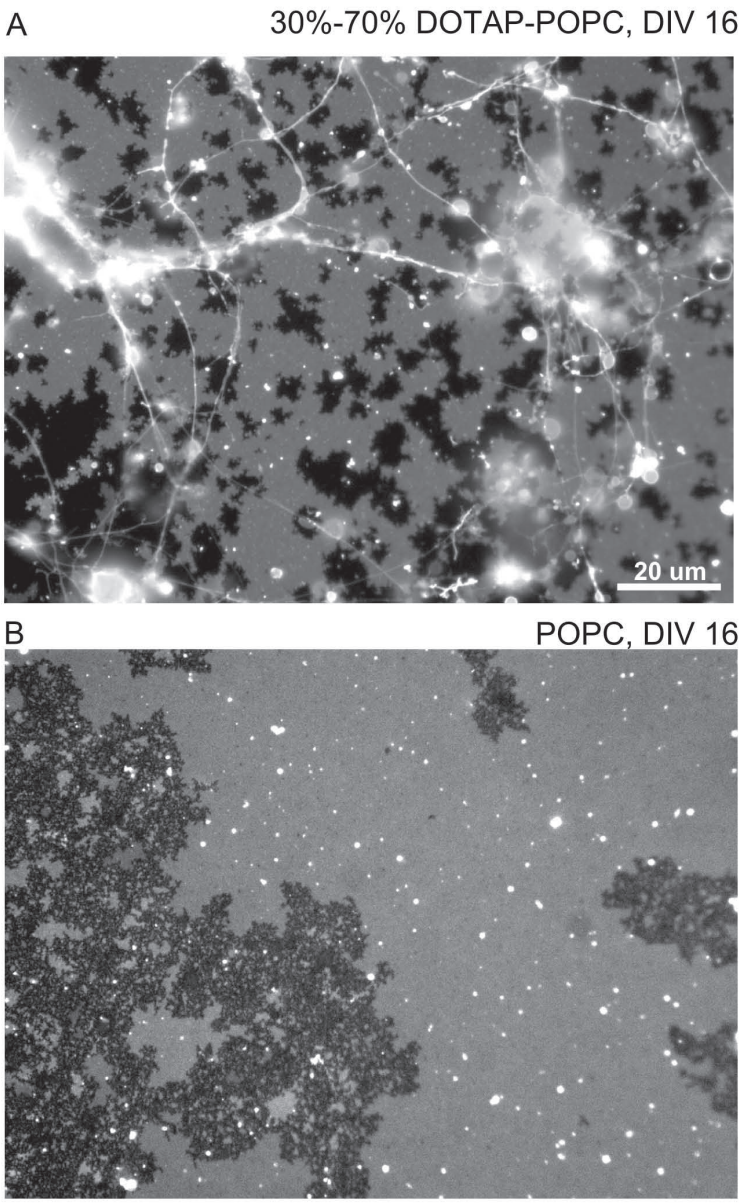

Figure 5.11: Degradation of SLBs in cell culture. (A)30%-70% POPC-DOTAP on DIV 16. Neurites are seen growing on the SLB. (B) POPC SLB of the same age in the dish with neurons. The scale bar is the same for both images.

Chapter 6

SLB with incorporated ephrin A5 for neuronal cell culture

OK, you can try this. And then, when it doesn't work, do it my way.

Kristin Michael

6.1 Incorporation of ephrin A5 into SLB

6.1.1 Determination of the detergent concentration

In this work the method of protein incorporation from detergent solution was used to introduce ephrin A5 into lipid vesicles from which SLBs were made. The concentration of detergent necessary for this procedure should be determined very precisely because of two reasons. Firstly, if the concentration of the detergent is too low, it can not facilitate protein incorporation process to the necessary degree. Secondly, if the concentration is too high, lipid vesicles can be dissolved completely producing micelles.

The detergent used in the present work was *n*-octyl-β-D-glucoside. To determine the suitable concentration of detergent optical density (OD) of lipid vesicles suspension made of POPC was measured while increasing the amount of detergent in solution (see Chapter 3). The dependence of OD, measured at the wavelength 500 nm, on the concentration of detergent is shown in fig. 6.1.

Initially, with the increase of the detergent concentration OD decreased most likely due to breaking of the relatively big aggregates of vesicles. The particles become smaller and scatter less light. The following increase of OD is associated with the incorporation of the detergent molecules into the membrane of the vesicles: membrane's reflective and refractive properties change and, as a result, its light scattering characteristics. When a critical concentration is achieved (12 mM in the present case), the OD starts to decrease due to dissolution of vesicles and formation of small micelles. The peak of the curve represents the concentration where vesicles contain the maximum possible amount of detergent.

As seen in the fig. 6.1 this peak lies around 10-12 mM. This concentration was chosen for the following experiments.

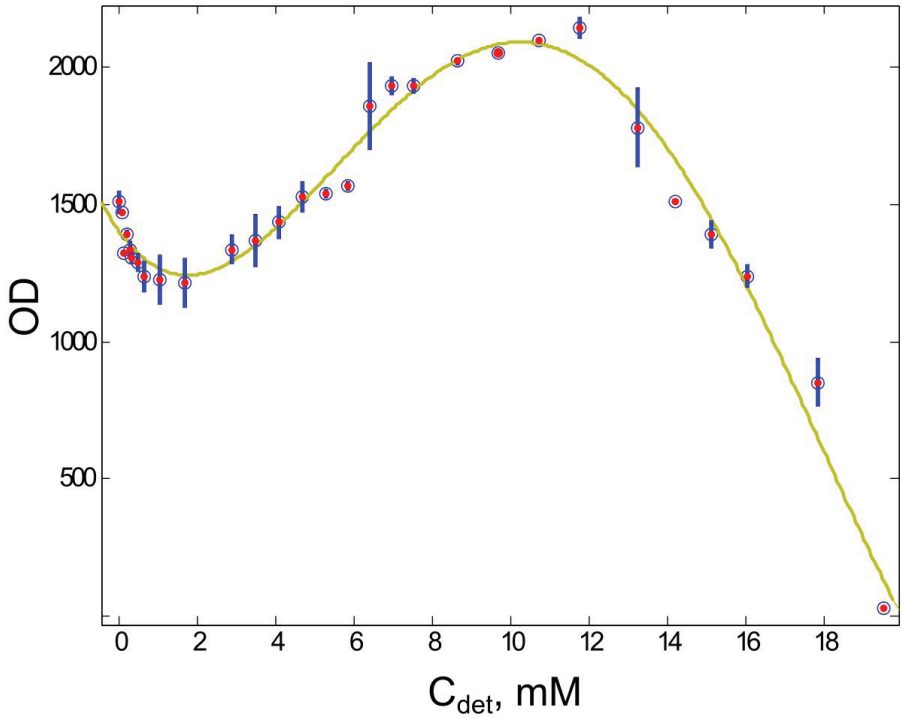

Figure 6.1: The dependence of optical density (OD) of suspension of lipid vesicles made of POPC on the concentration of detergent (*n*-octyl-β-D-glucoside). The measurements were done at λ=500 nm.

6.1.2 Immunostaining of SLB with incorporated ephrin A5

Ephrin A5 was incorporated into vesicles made of POPC (following the procedure described in Chapter 3) and the SLB was prepared by deposition of these vesicles. Presence of the protein in the bilayer was checked by immunostaining (as described in Chapter 3 and protocol in Appendix B). Except the SLB with ephrin A5 two other SLBs were stained for control. One was made of pure POPC and another one made of POPC but liposomes were treated with detergent without the protein to check if the detergent itself influenced attachment of the antibody. In the fig. 6.2 images of these SLBs are presented together with their fluorescence intensity profiles. All images were taken with the same exposure time. As one can see, fluorescence intensity of the SLB with ephrin A5 is almost three times higher than that of the control samples. This proves successful incorporation of ephrin A5 into the SLB.

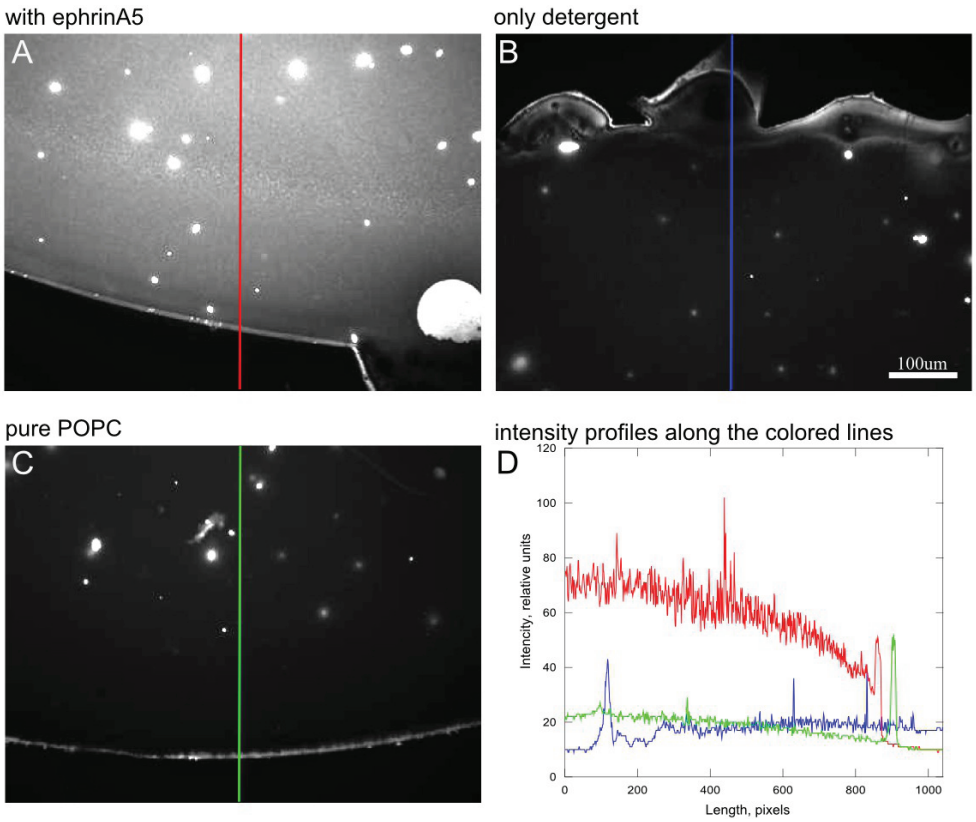

Figure 6.2: Immunofluorescence of lipid bilayers. Antibodies against ephrin A5 were applied. (A) The SLB with ephrin A5 reconstituted to liposomes from detergent solution. (B) The SLB made of liposomes treated with detergent, but without protein. (C) The SLB made of pure POPC. Exposure time is 1110 ms for all images. (D) Intensity profiles along the colored lines in images (A-C)

The bilayer itself stayed fluidic after protein incorporation procedure which was proved by FRAP. A spot in a bilayer with small amount of TexasRed-PE was bleached. This spot disappeared after some time (fig. 6.3); it proves that there was diffusion of the labeled molecules in the SLB. The calculated value of the diffusion coefficient was 1.1 um^2/s which a bit lower than for SLB made of POPC and labeled with NBD-PE (D=1.8 um^2/s). This difference is, on the one hand, due to different labels used. One the other hand, antibodies accumulated on the top of the SLB could slow down the movement of molecules in it.

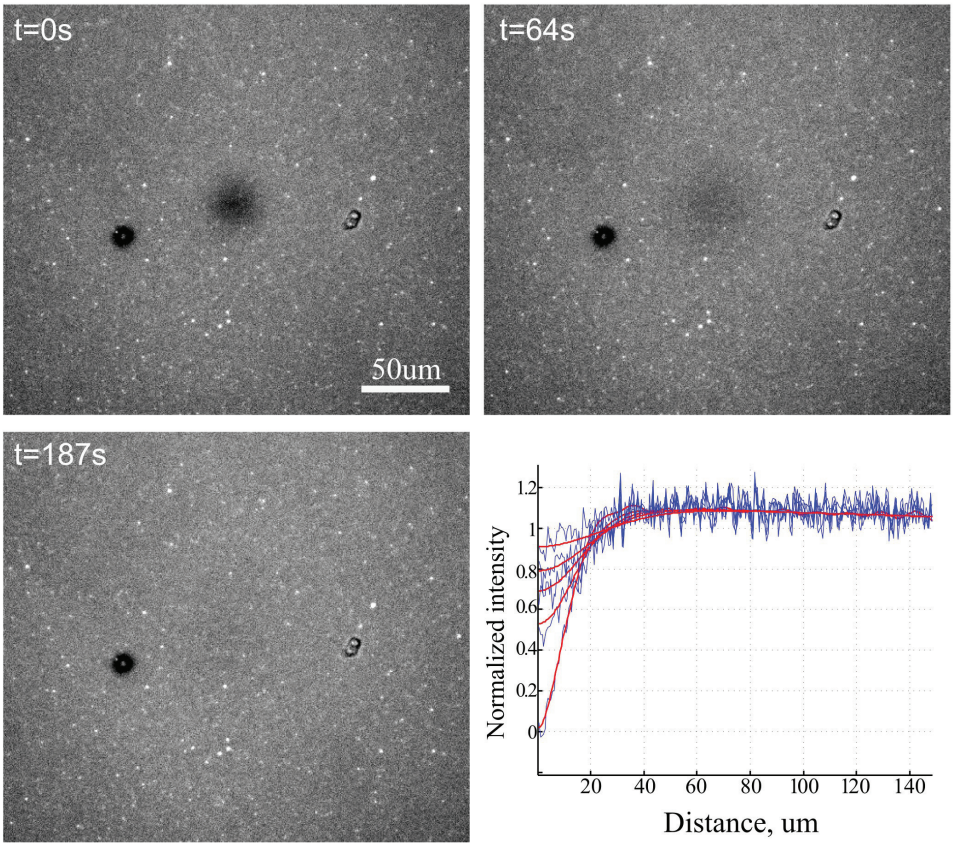

Figure 6.3: FRAP in the SLB with incorporated ephrin A5. The three micrographs show the recovery of the fluorescence in the bleached area. The graph represents the fitting of the experimental intensity profiles (blue curves) with the solutions of the Dirichlet problem based on the second Fick's law (red curves).

6.2 Neuronal cell culture on the ephrin A5 SLB

6.2.1 Cell growth and development

Primary rat cortical neurons were prepared as described in Chapter 3 and plated on the SLB with incorporated ephrin A5. In contrast to the pure POPC bilayers cells adhere to the SLB with ephrin. The reason for this can be the presence of Eph receptor not only in the synapses, but also in the somatic membrane. This can provide specific interaction between ephrin A5 in the SLB and the cell membrane. It is also feasible that ephrin creates possibilities for anchoring of other adhesion proteins in the somatic membrane, e.g. integrins.

The cells were monitored for several days in the culture and the number of cells and morphology were compared with the control samples. fig. 6.4 shows

neurons of DIV 6 growing on the SLB with ephrin A5 and on the control PLL coated glass surface. The morphology of the neuronal networks on both surfaces is similar. The culture on PLL seems to be slightly denser (the cells were plated at the same density of 80000 cells per 32 mm dish). As one could see from Chapter 3, SLBs made of pure POPC does not support the adhesion of cells. Thus, there is a strong reason to believe that the cells adhere to the SLB in this experiment due to presence of ephrin A5.

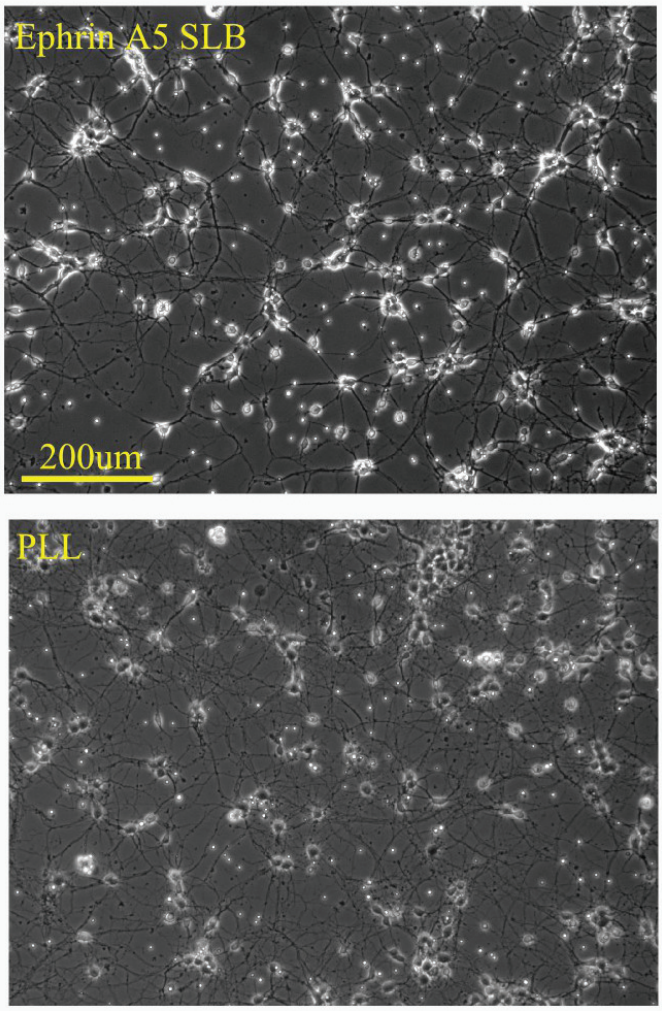

Figure 6.4: Neurons growing on the SLB with incorporated ephrin A5 (upper image) and on PLL coated glass (lower image). The micrographs were taken on DIV 6. The scale bar is the same for both images.

6.2.2 Synaptic activity of neurons growing on the SLB with ephrin A5

In order to investigate development of synapses in cell culture growing on SLB with incorporated ephrin A5 patch-clamp experiment were carried out. The aim of these experiments was to record postsynaptic currents and potentials to prove the presence of active synapses and to compare these data with the data obtained in the same experiments from the cells growing on control PLL coated surfaces. The cells were tested on DIV 6. This age was chosen, because normally neurons do not form mature synapses yet. However, ephrine A5 presented in the SLB could speed up synapse maturation as indicated in the literature [175].

In fig. 6.5 one can see the recordings of EPSP and EPSC made from neurons growing on ephrin A5. EPSPs, recorded in the current clamp mode.

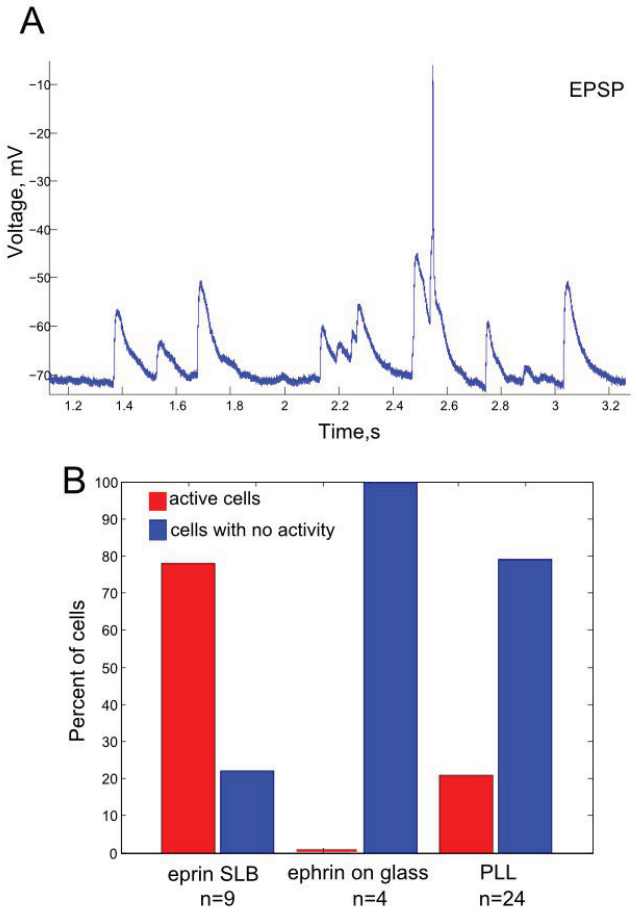

Figure 6.5: (A) The patch-clamp recording made in the current clamp mode. EPSPs are seen. In one case they lead to generation of the action potential. (B) Percentage of active cells on different surfaces.

The amplitude of injected current was chosen of such a value to keep potential in the cell close to resting potentials (around -70 mV) to ensure that the recorded EPSPs were spontaneous. The EPSPs have normal shape (as described in [176], [177]) and sometimes lead to the generation of the action potentials. Most of the cells on ephrin A5 SLB exhibited this activity: 7 of 9 tested cells generated spontaneous EPSP (fig. 6.5B).

Some neurons on control PLL coated surfaces on DIV 6 also exhibited similar activity: spontaneous EPSP and action potentials generations. The number of these active cells, however, was not very high compared to the number of inactive cells. Among 24 patched cell only 5 were active.

Another control surface was glass on which ephrin A5 was deposited using the same protocol as for PLL deposition (Appendix B). Among four tested on this surface neurons no one exhibited activity. This control was necessary to define if the SLB was important (or can facilitate) functioning of ephrin A5 by providing proper environment for the ephrin molecules.

One drawback of the presented experiments is that the density of cells was not controlled. The initial number of cells in the samples was the same (80000), but due to different factors influencing cell survival the final density on the DIV6 could be different in the different dishes. Moreover, the neurons themselves produced ephrine A5 and in a dense culture, where cells were in stronger contact with each other, this internal ephrin could play a role in synapse maturation. Future work should take this factor into account.

Chapter 7

Patterned SLB using GUV

We are researchers - we must produce a research

Holger Wigström

7.1 Characterization of GUV

GUV were prepared by electroformation method as described in Chapter 3 (exact protocol can be found in Appendix B). Produced vesicles contained small amount of fluorescently labeled lipid and were observed with fluorescence microscopy. In the fig. 7.1 one can see an example of produced liposomes made of POPC. The GUV had wide distribution in size: the largest vesicles were around 50-100 um in diameter but at the same time there were many small vesicles of several micrometers and less.

The liposomes were sedimented in the field of gravity to separate them by size. Bigger vesicles sank and could be collected from the bottom of a tube while small ones are still floating closer to the top (see Appendix B for details). This procedure led to an increase of the average size of the liposomes, though did not eliminate the small vesicles completely.

Some vesicles appeared to be multilamelar (fig. 7.1.). Nevertheless, multilamelarity was not a problem for rupturing of the vesicles and formation of the patches of the SLB on the substrate (as described later).

GUV were prepared not only with POPC but with a mixture of lipids consisting of 30% of DOTAP and 70% of POPC. Although exact measurements of the distribution of size were not done, these vesicles usually seemed to be smaller than POPC vesicles.

Both GUV made of POPC and of mixture of lipids ruptured upon touching the surface forming round SLB patches (fig. 7.2). The diameter of these patches depended on the size of the vesicles: the biggest observed patches were around 200-300 um.

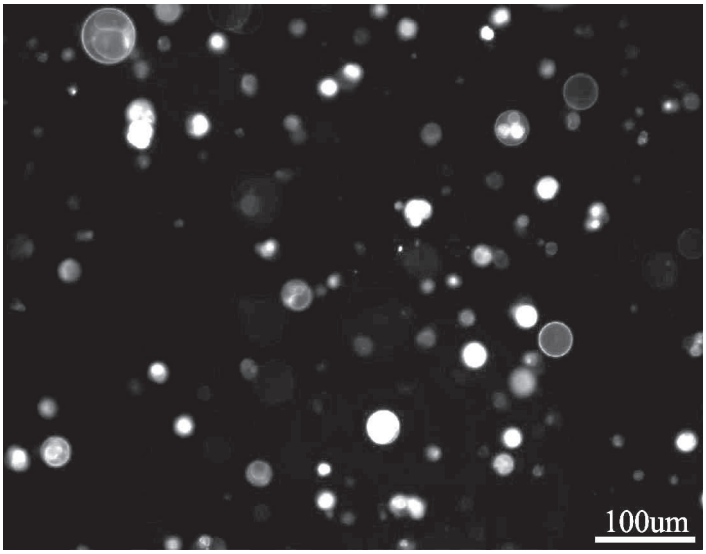

Figure 7.1: GUV prepared with POPC containing several percent of TexasRed-PE.

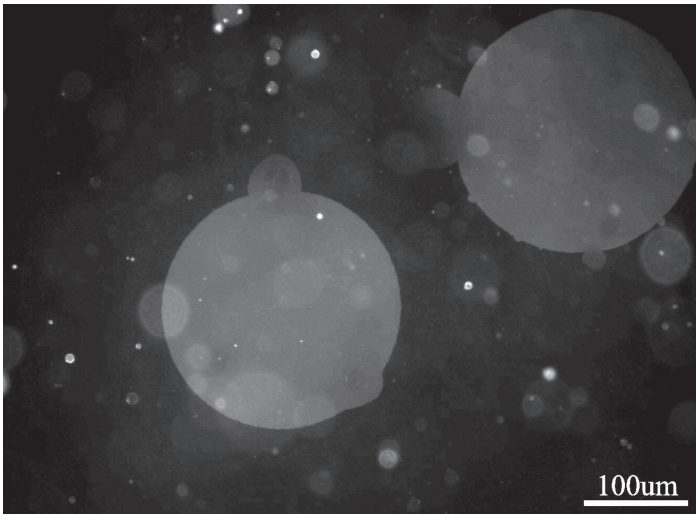

Figure 7.2: Patches of the SLB formed on the glass surface after rupturing of GUV

7.2 Characterization of the SLB on patterned substrates

Two types of substrates were used in this work: a chromium grid formed on glass by photolitography and a grid prepared by microcontact printing of proteins (PLL) on glass. Formation of SLBs on these substrates was first tested using SUV with the same procedure as for making positively chargeed SLB. Glass slides with Cr grid were activated in O2 plasma just before SUV application. In the case of PLL grids, glass slides were activated before printing. Flurorescence micrographs showed that the SLB was formed in each cell of the Cr grid (fig. 7.3).

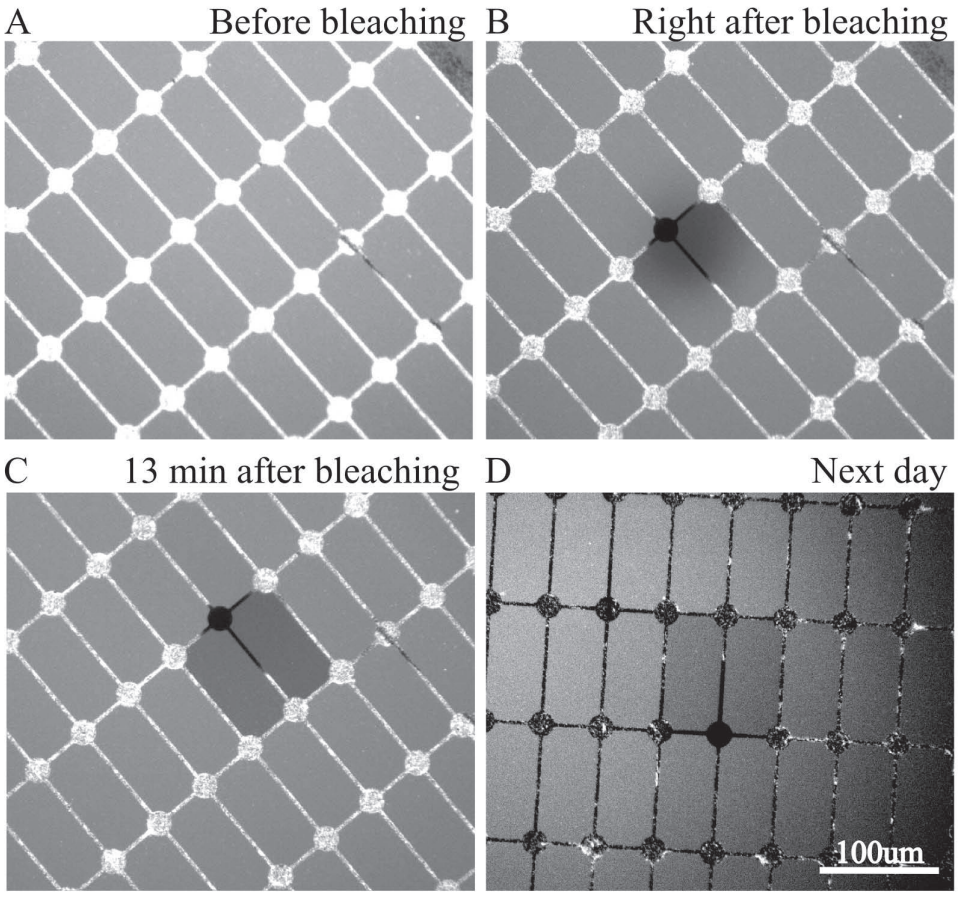

Figure 7.3: Bleaching of the SLB formed on glass patterned with the Cr. The bleached spot falls into two rectangles (B). These rectangles are darker than others in the image made 13 min after bleaching due to diffusion (C). The Cr lines are bright in the first three images (A-C) due to adsorption of liposomes. In the last image (D), made on the next day after bleaching, the lines are black as the liposomes were washed away.

FRAP experiments, presented in fig.7.3, proved that this SLB was fluid as the diffusion in each particular cell was observed but the lines of the grid made the border for the molecular motion in the SLB. The bleached spot was distributed over the two rectangles and they stayed darker than their neighbours until the next day. Accumulation of vesicles on the Cr lines was observed – fluorescence from the lines was higher than from inside of the squares. After some time the fluorescence signal became weaker and small black spots started to appear on the lines. After one day the lines became completely black indicating that the vesicles were washed away.

Micrographs of the SLB made in the cells of PLL grid printed on glass are shown in the fig. 7.4. As one can see, the SLB fills each triangle. The liposomes were also accumulated on some of the lines and, sometimes in the corners of the cells. FRAP experiments proved 2D fluidity of the SLB as the bleached molecules were distributed uniformly in the triangles touched by the bleached spot. The PLL lines also provided a border for diffusion but some of them were probably not complete. Some of triangles, that were very dark right after bleaching became brighter after 1h, most likely due to diffusion of the "bright" molecules from the adjacent triangles. Bright dots seen in some images are probably cylindrical vesicles that can be formed sometimes from the SLB (this effect was described in [70]).

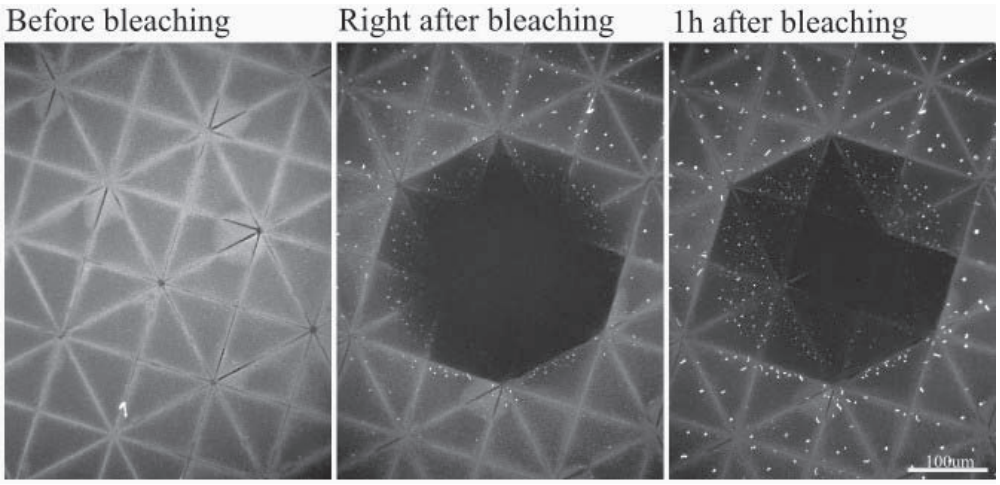

Figure 7.4: Bleaching of the SLB formed on glass patterned with the printed PLL

7.3 Formation of patterned SLB

Patterned SLBs were prepared using GUV made of mixture of POPC (70%) and DOTAP (30%), stained with TexasRed-PE (red) and SUV made of POPC and stained with NBD-PE (green). Cr grid on glass was used. First, GUV were deposited on this grid and after 3 min were washed away by a stream of buffer. This time was enough for some of GUV to rupture and form patches of the SLB. Some of the patches occupied several complete rectangles of the grid and parts of adjacent ones while others were small enough to fit into one rectangle (fig.7.5(A)). Probably some vesicles ruptured in an explosion manner as observed in specific patterns of the SLB patches. Such type of the SLB shape was never detected on plain glass, indicating that Cr line can promote this effect. It should be noted that in the present work the GUV were deposited randomly by injecting a small volume of the suspension into the dish with the patterned glass slide. But at the same time, it seems to be possible to manipulate a GUV by a micropipette, used for manipulations with cells. In this way one could get patched of SLB in the defined places.

After washing of GUV, SUV were applied. After incubation for at least 20 min they were washed by a stream of buffer. A picture of the sample taken through an optical red filter after this procedure is shown in fig.7.5(B). All empty rectangles were filled with new (green-stained) SLB which is not seen in the image. In the cells partially occupied by red-stained SLB, new SLB was also formed in the unoccupied area.

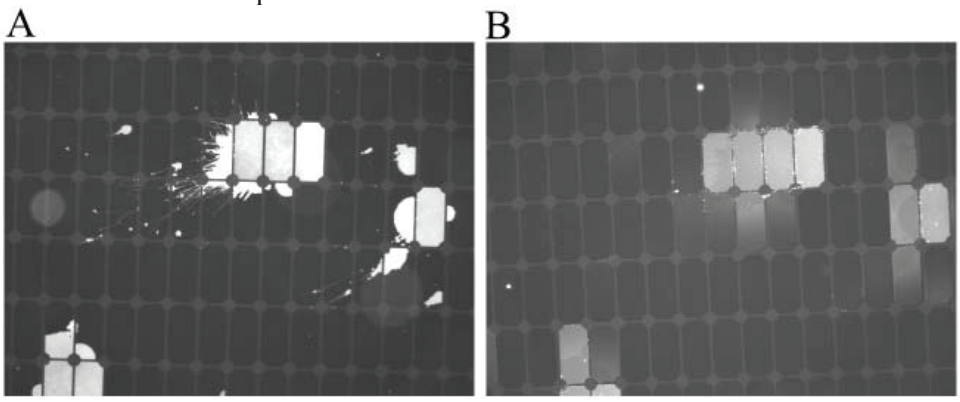

Figure 7.5: Preparation of the patterned SLB. (A) Patches of the SLB formed after rupturing GUV stained with the red dye. (B) The SLB after application of SUV stained with the green dye. Both images were taken through the red optical filter. Some boxes were filled with the SLB not completely after GUV application. After addition of SUV the SLB in these boxes contained the mixture of lipids

In these cells two types of the SLB were mixed due to diffusion which is seen in fig. 7.5(B) as decrease of brightness red fluorescent dye. In some cells a gradient of brightness or even a border between bright and dark parts can be seen

This indicates that the diffusion process was not completed. But after some time the diffusion process should reach equilibrium and the distribution of the fluorescence should become uniform.

Thus, one obtains a patterned SLB consisted of rectangular patches made of POPC-DOTAP mixture (concentration DOTAP in some of them is lower due to mixing in additional POPC) and patches filled with the SLB made of pure POPC. Several examples of such SLBs are shown in fig. 7.6.

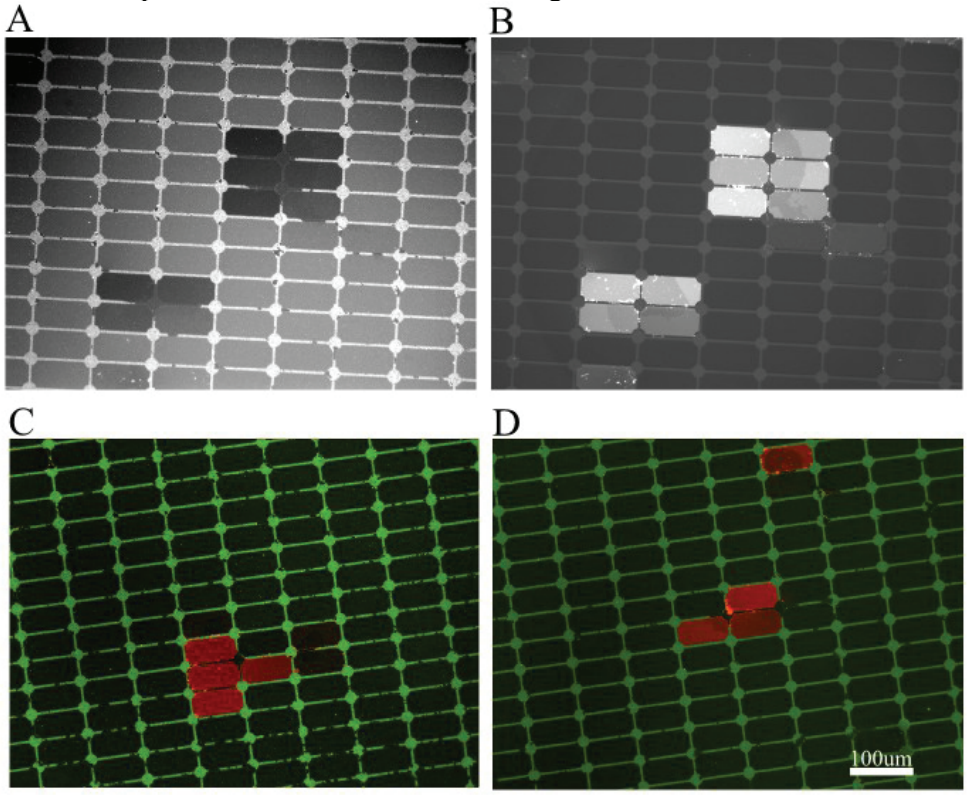

Figure 7.6: Patterned SLBs. (A) An image of the patterned SLB taken through the red optical filter. (B) The same SLB as in (A), but acquired in the green optical filter (C-D) Images of the patterned SLBs made using the combination of the red and green filters. The scale bar is identical for all images.

Fig. 7.6(A) shows the patterned SLB as seen in the green channel. Patches of SLB made of POPC-DOTAP mixture are seen as dark rectangles. In fig. 7.6(B) the same place of the sample is shown in the red channel. The rectangles that were dark, are bright now, while surroundings are dark. The images shown in fig. 7.6(C) and (D) are superpositions of images in both channels. Providing the results described in Chapter 4 one can conclude this pattern can be useful for cell guiding, as pure POPC SLB is cell repellent, while positively charged SLB provides cell adhesion.

Chapter 8

Discussion and conclusions

The future is not available now. Please call back later.

Egor Bartkevich

8.1. General discussion

The present work is devoted to the supported lipid bilayers. It examines the possibility of using an SLB as a platform for neuronal cell culture which can provide many advantages for research and biomedical applications, as shortly reviewed in Chapter 2. Unique properties of the SLB give the possibility to create a "phantom cell" on the solid surface [80]. Real cells sitting on such a surface would "think" that they are contacting another cell in their natural environment. This would increase biocompatibility. Mechanical properties of the surface would also be closer to biological values. Such a surface can not only increase survival of the cells, but also provide possibilities for studying many important cell functions such as adhesion and signaling. However, the SLB has not been used for experiments with cells very intensively. Usually cells do not adhere to the SLB made of natural phosphatidylcholine lipids, as was shown in literature [104–106]. To serve as a platform for the cell culture, the SLB should be functionalized in an appropriate way.

A simple way to provide cell adhesion to the SLB by adding positively charged lipids (DOTAP) was developed in the present work (Chapter 4). This method does not exploit complicated compounds, such as membrane proteins, peptides or other polymers which should be incorporated into the SLB or chemically bound to the lipid molecules [109–113]. The procedure of SLB functionalization with positively charged lipids is also very simple. There are essentialy no additional steps introduced into the protocol: lipids are just mixed while being dissolved in the chloroform in the initial step of the liposome preparation.

While providing adhesion for the cells, the positively charged bilayer is not overloaded with big adhesion molecules. This gives wider possibilities to introduce other molecules into the SLB (which are only functional, not adhesive)

without the risk of interference from the adhesive molecules. Thus, the positively charged SLB provides a basic platform for cells which can be extended by incorporating membrane proteins to study cell signaling phenomena.

The possibility of using SLB for studying cell signaling processes was also shown in this work (Chapter 5). A well known synaptic protein – Ephrin A5 [99] was incorporated into the SLB and its influence on neuronal development was studied. It was shown that Ephrin A5 did provide adhesion for primarily neurons (it is possible as Ephrin is an adhesion molecule) and facilitated their development. The later was proved by patch clamp recordings from the cells growing on the SLBs with Ephrin A5: 80% of tested neurons exhibited spontaneous synaptic activity on DIV 6. At the same time, only 20% of neurons of the same age growing on the control PLL coated surface were found to have spontaneously active synapses. The cells growing on Ephrin A5 simply deposited on glass didn't show synaptic activity. This supports a hypothesis discussed in literature that the Ephrin A5 can perform its functions only by being clustered in a proper way, which is provided by the bilayer of the cell membrane *in vivo* and can be provided by the SLB *in vitro* [99].

For better integration with recording devices, it is favorable to have the possibility to pattern a cell culture. This can be useful to guide cells to the recording sites of the MEAs, FET or nanowire arrays. Thus, patterning of the SLB is an important step on the way to use it as a universal cell culture platform. In the present work, a new method of SLB patterning has been developed (Chapter 6). It utilizes GUV that form patches of SLB on the surface upon rupturing on it. Being confined in printed or lithographically defined structures, these patches can be separated from each other. Thus, areas filled with bilayers of different types can be formed on the same surface. GUV can be manipulated by a micropipette which provides the possibility to position them precisely. The developed method has an advantage: GUVs and the SLB patches formed from them are always kept and manipulated under water. Thus, there is no risk of exposing the surface to air, which destroys the SLB.

The SLBs prepared in this work were characterized using FRAP. This method allowed the quality of the SLBs to be verified, to prove their 2D fluidity and to measure diffusion coefficients. A new computational algorithm was developed to analyze FRAP data that required neither an assumption about initial profile of the bleached spot, nor short bleaching time (as in the case of classical methods [128]). A MatLab based software was developed for this data processing (Appendix C).

Stability of the SLB can limit possible applications. As was shown in Chapter 4, holes appear in the SLB and become bigger with time. Although degradation of the SLB does take place, it is slow enough that big areas stay covered by the SLB, even after several weeks. The remaining SLB maintains its

natural 2D fluidity, which was proven by FRAP. It also supports cell growth for 10 days and longer. Thus, the SLB can be used as a platform for cell culture suitable to study many biological phenomena.

8.2. Conclusions

On the basis of the results of the present work several conclusions can be drawn:

1. SLB containing DOTAP support adhesion and growth of primary neurons in culture for at least 10 days.
2. Fluidity of the SLB decreases with the increasing DOTAP concentration.
3. Positive charge of the SLB is most likely responsible for adhesion of cells but fluidity of the SLB can also influence adhesion.
4. Ephrin A5 can be successfully incorporated into the SLB by reconstitution from detergent
5. SLBs with Ephrin A5 support adhesion and growth of neurons
6. There is a strong reason to believe that Ephrin A5 in the SLB speeds up maturation of the synapses.
7. Patterned SLB can be produced using GUVs.
8. Stability of the SLB both in cell culture conditions and without cells is limited but sufficient to carry out experiments with cells.

These conclusions should be taken into account when using the SLB for cell research or for biomedical applications.

8.3. Outlook

Using the SLB as a platform for cell culture, one can advance fundamental research in the field of cell adhesion and cell signaling. Adhesion of cells to the artificial membrane built on the surface that containes specifically chosen proteins can be studied instead of studying interaction between two cells. Advanced methods can be implemented here. Adhesion of cells to the SLB can be studied by TIRF microscopy. Using such modification of this method as VA-TIRF, one can define the distance from the surface to the cell membrane, which is more difficult (if possible at all) for cell-cell interactions. Such advanced methods as SPR, nanoparticle enhanced SPR, ellipsometry and QCM-D can also be implemented for studying cell adhesion to the SLB.

Along with studying cell adhesion, cell signaling can be studied. Investigations started in the frame of this work showing the influence of Ephrin on cell maturation and synapse formation should be continued. In addition to

statistical improvements of already obtained data, studies of synapse morphology and investigation of membrane protein expression should be done. The morphology can be also studied using TIRF. Other membrane proteins can be tested. If these proteins do not provide adhesion for cells, positively charged bilayers can be used.

Not only fundamental studies, but also applied areas of research can benefit from using the SLB as a platform for cell culture. Among them one can underline neuroelectronic interfacing. There are many attempts to establish interface between neurons and electronic devices using planar arrays of microelectrodes (MEA), field effect transistors (FET) arrays or nanowire (NW) arrays [100], [101]. There has been some success achieved but some problems remain to be overcome concerning biocompatibility, adhesion and mechanical properties of the electronic chips. Biocompatibility can be improved using the SLB as it represents a biomimetic surface and can mimic the natural environment for neurons.

Adhesion of neurons to the electrode sites is important and should be as strong as possible to reduce the gap between the cell and the electrode, thus reducing the leakage current and making recorded signals higher. SLB on the surface of a chip can help to improve cell adhesion (fig. 7.1(A)).

In the area of SLB applications for neuroelectronic interfaces an interesting idea of an artificial synapse arises. It is based on possibilities of patterning SLB and incorporating into that SLB specific synaptic proteins that can promote synapse formation at a certain place on the surface, in particular over recording sites (fig. 7.1(B)). Special receptors for neurotransmiters should be incorporated into the SLB to detect synaptic transmission. This is complicated because of difficulties of membrane protein purification and incorporation but other possibilities exist. In the case of using nanowires, an incoming AP can be detected. Redox active neurotransmiters such as dopamine or adrenaline can be detected electrochemically [178]. For this detection, neurotransmitter molecules must be provided access to the electrode. This can be achieved, for example, by using nanoporous materials (nanoporous Si or Al_2O_3) on which lipid bilayer could be formed.

Stability of the SLB is an important issue and should be taken into account before using the SLB. As was shown in the present work, holes appear in the SLB and if an application requires a confluent bilayer, it can become a problem. However, it seems to be possible to improve the stability of the SLB. For example, air stable SLB can be produced by tethering lipids to the surface [137], by covering the bilayer with proteins or polymers [179] or by introducing trehalose into solution [180]. Similar methods could be used to improve long term stability of the SLB, which would increase the range of its applications.

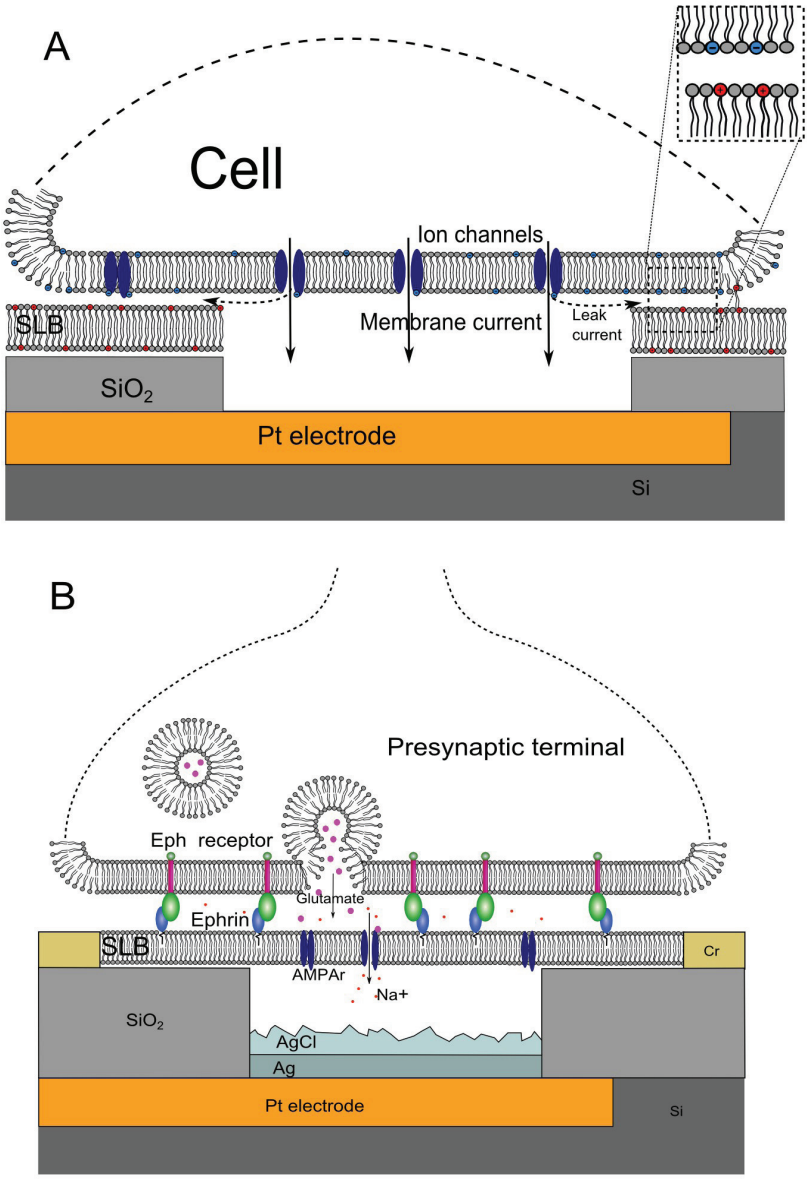

Figure 8.1: (A)A schematic representation of the SLB enhanced MEA: Positively charged SLB is formed on the surface of the chip (the area of the electrode stays free as liposomes can not fuse on metall). Due to electrostatic interaction of negatively charged cell membrane with the SLB the cell adheres to it tightly, reducing the gap between the cell membrane and the surface making the leak current lower. (B)The concept of an artificial synapse using SLB: a lipid bilayer is suspended over a planar AgCl electrode (AgCl is used to measure currents) of a MEA. Synapse adhesion protein (Ephrin) promotes formation of the synapse. Receptors, incorporated into the SLB (AMPAr in the present scheme) sense synaptic vesicle release and pass ions upon neurotransmiter binging.

Acknowledgments

It had been a really long way since I decided to do my PhD, the way with many turns and obstacles which made it harder. But at the same time there were many people who helped me to pass through everything and finally come to this place where I am.

First of all I'd like to thank to my supervisor – **Prof. Andreas Offenhäusser**: for the possibility to work at ICS-8 and to use advanced research equipment and infrastructure of the institute, for the supervision, for appreciating my opinion and giving me a lot of freedom in planing the experiments.

I'd like to thank to my colleagues form ICS-8 how directly helped me in my work:

Vanessa Maybeck for helping me in the lab, for teaching me many things especially concerning biology, for useful and interesting discussions of not only my work but also general scientific topics, for reading my papers and correcting my poor English.

Jonas Albers for great help with patch clamp experiments.

Ida Delac – our summer student – for help in the lab and for forcing me to help her with her project, as I could learn new things and advance my research.

Alexey Yakushenko for a possibility to discuss many topics (work and not only) in my native language, for ideas and advices, and also for reading a part of this thesis and making suggestions about it.

Philipp Rinklin for translating the abstract of this thesis to German.

Ranjita Ghoshmoulick for the collaboration, for helping with experiments, for finding useful papers about ephrin.

Especially I would like to mention **Kristin Elisabeth Michael** who were supervising me at the very beginning of my work in Jülich. She is no longer with us and will not be able to read these acknowledgments. I am happy that I had time to tell her that she was the best teacher who ever taught me how to work in the lab.

Our technical assistants at ICS-8:

Rita Fricke for teaching me useful tricks of cortex preparation and for preparing cells.

Bettina Breuer and **Steffani Zummengen** for preparing cells and keeping our labs in order.

Marko Banzet and **Michael Prömpers** for producing chips and for maintaining some devices in our labs.

All **other members of ICS-8** for creating nice and friendly atmosphere at the institute which helped to work greatly.

I'd like to thank to people from ICS-7:

Zhanna Santybayeva for usefull and interesting discussions, for proposals of collaboration, for being a good friend and for reading some parts of this thesis.

Dr. Agnes Csiszar for providing possibilities of using her divices and for very useful discussions concerning DOTAP lipisomes and bilayers.

I'd like to thank to my former teachers and supervisors, who taught me and influenced me a lot leading to the present thesis and my friends and family.

Holger Wigström – my former supervisor from Sweeden – he was like a father for me during first visit abroad. In his lab I learned a lot of useful techniques which helped me in the present work.

Pavel Bulay – my first supervisor, friend and colleague who inspirited me once to become a biophysicist and taught me many very important things concerning general work in the lab, modeling and scientific writing.

Ekaterina Schamova for being a good friend for all this time since our student years in Belarus. For always being ready to help in particular with this thesis.

Many thanks to my Jülich friends **Sergey Pud, Viktor Sydoruk, Francisco Carrega, Oliviera Corculanin, Kamilya Zhenusova** for making me feel not so lonely; to **Svetlana Borisova** for showing me that there are people nearby who share my points of view about this world.

Thanks to my **Mom** and **brother** for their love and attention, for reminding me that I have a family.

Also, I must thank to Deutscheforschungsgemeinschaft for providing financial support for me via GK Bionik.

DFG Deutsche Forschungsgemeinschaft

BIONIK GRADUATE Bonn - Jülich - Aachen

At the end, I would like to thank a lot and express my great respect to developers of free and opensource software – Linux kernel, MintLinux OS and OpenOffice. Unfortunately people don't pay attention to these great software pieces. They helped me a lot in my work. This thesis was created in OpenOffice. My home computer works under Linux Mint.

Linux Mint from freedom came elegance

Apache OpenOffice™

Appendix A

Materials and equipment

A.1 Materials

Table A.1 List of materials

Material	Notes	Supplier	Catalogue number
Glass cover-slips	Diameter = 30mm, Thickness #1 or #2	Thermo Fisher Scientific Inc.	
Hellmanex	Hellmanex II or Hellmanex III	Hellma GmbH & Co	
PBS	According to the Protocol B13		
DPBS	PBS with Ca^{2+} and Mg^{2+}, 10x	Life Technologies	14080
POPC	In chloroform	Avanti Polar Lipids, Inc	850457C
DOTAP	In chloroform	Avanti Polar Lipids, Inc	890890C
NBD-PE	In chloroform	Avanti Polar Lipids, Inc	810155C
Texas Red-PE	Powder	Life Technologies	T1395MP
Ephrin A5	Powder	R and D systems	374-EA-200
n-octyl-β-D-glucoside	Powder	Avanti Polar Lipids, Inc	850511P
HBSS		Sigma-Aldrich, Gmbh	H6648
Neurobasal medium		Life Technologies	21103
B27 supplement		Life Technologies	17504-044
L-glutamine	Aliquoted, freezed	Sigma-Aldrich, Gmbh	

Gentomicin	Aliquoted	Sigma-Aldrich, Gmbh	G1397
Trypan blue		Sigma-Aldrich, Gmbh	T8154
Poly-l-lysine	Aliquoted, freezed	Sigma-Aldrich, Gmbh	P1399
GBSS		Sigma-Aldrich, Gmbh	G9779
Calcein AM	Aliquoted, freezed		
Ephrin Ab-Goat IgG	Powder	R and D systems	AF3743
Powder	Powder	Life Technologies	A-11015
SDS		Sigma-Aldrich, Gmbh	L6026
Sylgard 184 Silicone elastomer	PDMS	Dow corning	

A.2 Equipment

Table A.2 List of devices

Equipment	**Specification**	**Manufacturer**
Ultrasonic bath	Bandelin Sonorex	Sonorex
Plasma oven	Plasma system PICO	Diener Electronics
Avanti mini extruder		Avanti Polar Lipids, Inc
Spectrophotometer	PerkinElmer Lambda 900	PerkinElmer, Inc
Inverted microscope	Axiovert 200	Carl Zeiss, Gmbh
Upright microscope	AxioScope	Carl Zeiss, Gmbh
Upright microscope	ApoTome	Carl Zeiss, Gmbh
Laser		Rapp Opto-Electronics
Neubauer counting chamber		Marienfeld-Superior
Patch clamp amplifier	HEKA EPC9	HEKA Elektronik Dr. Schulze GmbH
Vesicle Prep Pro	Device for GUV electroformation	Nanion technologies
NanoSight LM10	Nanoparticle tracking system	NanoSight, Ltd
Q-Sense E4	QCM-D device	BiolinScientific/Q-Sense

Appendix B

Protocols

B.1 Preparation of small unilamellar vesicles (SUV)

Devices
Avanti mini extruder
Vacuum pump

Materials
Lipids from:

Avanti:	POPC – 25mg/ml DOTAP – 25mg/ml NBD-PE – 1mg/ml
Invitrogen:	TexasRed-DHPE – 1mg/ml

Chloroform

Procedure

1. Mix lipids and dilute them in chloroform in a glass flask in such a way that the final concentration is 10mg/ml. Check if the flask is clean. Rinse it with chloroform before using.

! The examples of dilutions (in each case you have 500ul of lipids of 10mg/ml):

Table B1.1 Examples of dilutions

	0% DOTAP (no label)	0% DOTAP	5% DOTAP	30% DOTAP	100% DOTAP
Chlorophorm	300ul	300ul	300ul	300ul	300ul
POPC	200ul	200ul	190ul	140ul	0ul
DOTAP	0ul	0ul	10ul	60ul	200ul
NBD-PE (or TexasRed	0ul	10ul	10ul	10ul	10ul

❗ Lipids should always be stored in a freezer in glass vials closed with Teflon lids and sealed with parafilm

❗ Warm up the vials with lipids to room temperature before opening them when you take them out of the freezer. If you open the vial when it is still cold, humidity from air can precipitate on the inner wall of the vial and spoil lipids.

❗ Work with lipids under the chemical hood.

❕ It's OK to use plastic pipette tips to take lipids in chloroform, if you do it quickly

2. Make lipids dry on the walls of the flask under the stream of nitrogen. Rotate the flask to spread lipids uniformly. Leave the flask in vacuum for 1h to remove residue of chloroform.

3. Add buffer to dried lipids to get final concentration 5mg/ml (if you have 500ul of lipids of 10mg/ml add 1ml of buffer). Shake intensively. Large multilamelar vesicles (LMV) should be produced. You can sonicate LMV in a bath sonicator on ice to make them smaller and break clusters down.

4. Extrude vesicles using Avanti mini extruder.

4.1 assemble the extruder (see fig. B1.1 and instructions at the Avanti Polar Lipids, Inc. web page [123]):

❗ Work with gloves, use a tweezers

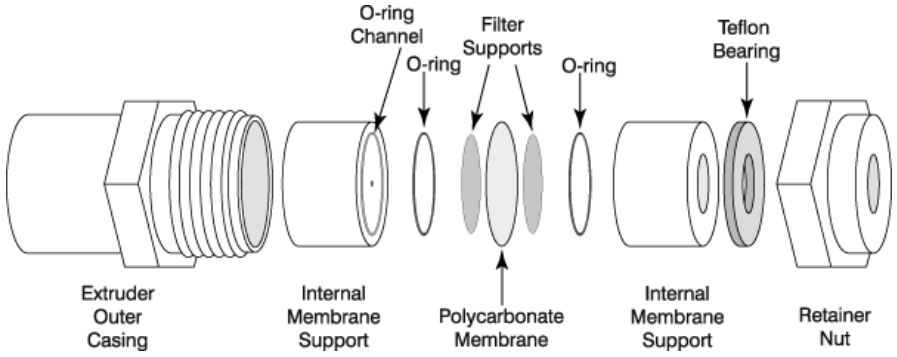

Figure B1.1: The diagram showing the assembly of the Avanti mini extruder [123].

4.1.1 position an O-ring in the O-ring channel of each internal membrane support

4.1.2 lightly wet the filters with mili-Q water supports they can't fall off.

4.1.3 put one of the internal membrane supports into the extruder outer casing

4.1.4 lay a membrane on the O-ring with a tweezers.

❗ CRUCIAL STEP . The membrane must be perfectly in place, sealed, and not folded !

4.1.5 put another internal membrane support on top, insert a Teflon bearing into the retainer nut, screw the nut tight on the casing.

4.1.6 put it into the extruder holder

4.2 Fill one syringe with LMV and insert into the nut side of the extruder, the empty one on the casing side.

4.3 Operate the syringes so that the contents pass through the membrane at least 11 times. Small unilamelar vesicles (SUV) are produced.

❗ Always do odd number of times. Finish in the syringe which was initially empty.

4.4 Put SUV into a glass vial. Store them in a fridge.

❗ Don't use plastic for storing liposomes.

4.5 Rinse the syringes with 2ml Ethanol and 10 ml milli-Q water. Rinse membrane supports, O-rings and Teflon bearing first with Ethanol, then with milli-Q water. Leave them on tissue to dry.

B.2 Glass slides cleaning for SLB preparation

Devices
Ultrasonic bath

Materials
Hellmanex 2%
Glass coverslips

Procedure

1. Chose glass slides or cover slips of suitable size and shape.
2. Put the glass slides into a holder in such a way that they cannot scratch each other and sonicate them in Hellmanex 2% and then rinse extensively by deionized water.

   ❗ While drying water should spread on the surface uniformly producing thing layer on which lines of interference of light should be seen. If water does not produce the thin layer but forms drops, it means that the surface is not clean enough. In this case repeat sonication in Hellmanex2% and

rinsing again.
3. Rinse glass slides with miliQ water.
4. Make the glasses dry by nitrogen stream or in a dryer.
5. Activate the glass slides by oxygen plasma in plasma oven (5 min, pressure 4.0, generator 0.4). Immediately go to the next step.

B.3 Preparation of the Supported lipid bilayers (SLB) by vesicle fusion

1. Put the glass slide into a Petri dish. Put PDMS wells on to the glass slide. Be sure that they stick tightly to the surface.

   ! These squares are necessary to prevent exposure of the SLB to air while rinsing or changing of solution. It also helps to make the SLB of different type on one glass slide in the same Petri dish.
2. Dilute liposomes to 0.1mg/ml with a buffer containing Ca and Mg ions.
3. Apply vesicles on the glass slide – 100ul per 1cm^2.
4. Wait for 20 – 30 min.
5. Rinse the SLB with a flow of buffer to remove excess of vesicles using a syringe – 20ml of buffer per 1cm2. Avoid bubbles.

   ! Don't expose lipid bilayers to air – they are immediately destroyed.

B.4 Optical density measurements

Devices
Spectrophotometer

Materials
N-octyl-β-D-glucoside - 100mM water solution
POPC liposomes 5mg/ml (the concentration may be lower due to losing of lipids during extrusion)

Procedure
1. Rinse the cuvettes with 70% ethanol and then with milli-Q water.
2. Fill both cuvettes with PBS and make reference measurement.
3. Remove solution from the sample cuvette and add 950ul of PBS and 600ul of POPC liposomes.
4. Measure OD adding step by step small amount of detergent solution (around 10 ul).

   ! Use small magnetic rotor to steer the solution right in the cuvette. Steer

the solution before each measurement. Add detergent while steering to minimize effect of local concentration increase.

B.5 Ephrin A5 reconstitution from detergent

Devices
Avanti mini extruder
Vacuum pump

Materials
POPC – 25 mg/ml in chloroform,
Ephrin A5- 200mg/ml, 25ul aliquots, kept in the freezer
N-octyl-β-D-glucoside - 100mM water solution

Procedure
1. Mix 25ul of POPC solution with 200ul chloroform in a glass flask. Check if the flask is clean. Rinse it with chloroform before using.
2. Dry lipids on the walls of the flask under the stream of nitrogen. Rotate the flask to spread lipids uniformly. Leave the flask in vacuum for 1h to remove residue of chloroform.
3. Mix 425ul of PBS with 50ul detergent solution and then with and 25ul ephrin A5 solution. Total volume is 500ul. Shake intensively to produce large multilamelar vesicles (LMV). Do not use ultrasound to prevent protein denaturation.
4. Extrude vesicles using Avanti mini extruder as described in Protocol B1.
5. Use produced proteoliposomes right after preparation

B.6 Immunofluorescence of lipid bilayers

Materials
Primarily Ab: ephrin Ab -Goat IgG (R&D,AF3743), 100ul/ml, aliquots 25ul
Secondary Ab: Alexa Fluor® 488 donkey anti-goat IgG (H+L), 2 mg⁄mL (Invitrogen, A-11055),

Procedure
1. Produce the SLB from proteoliposomes as described in Protocol B.3.
2. Fill the dishes with excess of buffer and left for ~30 min to remove residues of detergent
3. Dilute 20 ul of primarily Ab solution in 125 ul of PBS. Add 20 ul of this mixture into each well.

! No blocking buffer is required

4. Incubation 1.5h at room temperature.
5. Wash with the gentle stream of PBS.
6. Dilute 10 ul of primarily Ab solution in 1 ml of PBS. Add ~50ul of this solution to each well.
7. Incubation 1.5h at room temperature.
8. Wash with the gentle stream of buffer. The samples are ready for taking images with fluorescent microscope.

B.7 FRAP

1. Take a reference image with Axiovision.
2. Shut down Axiovision and start RapOptoelectronics software to control the laser.
3. Close the shutter of the fluorescent lamp. Bleach a spot in the centre of the field of view (~1 min, ~30% of power of the laser).
4. Shut down RapOptoelectronics software. Start Axiovision. Take images with ~1 min interval.

   ! Keep the shutter of the fluorescent lamp closed between image acquisition to prevent bleaching of the sample.
5. Use Simple FRAP analyser software to calculate diffusion coefficient (Appendix C).

B.8 PLL coating

1. Dilute PLL to 10 ug/ml.
2. Treat glass cover slips in flame (to sterilize them), wait several seconds to cool them down and put them in to Petri dishes.
3. Apply 1 ml of PLL solution to each Petri dish. Incubate for 20 min.
4. Wash the samples very gently with PBS twice. Fill the dishes with PBS and keep at 4°C.

B.9 Cortex preparation

(based on the protocol from [181])

This protocol is performed under sterile conditions. Cortical neurons are prepared from E18 Wistar rat embryos, mechanically dissociated, and plated onto in vitro growth substrates by the following protocol:

1. Remove brain in 1.5 mL HBSS− on ice.

2. Isolate cortex without dura and transfer to 7 mL HBSS− in a 15 mL Falcon tube. Pool as many cortices as necessary, always storing on ice.
3. Reduce the volume of HBSS− to 1 mL per brain.
4. Mechanically dissociate cells with a silanized, fire polished, glass pipette.
5. Add one volumes HBSS+ and allow to settle for 3 min on ice.
6. Transfer 1 ml from the top of the preparation to a clean tube with 5 ml of NB.
7. Centrifuge at 200 g for 3 min.
8. Aspirate HBSS and resuspend the pellet in 1 mL supplemented NB media.
9. Dilute trypan blue 1:2 in NB media, then add 1 volume of cell suspension for live dead staining. The final mixture is 1:2:1, trypan blue:NB:cell suspension. 25 µL is the standard volume for trypan blue.
10. Count live (not blue) cells in a Neubauer chamber and dilute to appropriate plating concentrations in NB. Distribute to substrates.
11. Let substrates stand at room temperature for 10 min, then transfer to a 37°C 5% CO2 humidified incubator.
12. After 1-4 hours of adhesion, remove half of media and replace with fresh NB. Then change half of the media every 3-4 days.

B.10 Cell staining with calcein-AM

1. Dilute calcein-AM: 1 ul per 1 ml of PBS contained Ca^{2+} and Mg^{2+} ions.
2. Replace cell culture medium to calcein-AM solution.
   ❗ Warm up all solutions to 37°C before adding them to cells.
3. Incubate at 37°C for 5 min.
4. Replace calcein-AM solution with PBS contained Ca^{2+} and Mg^{2+} ions. The samples are ready to take pictures.

B.11 Preparation of GUV

Devices
Vesicle Prep Pro
Vacuum pump

Materials
POPC – 25 mg/ml in chloroform
Glucose solution – 200mM
Chloroform.

Procedure

1. Dilute lipids: 50 ul of POPC with 100 ul of chloroform.
   ❗ Consider notes from Protocol B1
2. Put 20 ul of the lipid solution on the conduction surface of the ITO-coated slide.
3. Let chloroform to evaporate. Leave the slide in vacuum for ~1 h to remove the residues of solvent.
4. Place the ITO slide into the device and a rubber o-ring on the slide around the dry lipid film.
5. Add around 300 ul of glucose solution.
6. Place the second ITO slide on the top, close the Vesicle Prep Pro and run the protocol: frequency -10 Hz, amplitude – 2.5 V, temperature – 25°C, rise time – 100 min, main time – 300 min, fall time – 100 min.
7. When the protocol is finished collect vesicles with a pipette.

B.12 Protein microcontact printing

1. Clean stamps for 5-10 minutes in 70% Ethanol
2. Work on ice and make the protein solution (10mL GBSS + 100µL PLL)
3. Dry the stamps in a Nitrogen stream
4. Put the stamps for 20 minutes in the protein solution
5. Dry the stamps carefully in a gentle Nitrogen stream.
   ❗ Work carefully, so that you don't blow the proteins away from the stamp surface.
6. Place a PDMS stamp on the coverslip, put 10 g weight and leave it for 3-5 min.
7. Remove the stamp and store the substrate at 4°C until plating cells.
   ❗ Pull it directly up to prevent smashing the printed structures

B.13 PBS formulation

Table B13.1 PBS formulation

Salt	Molar mass, g/mol	Concentration, mM	Concentration, g/L
NaCl	58.44	137	8
KCL	74.55	2.7	0.2
Na_2HPO_4	141.96	8.7	1.24
NaH2PO4xH2O	138	1.48	0.2

Appendix C

"Simple FRAP analyser" software

C.1 Software description

Simple FRAP analyser is a MATLAB based software designed to process data of photobleaching experiments and calculate diffusion coefficient. It consists of several functions. The main function is called SimpleFrapAnalyzer. It accepts the required parameters, calls other functions responsible for data processing and returnes calculate data. This function has the following format:

```
[D,dD,u_ex,u_ca,t]=SimpleFrapAnalyzer(DirPath,Dinit,PixelSize,X,fi1,fi2,n)
```

Output:
D – diffusion coefficients (m^2/s)
dD – variance of D (m^2/s)
u_ex – an array of experimentally measured intensity profiles
u_ca – an array of calculated intensity profiles
t – an array of time points

Input:
DirPath – path to a folder with FRAP images
Dinit – initial guess about diffusion coefficient (m^2/s)
PixelSize – real size of the pixel in the image (m)
X – is an array [x1 x2] to specify the coordinates of the centre of the bleached spot. If 0 is provided, the program will try to find the centre automatically (pixels)
fi1 – start angle for circular averaging (degree)
fi2 – end angle for circular averaging (degree)
n – number of therms in the solution. Usually 50 is enough.

The SimpleFrapAnalyzer calls first the ReadFrapData function. It reads the image files and extract profiles of intensity and time points. Files should be named in a special way: a file name should contain a word 'time' directly followed by the

time in hh-mm-ss format, e.g. popc-b1-time16-00-48.jpg. The file with the reference image should contain a word 'reference' in its name, e.g. popc-b1-reference.jpg. The ReadFrapData function subtract the reference image from all the other images which helps to get rid of uneven illumination. If the coordinates of centre (x1,x2) of the spot was not specified, it calls the FindSpotCentre function which tries to find them. Then the function RadialMean is called which calculates the intensity profiles for each image. A function FitD first calls the PolarDifSolv function (which finds the solution of the diffusion equation) and then performs the fitting algorithm.

While working the program returns messages in the MATLAB Command Window informing the user about the procedure which is being done at the moment. It displays the centre of the spot in first image for the user to have possibility to check visually correctness of the centre finding. In the separate figure extracted intensity profiles together with the calculated ones are plotted (fig. C1.1).

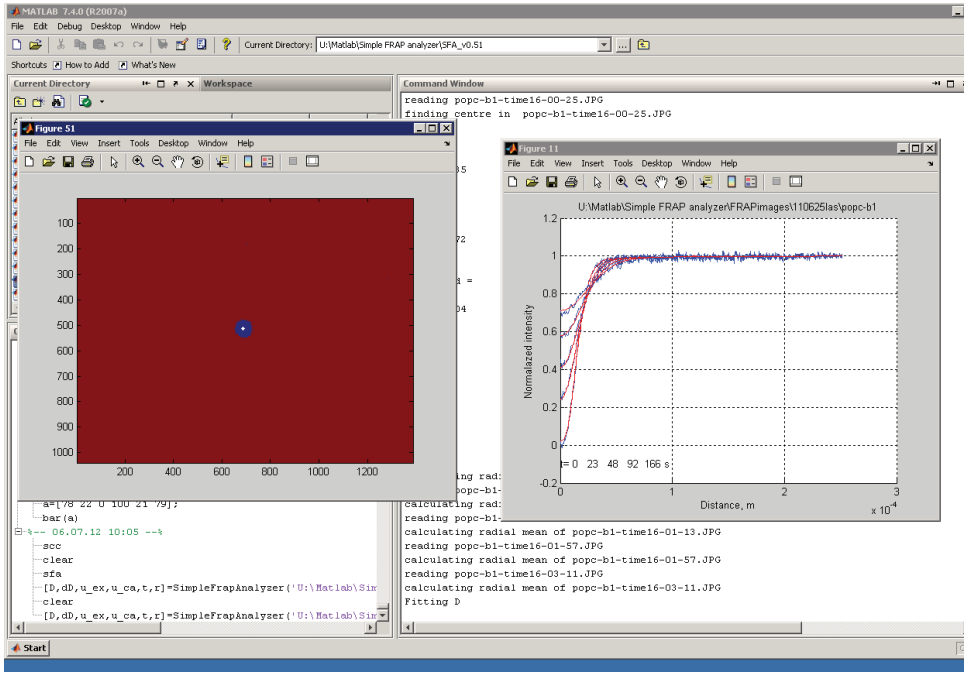

Figure C1.1: A screen shot representing the result of work of "Simple FRAP analyzer" program. In the MatLab figure 51 the binarized image of the bleached spot is shown. The centre found by the program is depicted by the white dot. The MatLab figure 11 represents the experimental profiles of intensity (blue curves) and analytically calculated profiles (red curves). In the MatLab command window messages about currently running procedures are shown.

C.2 Source code

SimpleFrapAnalyzer.m

```
function
[D,dD,u_ex,u_ca,t]=SimpleFrapAnalyzer(DirPath,Dinit,PixelSize,X,fi1,fi2,n)
%Output:
%D - diffusion coefficients (m2/s)
%dD - variance of D (m2/s)
%u_ex - an array of experimentally measured intensity profiles
%u_ca - an array of calculated intensity profiles
%t - an array of time points
%Input:
% DirPath='U:\Matlab\Simple FRAP analyzer\FRAPimages\Simulation\simulation';
% Dinit - initial guess about diffusion coefficient (m2/s);
% PixelSize - real size of a pixel in the image (m);
%X=[x1,x2] - coordinates of the centre of the spot. If X=0 x1,x2 will be
found automatically.
i1 - start angle for circular averaging (degree)
fi2 - end angle for circular averaging (degree)
n - number of therms in te solution. Usually 50 is enough.
[u_ex,t]=ReadFrapData(DirPath,X,fi1,fi2);
[D,dD,u_ca]=FitD(u_ex,Dinit,PixelSize,t,n);

x=PixelSize*[1:length(u_ex(1,:))];
h11=figure(11);hold on;
grid on
for i=1:length(u_ex(:,1))
    plot(x,u_ex(i,:));plot(x,u_ca(i,:),'r')
end
xlabel('Distance, m');
ylabel('Normalazed intensity');
title(num2str(DirPath));
text(x(1),-0.1,['t= ',num2str(t),' s']);
text(x(1),1.1,['D= ',num2str(D*1e12),' +-',num2str(dD*1e12),' um^2/s']);
```

ReadFrapData.m

```
function [u_ex,t]=ReadFrapData(DirPath,X,fi1,fi2)
%This function reads fluorescence recovery images placed in DirPath and
extract intensity profiles u_ex as well as time of image aquisition
%(it is specified in filenames in the following way: *timehh-mm-ss*.*)

u_ex=[];
d=dir(DirPath);
i=0;
t=1;
ref_on=0;
for j=1:length(d)
    s=d(j).name;
    if isempty(strfind(s,'reference'))~=1
        s_ref=s;
        ref_on=1;
    end
end
if ref_on==1
```

```
    Iref=double(imread([DirPath,'/',s_ref]));
else
    Iref=0;
end
for j=1:length(d)
            s=d(j).name;
            if isempty(strfind(s,'time'))~=1%we ignore everything except
files containing 'time' in their names
               i=i+1;
                %finding and extracting time
                k = strfind(s, 'time');
                if ~isempty(k)
                    hh(i)=str2num(s(k+4:k+5));
                    mm(i)=str2num(s(k+7:k+8));
                    ss(i)=str2num(s(k+10:k+11));
                else
                 t=0;
                end
               %
                disp(['reading ',s]);
                I1=double(imread([DirPath,'/',s]));
                I1=I1-Iref;
               if i==1%finding centre only for the first image
                    if X==0
                        disp(['finding centre in  ',s]);
                        [x1,x2]=FindSpotCentre(I1,1)
                    else
                        x1=X(1);
                        x2=X(2);
                    end
               end
              disp(['calculating radial mean of ',s]);
               Ir=RadialMean(I1,x1,x2,fi1,fi2,32);
               mIr=mean(Ir,2);
               %plot(mIr);pause(1)
               u_ex=[u_ex,mIr];
         end
end
u_ex=u_ex';
u_ex1=u_ex;
len=length(u_ex(1,:));
for i=1:length(u_ex(:,1))
    u_ex1(i,:)=(u_ex(i,:)-mean(u_ex(i,round(0.9*len):len))+
(mean(u_ex(1,round(0.9*len):len))-mean(u_ex(1,1:5))))...
                /abs(mean(u_ex(1,round(0.9*len):len))-mean(u_ex(1,1:5)));
end
u_ex=u_ex1;
if t~=0
    t=FrapTimeSteps(hh,mm,ss);
end
```

FitD.m

```
function [D,dD,u_ca]=FitD(u_ex,Dinit,scale,t,n)
%This function fits the solutions of the diffusion equations in polar
coordinates to experimental intensity profiles (u_ex) by searching for
suitable diffusion coefficient (D)
%u_ex - experimental intensity profiles. It is extracted from images by
```

```
ReadFrapData
%u_ca - an array of calculated intensity profiles
%Dinit - initial guess about diffusion coefficient (m2/s);
%scale - PixelSize
%D - diffusion coefficients (m2/s)
%dD - variance of D (m2/s)
%t - an array of time points
D=Dinit;
u0=u_ex(1,:);
r0=length(u0)*scale;%r0 - radius of the area under consideration
ur0=mean(u_ex(1,length(u_ex)-20:length(u_ex)));%ur0 - boundary condition at
the point r0
Dnum=11;
mindu1=1;
k=0.1;
disp('Fitting D');
while 1
    for i=1:Dnum
        Drange(i)=D+k*D*(5-(i-1));
    end
    du=zeros(1,length(Drange));
    for j=1:length(Drange)
        for i=1:length(t)
                    u=PolarDifSolv(u0,Drange(j),r0,t(i),n,ur0);
                    du(j)=du(j)+sum((u-u_ex(i,:)).^2)/length(u);
        end
        du(j)=du(j)./length(t);
    end
    [mindu2,minj]=min(du)
    D=Drange(minj)
    if (minj~=1)&&(minj~=length(Drange))
        k=k/1.5;
    else
        k=k;
    end
    if abs(mindu1-mindu2)<0.005*mindu2
        disp('The accuracy of 1% has been archived. Process stopped.')
        break;
    end
    mindu1=mindu2;
end
dD=k*D;
u_ca=[];
t(1)=0.01*t(2);
for i=1:length(t)
    u_ca=[u_ca;PolarDifSolv(u0,D,r0,t(i),n,ur0)];
end
```

PolarDifSolv.m

```
function u=PolarDifSolv(u0,D,r0,t,n,ur0)
%This function solves the Dirichlet problem for the diffusion equation in
polar coordinates
%u0 - initial condition (a vector)
%D - diffusion coefficient
%r0 - radius of the area under consideration
%t - time (size = 1x1)
%n - number of terms of the row of the solution // ~50 was OK
```

```
%ur0 - boundary condition - u(r0)=const
N=length(u0);
dr=r0/N;
r=dr:dr:r0;
u=zeros(1,N);
u0=u0-ur0;
for m=1:n
    mu0m=BesselJzero(m);
    f=u0.*r.*besselj(0,mu0m*r/r0);
    Cm=2*trapz(r,f)/(r0*besselj(1,mu0m))^2;
    u=u+Cm*besselj(0,mu0m*r/r0)*exp(-D*(mu0m/r0)^2*t);
end
u=ur0+u;
```

FindSpotCentre.m

```
function [x1,x2]=FindSpotCentre(I,ShowResult)
%This function finds coordinates of a dark spot on a bright background
I=double(I);
%setting threshold between min and mean value of intensity
Imin=min( Smooth1D(min(I)',round(0.03*length(I(1,:)))) )
Imean=mean( Smooth1D(mean(I)',round(0.03*length(I(1,:)))) )
threshold=Imin+(Imean-Imin)/2
%Making the image black and white
I1=gray2bw(I,threshold);
%
SI1=sum(I1);%
SI2=sum(I1');
nx1=round(0.03*length(SI1));
nx2=round(0.03*length(SI2));
sSI1=Smooth1D(SI1',nx1);
sSI2=Smooth1D(SI2',nx2);
[mins1,x1]=FindLocalMin1D(sSI1,nx1);
[mins2,x2]=FindLocalMin1D(sSI2,nx2);
if length(x1)>1
    [a,b]=min(mins1);
    x1=x1(b);
end
if length(x2)>1
    [a,b]=min(mins2);
    x2=x2(b);
end
if ShowResult
    figure(51);image(I1*128);hold on
    plot(x1,x2,'ko');hold off
end
```

gray2bw.m

```
function I1=gray2bw(I,threshold)
%Converts an image I to a black and white image I1 according to the specified
threshold
I=double(I);
I1=I-threshold;
I1=sign(sign(I1)+1);
```

RadialMean.m

```
function Ir=RadialMean(I,x1,x2,fi1,fi2,n)
%I - image to be analyzed
%x1,x2 - coordinates of the centre of the spot
%fi1,fi1 - angles in degrees to start and finish averaging
%n - number of profiles to average
sz=size(I);
a1=length(I(x2,x1:sz(2)));
a2=x1;
a3=length(I(x2:sz(1),x1));
a4=x2;
R=min([a1,a2,a3,a4])-10;
dfi=(fi2-fi1)*pi/(180*n);
Ir=zeros(R,n);
b=zeros(R,1);
for i=1:n
    fi=fi1*pi/180+dfi*(i-1);
    for j=1:R
        xj=x1+round(j*cos(fi));
        yj=x2+round(j*sin(fi));
        b(j)=I(yj,xj);
    end
Ir(:,i)=b;
end
```

Bibliography

[1] B. Alberts, A. Johnson, J. Lewis, M. Raff, and K. Roberts, “Cell Movements and the Shaping of the Vertebrate Body,” in *Molecular Biology of the Cell*, Garland Science, 2002.

[2] S. Singer and G. Nicolson, “The fluid mosaic model of the structure of cell membranes,” *Science*, vol. 175, no. 4023, pp. 720–731, 1972.

[3] “Cell membrane,” *Wikipedia*. 2012.

[4] E. Sackmann, “Biological membranes architecture and function,” in *Handbook of biological physics*, vol. 1, 1995, pp. 1–62.

[5] “Extracellular matrix,” *Wikipedia*. 2012.

[6] G. J. Doherty and H. T. McMahon, “Mediation, modulation, and consequences of membrane-cytoskeleton interactions.,” *Annual review of biophysics*, vol. 37, pp. 65–95, Jan. 2008.

[7] P. Devaux, “Specificity of lipid-protein interactions as determined by spectroscopic techniques.,” *Biochimica et biophysica acta*, vol. 822, pp. 63–125, 1985.

[8] R. Gennis, *Biomembranes: molecular structure and function*. Springer, 1989.

[9] A. Gardas, “A structural study on a macro-glycolipid containing 22 sugars isolated from human erythrocytes.,” *European journal of biochemistry*, vol. 68, no. 1, pp. 177–83, Sep. 1976.

[10] J. Laitinen, R. Löppönen, J. Merenmies, and H. Rauvala, “Binding of laminin to brain gangliosides and inhibition of laminin-neuron interaction by the gangliosides.,” *FEBS letters*, vol. 217, no. 1, pp. 94–100, Jun. 1987.

[11] P. Yeagle, “Modulation of membrane function by cholesterol,” *Biochimie*, pp. 1303–1310, 1991.

[12] “Nernst equation,” *Wikipedia*. 2012.

[13] “Goldman equation,” *Wikipedia*. 2012.

[14] “Action potential,” *Wikipedia*. 2012.

[15] “Introduction to the Nervous System.” [Online]. Available: http://students.cis.uab.edu/nkm188/project_back2.html.

[16] G. Ehrenstein, “Surface charge,” in *Biophysics Textbook Online*, .

[17] N. Lakshminarayanaiah and K. Murayama, “Estimation of surface charges in some biological membranes.,” *The Journal of membrane biology*, vol. 23, no. 3–4, pp. 279–92, Jan. 1975.

[18] J. D’arrigo, “Possible screening of surface charges on crayfish axons by polyvalent

metal ions," *The Journal of physiology*, pp. 117–128, 1973.

[19] D. Gilbert, "Fixed surface charges," in *Biophysics and physiology of excitable membranes*, W. Adelman, Ed. Van Nostrand Reinhold, New York, 1971, p. 359.

[20] "Entropic force," *Wikipedia*. 2012.

[21] V. Luzzati, T. Gulik-Krzywicki, and A. Tardieu, "Polymorphism of lecithins," *Nature*, vol. 218, pp. 1031–1034, 1968.

[22] V. Luzzati, "X-ray diffraction studies of lipid-water systems," *Biological membranes*, vol. 1, pp. 71–123, 1968.

[23] C. Tilcock and P. Cullis, "On the validity of 31 P-NMR determinations of phospholipid polymorphic phase behaviour," *Chemistry and physics of lipids*, vol. 40, pp. 47–56, 1986.

[24] P. Cullis and B. Kruijff, "Lipid polymorphism and the functional roles of lipids in biological membranes," *Biochimica et Biophysica Acta (*, vol. 559, pp. 399–420, 1979.

[25] P. Cullis, B. D. Kruijff, and M. Hope, "Structural properties of phospholipids in the rat liver inner mitochondrial membrane. A 31P-NMR study," *BBA*, vol. 600, pp. 625–635, 1980.

[26] A. Blume, "Apparent molar heat capacities of phospholipids in aqueous dispersion. Effects of chain length and head group structure," *Biochemistry*, vol. 22, no. 23, pp. 5436–5442, Nov. 1983.

[27] G. Tresset, "The multiple faces of self-assembled lipidic systems.," *PMC biophysics*, vol. 2, no. 1, p. 3, Jan. 2009.

[28] J. M. Seddon and R. H. Templer, "Polymorphism of Lipid-Water Systems," in *Handbook of biological physics*, vol. 1, 1995, pp. 97–160.

[29] a Tardieu, V. Luzzati, and F. C. Reman, "Structure and polymorphism of the hydrocarbon chains of lipids: a study of lecithin-water phases.," *Journal of molecular biology*, vol. 75, no. 4, pp. 711–33, Apr. 1973.

[30] J. M. Seddon, "Structure of the inverted hexagonal (HII) phase, and non-lamellar phase transitions of lipids.," *Biochimica et biophysica acta*, vol. 1031, no. 1, pp. 1–69, Feb. 1990.

[31] P. Kekicheff and B. Cabane, "Between cylinders and bilayers: structures of intermediate mesophases of the SDS/water system," *Journal de Physique*, vol. 48, pp. 1571–1583, 1987.

[32] P. Mariani, V. Luzzatil, and H. Delacroix, "Cubic Phases of Lipid-containing Systems. Structure Analysis and Biological Implications," *J. Mol. Biol.*, vol. 204, pp. 165–189, 1988.

[33] I. Pascher, M. Lundmark, and P. Nyholm, "Crystal structures of membrane lipids eclipsed," vol. 1113, pp. 339–373, 1992.

[34] A. Blaurock, "Structure of the crystalline bilayer in the subgel phase of dipalmitoylphosphatidylglycerol.," *Biochemistry*, vol. 25, no. 2, pp. 299–305, Jan. 1986.

[35] J. L. Ranck, T. Keira, and V. Luzzati, "A novel packing of the hydrocarbon chains in lipids. The low temperature phases of dipalmitoyl phosphatidyl-glycerol.," *Biochimica et biophysica acta*, vol. 488, no. 3, pp. 432–41, Sep. 1977.

[36] W. Tsuzuki, “Cis-Trans Isomerization of Carbon Double Bonds in Monounsaturated Triacylglycerols Via Generation of Free Radicals.,” *Chemistry and physics of lipids*, vol. 163, no. 7, pp. 741–5, Sep. 2010.

[37] A. Zachowski, “Phospholipids in animal eukaryotic membranes: transverse asymmetry and movement.,” *Biochemical Journal*, vol. 14, pp. 1–14, 1993.

[38] T. Pomorski, S. Hrafnsdóttir, P. F. Devaux, and G. van Meer, “Lipid distribution and transport across cellular membranes.,” *Seminars in cell & developmental biology*, vol. 12, no. 2, pp. 139–48, Apr. 2001.

[39] “The Nanion Technologies GmbH web page.” [Online]. Available: http://www.nanion.de/images/stories/images/p44_1_GUV.jpg.

[40] “Liposome,” *Encyclopædia Britannica, Inc.* 2012.

[41] K. Matsuzaki, O. Murase, K. Sugishita, S. Yoneyama, K. Akada, M. Ueha, a Nakamura, and S. Kobayashi, “Optical characterization of liposomes by right angle light scattering and turbidity measurement.,” *Biochimica et biophysica acta*, vol. 1467, no. 1, pp. 219–26, Jul. 2000.

[42] C. Grabielle-Madelmont, “Characterization of loaded liposomes by size exclusion chromatography,” *Journal of Biochemical and Biophysical Methods*, vol. 56, no. 1–3, pp. 189–217, Jun. 2003.

[43] S. K. Wiedmer, J. Hautala, J. M. Holopainen, P. K. Kinnunen, and M. L. Riekkola, “Study on liposomes by capillary electrophoresis.,” *Electrophoresis*, vol. 22, no. 7, pp. 1305–13, Apr. 2001.

[44] L. Mayer and M. Hope, “Vesicles of variable sizes produced by a rapid extrusion procedure,” *Biochimica et Biophysica Acta (BBA)-*, vol. 858, pp. 161–168, 1986.

[45] N. Skalko, J. Bouwstra, F. Spies, M. Stuart, P. M. Frederik, and G. Gregoriadis, “Morphological observations on liposomes bearing covalently bound protein: studies with freeze-fracture and cryo electron microscopy and small angle X-ray scattering techniques.,” *Biochimica et biophysica acta*, vol. 1370, no. 1, pp. 151–60, Mar. 1998.

[46] R. Biltonen and D. Lichtenberg, “The use of differential scanning calorimetry as a tool to characterize liposome preparations,” *Chemistry and physics of lipids*, vol. 64, pp. 129–142, 1993.

[47] C. Demetzos, “Differential Scanning Calorimetry (DSC): a tool to study the thermal behavior of lipid bilayers and liposomal stability.,” *Journal of liposome research*, vol. 18, no. 3, pp. 159–73, Jan. 2008.

[48] G. Riquelme, E. Lopez, L. M. Garcia-segura, J. A. Ferragut, and J. M. Gonzalez-ros, “Giant Liposomes : A Model System in Which To Obtain Patch-Clamp Recordings,” *Biochemistry*, vol. 29, pp. 1 121 5–1 1222, 1990.

[49] D. Lasic, *Medical applications of liposomes*. Amsterdam: Elsevier, 1998.

[50] a Chonn and P. R. Cullis, “Recent advances in liposomal drug-delivery systems.,” *Current opinion in biotechnology*, vol. 6, no. 6, pp. 698–708, Dec. 1995.

[51] D. Lasic, “Applications of Liposomes,” in *Handbook of biological physics*, R. Lipowsky and E. Sackmann, Eds. Elsevier, 1995.

[52] D. D. Lasic, “Novel applications of liposomes.,” *Trends in biotechnology*, vol. 16, no. 7, pp. 307–21, Jul. 1998.

[53] M. Tanaka, A. P. Wong, F. Rehfeldt, M. Tutus, and S. Kaufmann, “Selective deposition of native cell membranes on biocompatible micropatterns.,” *Journal of the American Chemical Society*, vol. 126, no. 10, pp. 3257–60, Mar. 2004.

[54] K. a Edwards and A. J. Baeumner, “Analysis of liposomes.,” *Talanta*, vol. 68, no. 5, pp. 1432–41, Feb. 2006.

[55] K. a Edwards and A. J. Baeumner, “Liposomes in analyses.,” *Talanta*, vol. 68, no. 5, pp. 1421–31, Feb. 2006.

[56] “Monolayer,” *Wikipedia*. 2012.

[57] “Langmuir–Blodgett film,” *Wikipedia*. 2012.

[58] P. Mueller, D. Rudin, and H. T. Tien, “Reconstitution of cell membrane structure in vitro and its transformation into an excitable system,” *Nature*, 1962.

[59] P. Mueller, D. Rudin, and H. Tien, “Methods for the formation of single bimolecular lipid membranes in aqueous solution,” *The Journal of Physical*, 1963.

[60] E. T. Castellana and P. S. Cremer, “Solid supported lipid bilayers: From biophysical studies to sensor design,” *Surface Science Reports*, vol. 61, no. 10, pp. 429–444, Nov. 2006.

[61] L. Q. Gu, O. Braha, S. Conlan, S. Cheley, and H. Bayley, “Stochastic sensing of organic analytes by a pore-forming protein containing a molecular adapter.,” *Nature*, vol. 398, no. 6729, pp. 686–90, Apr. 1999.

[62] F. Gómez-Lagunas, A. Peña, A. Liévano, and A. Darszon, “Incorporation of ionic channels from yeast plasma membranes into black lipid membranes.,” *Biophysical journal*, vol. 56, no. 1, pp. 115–9, Jul. 1989.

[63] P. V. Gelder and F. Dumas, “Understanding the function of bacterial outer membrane channels by reconstitution into black lipid membranes,” *Biophysical chemistry*, 2000.

[64] a Studer, S. Demarche, D. Langenegger, and L. Tiefenauer, “Integration and recording of a reconstituted voltage-gated sodium channel in planar lipid bilayers.,” *Biosensors & bioelectronics*, vol. 26, no. 5, pp. 1924–8, Jan. 2011.

[65] B. Suarez-Isla, K. Wan, and J. Lindstrom, “Single-channel recordings from purified acetylcholine receptors reconstituted in bilayers formed at the tip of patch pipets,” *Biochemistry*, 1983.

[66] J. L. Gornall, K. R. Mahendran, O. J. Pambos, L. J. Steinbock, O. Otto, C. Chimerel, M. Winterhalter, and U. F. Keyser, “Simple reconstitution of protein pores in nano lipid bilayers.,” *Nano letters*, vol. 11, no. 8, pp. 3334–40, Aug. 2011.

[67] E. K. Schmitt, C. Weichbrodt, and C. Steinem, “Impedance analysis of gramicidin D in pore-suspending membranes,” *Soft Matter*, vol. 5, no. 17, p. 3347, 2009.

[68] E. K. Schmitt, M. Nurnabi, R. J. Bushby, and C. Steinem, “Electrically insulating pore-suspending membranes on highly ordered porous alumina obtained from vesicle spreading,” *Soft Matter*, vol. 4, no. 2, p. 250, 2008.

[69] S. Kresák, T. Hianik, and R. L. C. Naumann, “Giga-seal solvent-free bilayer lipid membranes: from single nanopores to nanopore arrays,” *Soft Matter*, vol. 5, no. 20, p. 4021, 2009.

[70] L. K. Tamm and H. M. McConnell, “Supported phospholipid bilayers.,” *Biophysical journal*, vol. 47, no. 1, pp. 105–13, Jan. 1985.

[71] V. Kiessling, M. K. Domanska, D. Murray, C. Wan, and L. K. Tamm, “Supported Lipid Bilayers : Development and Applications in Chemical Biology,” *Chemical Biology*, 2008.

[72] M. Tanaka and E. Sackmann, “Polymer-supported membranes as models of the cell surface.,” *Nature*, vol. 437, no. 7059, pp. 656–63, Sep. 2005.

[73] E. Sinner, “Functional tethered membranes,” *Current opinion in chemical biology*, vol. 5, no. 6, pp. 705–11, Dec. 2001.

[74] I. Köper, “Insulating tethered bilayer lipid membranes to study membrane proteins,” *Molecular BioSystems*, vol. 3, no. 10, p. 651, 2007.

[75] B. a Cornell, V. L. Braach-Maksvytis, L. G. King, P. D. Osman, B. Raguse, L. Wieczorek, and R. J. Pace, “A biosensor that uses ion-channel switches.,” *Nature*, vol. 387, no. 6633, pp. 580–3, Jun. 1997.

[76] O. Worsfold, N. H. Voelcker, and T. Nishiya, “Biosensing using lipid bilayers suspended on porous silicon.,” *Langmuir : the ACS journal of surfaces and colloids*, vol. 22, no. 16, pp. 7078–83, Aug. 2006.

[77] H. M. Keizer, B. R. Dorvel, M. Andersson, D. Fine, R. B. Price, J. R. Long, A. Dodabalapur, I. Köper, W. Knoll, P. a V. Anderson, and R. S. Duran, “Functional ion channels in tethered bilayer membranes--implications for biosensors.,” *Chembiochem : a European journal of chemical biology*, vol. 8, no. 11, pp. 1246–50, Jul. 2007.

[78] M. Trojanowicz, “Miniaturized biochemical sensing devices based on planar bilayer lipid membranes,” *Journal of Analytical Chemistry*, vol. 371, no. 2, pp. 246–260, Sep. 2001.

[79] R. P. Richter, R. Bérat, and A. R. Brisson, “Formation of solid-supported lipid bilayers: an integrated view.,” *Langmuir : the ACS journal of surfaces and colloids*, vol. 22, no. 8, pp. 3497–505, Apr. 2006.

[80] E. Sackmann, “Supported membranes: scientific and practical applications.,” *Science (New York, N.Y.)*, vol. 271, no. 5245, pp. 43–8, Jan. 1996.

[81] J. Raedler, H. Strey, and E. Sackmann, “Phenomenology and Kinetics of Lipid Bilayer Spreading on Hydrophilic Surfaces,” *Langmuir*, vol. 11, no. 11, pp. 4539–4548, Nov. 1995.

[82] O. P. Karlsson and S. Löfås, “Flow-mediated on-surface reconstitution of G-protein coupled receptors for applications in surface plasmon resonance biosensors.,” *Analytical biochemistry*, vol. 300, no. 2, pp. 132–8, Jan. 2002.

[83] Y. Domanov, “Supported lipid bilayer: properties, preparation and applications.” 2008.

[84] “Cell surface receptor,” *Wikipedia*. 2012.

[85] “G protein-coupled receptor,” *Wikipedia*. 2012.

[86] W. K. Kroeze, D. J. Sheffler, and B. L. Roth, “G-protein-coupled receptors at a glance.,” *Journal of cell science*, vol. 116, no. Pt 24, pp. 4867–9, Dec. 2003.

[87] U. Cavallaro and E. Dejana, “Adhesion molecule signalling: not always a sticky business,” *Nature Reviews Molecular Cell Biology*, vol. 12, pp. 189–197, 2011.

[88] M. B. Dalva, A. C. McClelland, and M. S. Kayser, “Cell adhesion molecules: signalling functions at the synapse.,” *Nature reviews. Neuroscience*, vol. 8, no. 3, pp.

206–20, Mar. 2007.

[89] K. Gerrow and A. El-Husseini, “Cell adhesion molecules at the synapse,” *Frontiers in Bioscience*, vol. 11, pp. 2400–2419, 2006.

[90] S. Murase and E. M. Schuman, “The role of cell adhesion molecules in synaptic plasticity and memory.,” *Current opinion in cell biology*, vol. 11, no. 5, pp. 549–53, Oct. 1999.

[91] P. Scheiffele, “Cell-cell signaling during synapse formation in the CNS.,” *Annual review of neuroscience*, vol. 26, pp. 485–508, Jan. 2003.

[92] M. Yamagata, J. R. Sanes, and J. a Weiner, “Synaptic adhesion molecules,” *Current Opinion in Cell Biology*, vol. 15, no. 5, pp. 621–632, Oct. 2003.

[93] M. Hortsch and H. Umemori, Eds., *The sticky synapse*. Springer.

[94] D. Arvanitis and A. Davy, “Eph/ephrin signaling: networks,” *Genes & development*, vol. 22, pp. 416–429, 2008.

[95] A. Rodenas-Ruano, M. a Perez-Pinzon, E. J. Green, M. Henkemeyer, and D. J. Liebl, “Distinct roles for ephrinB3 in the formation and function of hippocampal synapses.,” *Developmental biology*, vol. 292, no. 1, pp. 34–45, Apr. 2006.

[96] E. B. Pasquale, “Eph-ephrin bidirectional signaling in physiology and disease.,” *Cell*, vol. 133, no. 1, pp. 38–52, Apr. 2008.

[97] M. E. Pitulescu and R. H. Adams, “Eph/ephrin molecules--a hub for signaling and endocytosis.,” *Genes & development*, vol. 24, no. 22, pp. 2480–92, Nov. 2010.

[98] I. C. Grunwald, M. Korte, G. Adelmann, A. Plueck, K. Kullander, R. H. Adams, M. Frotscher, T. Bonhoeffer, and R. Klein, “Hippocampal plasticity requires postsynaptic ephrinBs,” *Nature neuroscience*, vol. 7, no. 1, pp. 33–40, Jan. 2004.

[99] K. Kullander and R. Klein, “Mechanisms and functions of Eph and ephrin signalling.,” *Nature reviews. Molecular cell biology*, vol. 3, no. 7, pp. 475–86, Jul. 2002.

[100] A. Offenhäusser and W. Knoll, “Cell-transistor hybrid systems and their potential applications,” *TRENDS in Biotechnology*, vol. 19, pp. 62–66, 2001.

[101] P. Fromherz, “Neuroelectronic interfacing: semiconductor chips with ion channels, nerve cells, and brain,” *Nanoelectronics and information technology*, vol. 54, no. 2, pp. 781–810, 2003.

[102] G. G. Wallace, S. E. Moulton, and G. M. Clark, “Electrode-Cellular Interface,” *Science*, vol. 324, no. April, pp. 185–186, 2009.

[103] M. Trojanowicz and A. Mulchandani, “Analytical applications of planar bilayer lipid membranes.,” *Analytical and bioanalytical chemistry*, vol. 379, no. 3, pp. 347–50, Jun. 2004.

[104] A.-S. Andersson, K. Glasmästar, D. Sutherland, U. Lidberg, and B. Kasemo, “Cell adhesion on supported lipid bilayers.,” *Journal of biomedical materials research. Part A*, vol. 64, no. 4, pp. 622–9, Mar. 2003.

[105] L. Kam and S. G. Boxer, “Cell adhesion to protein-micropatterned-supported lipid bilayer membranes.,” *Journal of biomedical materials research*, vol. 55, no. 4, pp. 487–95, Jun. 2001.

[106] A. E. Oliver, V. Ngassam, P. Dang, B. Sanii, H. Wu, C. K. Yee, Y. Yeh, and A. N.

Parikh, “Cell attachment behavior on solid and fluid substrates exhibiting spatial patterns of physical properties.,” *Langmuir : the ACS journal of surfaces and colloids*, vol. 25, no. 12, pp. 6992–6, Jun. 2009.

[107] O. Ivanova, “The use of phospholipid film for shaping cell cultures,” *Nature*, 1973.

[108] L. B. Margolis, E. J. Vasilieva, J. M. Vasiliev, and I. M. Gelfand, “Upper surfaces of epithelial sheets and of fluid lipid films are nonadhesive for platelets.,” *Proceedings of the National Academy of Sciences of the United States of America*, vol. 76, no. 5, pp. 2303–5, May 1979.

[109] D. Thid, K. Holm, P. S. Eriksson, J. Ekeroth, B. Kasemo, and J. Gold, “Supported phospholipid bilayers as a platform for neural progenitor cell culture.,” *Journal of biomedical materials research. Part A*, vol. 84, no. 4, pp. 940–53, Mar. 2008.

[110] B. Ananthanarayanan, L. Little, D. V. Schaffer, K. E. Healy, and M. Tirrell, “Neural stem cell adhesion and proliferation on phospholipid bilayers functionalized with RGD peptides.,” *Biomaterials*, vol. 31, no. 33, pp. 8706–15, Nov. 2010.

[111] C.-J. Huang, N.-J. Cho, C.-J. Hsu, P.-Y. Tseng, C. W. Frank, and Y.-C. Chang, “Type I collagen-functionalized supported lipid bilayer as a cell culture platform.,” *Biomacromolecules*, vol. 11, no. 5, pp. 1231–40, May 2010.

[112] S. Pautot, H. Lee, E. Y. Isacoff, and J. T. Groves, “Neuronal synapse interaction reconstituted between live cells and supported lipid bilayers.,” *Nature chemical biology*, vol. 1, no. 5, pp. 283–9, Oct. 2005.

[113] M. Baksh, C. Dean, S. Pautot, and S. DeMaria, “Neuronal activation by GPI-linked neuroligin-1 displayed in synthetic lipid bilayer membranes,” *Langmuir*, vol. 21, no. 23, pp. 10693–10698, 2005.

[114] K. D. Mossman, G. Campi, J. T. Groves, and M. L. Dustin, “Altered TCR signaling from geometrically repatterned immunological synapses.,” *Science (New York, N.Y.)*, vol. 310, no. 5751, pp. 1191–3, Nov. 2005.

[115] A. a Oliva, C. D. James, C. E. Kingman, H. G. Craighead, and G. a Banker, “Patterning axonal guidance molecules using a novel strategy for microcontact printing.,” *Neurochemical research*, vol. 28, no. 11, pp. 1639–48, Nov. 2003.

[116] S. Roth, G. Bugnicourt, M. Bisbal, S. Gory-Fauré, J. Brocard, and C. Villard, “Neuronal architectures with axo-dendritic polarity above silicon nanowires.,” *Small (Weinheim an der Bergstrasse, Germany)*, vol. 8, no. 5, pp. 671–5, Mar. 2012.

[117] J. T. Groves, “Micropatterning Fluid Lipid Bilayers on Solid Supports,” *Science*, vol. 275, no. 5300, pp. 651–653, Jan. 1997.

[118] J. T. Groves and S. G. Boxer, “Micropattern formation in supported lipid membranes.,” *Accounts of chemical research*, vol. 35, no. 3, pp. 149–57, Mar. 2002.

[119] P. Cremer, “Creating spatially addressed arrays of planar supported fluid phospholipid membranes,” *JOURNAL-AMERICAN CHEMICAL SOCIETY*, vol. 121, pp. 8130–8131, 1999.

[120] S. Kaufmann, J. Sobek, M. Textor, and E. Reimhult, “Supported lipid bilayer microarrays created by non-contact printing.,” *Lab on a chip*, vol. 11, no. 14, pp. 2403–10, Jul. 2011.

[121] a a Brian and H. M. McConnell, “Allogeneic stimulation of cytotoxic T cells by supported planar membranes.,” *Proceedings of the National Academy of Sciences of the*

United States of America, vol. 81, no. 19, pp. 6159–63, Oct. 1984.

[122] J. J. Cole, C. R. Barry, X. Wang, and H. O. Jacobs, "Nanocontact electrification through forced delamination of dielectric interfaces.," *ACS nano*, vol. 4, no. 12, pp. 7492–8, Dec. 2010.

[123] Http://www.avantilipids.com, "Avanti Polar Lipids, Inc. web page," 2012. [Online]. Available: http://www.avantilipids.com/index.php?option=com_content&view=article&id=243&Itemid=208&catnumber=850457.

[124] J.-L. Rigaud and D. Lévy, "Reconstitution of membrane proteins into liposomes.," *Methods in enzymology*, vol. 372, no. 2000, pp. 65–86, Jan. 2003.

[125] F. Sharom, "Reconstitution of membrane transporters," *Methods in molecular biology*, vol. 227, 2003.

[126] A. M. Seddon, P. Curnow, and P. J. Booth, "Membrane proteins, lipids and detergents: not just a soap opera.," *Biochimica et biophysica acta*, vol. 1666, no. 1–2, pp. 105–17, Nov. 2004.

[127] D. Martin, *Nanobiotechnology of biomimetic membranes*. Springer, 2006.

[128] D. Axelrod, D. E. Koppel, J. Schlessinger, E. Elson, and W. W. Webb, "Mobility measurement by analysis of fluorescence photobleaching recovery kinetics.," *Biophysical journal*, vol. 16, no. 9, pp. 1055–69, Sep. 1976.

[129] T. Meyvis, S. D. Smedt, and P. V. Oostveldt, "Fluorescence recovery after photobleaching: a versatile tool for mobility and interaction measurements in pharmaceutical research," *Pharmaceutical*, 1999.

[130] J. Lippincott-Schwartz, E. Snapp, and A. Kenworthy, "Studying protein dynamics in living cells.," *Nature reviews. Molecular cell biology*, vol. 2, no. 6, pp. 444–56, Jun. 2001.

[131] N. Klonis, M. Rug, I. Harper, M. Wickham, A. Cowman, and L. Tilley, "Fluorescence photobleaching analysis for the study of cellular dynamics," *European Biophysics Journal*, vol. 31, no. 1, pp. 36–51, Mar. 2002.

[132] E. a Reits and J. J. Neefjes, "From fixed to FRAP: measuring protein mobility and activity in living cells.," *Nature cell biology*, vol. 3, no. 6, pp. E145–7, Jun. 2001.

[133] "Fluorescence recovery after photobleaching," *Wikipedia*. 2012.

[134] O. N. Irrechukwu and M. E. Levenston, "Improved Estimation of Solute Diffusivity Through Numerical Analysis of FRAP Experiments," *Cellular and Molecular Bioengineering*, vol. 2, no. 1, pp. 104–117, Jan. 2009.

[135] P. Jönsson, M. P. Jonsson, J. O. Tegenfeldt, and F. Höök, "A method improving the accuracy of fluorescence recovery after photobleaching analysis.," *Biophysical journal*, vol. 95, no. 11, pp. 5334–48, Dec. 2008.

[136] J. Crank, *The mathematics of diffusion*. Oxford: Clarendon Press, 1979.

[137] Y. Deng, Y. Wang, B. Holtz, J. Li, N. Traaseth, G. Veglia, B. J. Stottrup, R. Elde, D. Pei, A. Guo, and X.-Y. Zhu, "Fluidic and air-stable supported lipid bilayer and cell-mimicking microarrays.," *Journal of the American Chemical Society*, vol. 130, no. 19, pp. 6267–71, May 2008.

[138] A. Offenhaeusser, S. Boecker-Meffert, T. Decker, R. Helpenstein, P. Gasteier, J. Groll, M. M?ller, A. Reska, S. Sch?fer, P. Schulte, and A. Vogt-Eisele, "Microcontact

printing of proteins for neuronal cell guidance," *Soft Matter*, vol. 3, no. 3, p. 290, 2007.

[139] M. C. Dixon, "Quartz crystal microbalance with dissipation monitoring: enabling real-time characterization of biological materials and their interactions.," *Journal of biomolecular techniques : JBT*, vol. 19, no. 3, pp. 151–8, Jul. 2008.

[140] G. Sauerbrey, "Verwendung von Schwingquarzen zur Wägung dünner Schichten und zur Mikrowägung," *Zeitschrift für Physik A Hadrons and Nuclei*, vol. 155, pp. 206–222, 1959.

[141] "http://www.q-sense.com/." .

[142] "NanoSight Ltd web page." .

[143] NanoSight Ltd, "Applications of Nanoparticle Tracking Analysis (NTA) in Nanoparticle Research," 2009.

[144] E. Neher and B. Sackmann, "Single-channel currents recorded from membrane of denervated frog muscle fibres," *Nature*, vol. 260, pp. 799–802, 1976.

[145] O. Hamill, A. Marty, E. Neher, and B. Sakmann, "Improved patch-clamp techniques for high-resolution current recording from cells and cell-free membrane patches," *Pflugers Archiv*, vol. 391, pp. 85–100, 1981.

[146] B. Safronov and W. Vogel, "Electrical Activity of Individual Neurons: Patch-Clamp Techniques," in *Modern Techniques in Neuroscience Research*, U. Windhorst and H. Johansson, Eds. Springer.

[147] B. Sakmann and E. Neher, *Single-channel recording*. Springer.

[148] J. Malmivuo and PlonseyR;, *Bioelectromagnetism*. Oxford University Press, 1995.

[149] "Метод локальной фиксации потенциала," *Wikipedia*. .

[150] "Immunofluorescence Method." [Online]. Available: http://www.bio.davidson.edu/Courses/genomics/method/IMF.html.

[151] "Immunofluorescence," *Wikipedia*. 2012.

[152] K. Akashi, H. Miyata, H. Itoh, and K. Kinosita, "Preparation of giant liposomes in physiological conditions and their characterization under an optical microscope.," *Biophysical journal*, vol. 71, no. 6, pp. 3242–50, Dec. 1996.

[153] T. D'Onofrio, A. Hatzor, and A. Counterman, "Controlling and measuring the interdependence of local properties in biomembranes," *Langmuir*, no. 25, pp. 8461–8466, 2003.

[154] Y. Yamashita, M. Oka, and T. Tanaka, "A new method for the preparation of giant liposomes in high salt concentrations and growth of protein microcrystals in them," *Biochimica et Biophysica*, vol. 1561, pp. 129–134, 2002.

[155] J. P. Reeves and R. M. Dowben, "Formation and properties of thin-walled phospholipid vesicles.," *Journal of cellular physiology*, vol. 73, no. 1, pp. 49–60, Feb. 1969.

[156] J. D. Castile and K. M. Taylor, "Factors affecting the size distribution of liposomes produced by freeze-thaw extrusion.," *International journal of pharmaceutics*, vol. 188, no. 1, pp. 87–95, Oct. 1999.

[157] N. Oku and R. C. MacDonald, "Differential effects of alkali metal chlorides on formation of giant liposomes by freezing and thawing and dialysis.," *Biochemistry*, vol.

22, no. 4, pp. 855–863, 1983.

[158] S. Kim and G. M. . Martin, “Preparation of cell-size unilamellar liposomes with high captured volume and defined size distribution,” *Biochimica et Biophysica Acta (BBA)-Biomembranes*, vol. 646, pp. 1–9, 1981.

[159] A. Moscho, O. W. E. Orwar, D. T. Chiu, B. P. Modi, and R. N. Zare, “Rapid preparation Rapid preparation of giant unilamellar vesicles,” *PNAS*, vol. 93, no. October, pp. 11443–11447, 1981.

[160] S. Pautot and B. Frisken, “Production of unilamellar vesicles using an inverted emulsion,” *Langmuir*, vol. 19, no. 10, pp. 2870–2879, 2003.

[161] K. S. Horger, D. J. Estes, R. Capone, and M. Mayer, “Films of agarose enable rapid formation of giant liposomes in solutions of physiologic ionic strength.,” *Journal of the American Chemical Society*, vol. 131, no. 5, pp. 1810–9, Feb. 2009.

[162] M. I. Angelova and D. S. Dimitrov, “Liposome electroformation,” *Faraday Discussions of the Chemical Society*, vol. 81, p. 303, 1986.

[163] A. Kumar and G. M. Whitesides, “Features of gold having micrometer to centimeter dimensions can be formed through a combination of stamping with an elastomeric stamp and an alkanethiol ‘“ink”’ followed by chemical etching,” *Applied Physics Letters*, vol. 63, no. 14, p. 2002, 1993.

[164] S. Alom Ruiz and C. S. Chen, “Microcontact printing: A tool to pattern,” *Soft Matter*, vol. 3, no. 2, p. 168, 2007.

[165] A. P. Quist, E. Pavlovic, and S. Oscarsson, “Recent advances in microcontact printing.,” *Analytical and bioanalytical chemistry*, vol. 381, no. 3, pp. 591–600, Feb. 2005.

[166] R. Fricke, P. D. Zentis, L. T. Rajappa, B. Hofmann, M. Banzet, A. Offenhäusser, and S. H. Meffert, “Axon guidance of rat cortical neurons by microcontact printed gradients.,” *Biomaterials*, vol. 32, no. 8, pp. 2070–6, Mar. 2011.

[167] C. K. Yeung, L. Lauer, A. Offenhäusser, and W. Knoll, “Modulation of the growth and guidance of rat brain stem neurons using patterned extracellular matrix proteins.,” *Neuroscience letters*, vol. 301, no. 2, pp. 147–50, Mar. 2001.

[168] Avanti Polar lipids, “Preparation of Liposomes.” .

[169] R. Richter, A. Mukhopadhyay, and A. Brisson, “Pathways of lipid vesicle deposition on solid surfaces: a combined QCM-D and AFM study.,” *Biophysical journal*, vol. 85, no. 5, pp. 3035–47, Nov. 2003.

[170] “Coefficient of determination,” *Wikipedia*. 2012.

[171] L. Zhang, T. a Spurlin, A. a Gewirth, and S. Granick, “Electrostatic stitching in gel-phase supported phospholipid bilayers.,” *The journal of physical chemistry. B*, vol. 110, no. 1, pp. 33–5, Jan. 2006.

[172] B. P. Bean, “The action potential in mammalian central neurons.,” *Nature reviews. Neuroscience*, vol. 8, no. 6, pp. 451–65, Jun. 2007.

[173] “Excitatory postsynaptic potential,” *Wikipedia*. 2012.

[174] M. Grandbois, H. Clausen-Schaumann, and H. Gaub, “Atomic force microscope imaging of phospholipid bilayer degradation by phospholipase A2.,” *Biophysical journal*, vol. 74, no. 5, pp. 2398–404, May 1998.

[175] Y. Akaneya, K. Sohya, A. Kitamura, F. Kimura, C. Washburn, R. Zhou, I. Ninan, T. Tsumoto, and E. B. Ziff, “Ephrin-A5 and EphA5 interaction induces synaptogenesis during early hippocampal development.,” *PloS one*, vol. 5, no. 8, p. e12486, Jan. 2010.

[176] D. Turner, “Waveform and amplitude characteristics of evoked responses to dendritic stimulation of CA1 guinea-pig pyramidal cells.,” *The Journal of Physiology*, vol. 395, pp. 419–439, 1988.

[177] A. Nicoll and A. Larkman, “Modulation of EPSP shape and efficacy by intrinsic membrane conductances in rat neocortical pyramidal neurons in vitro.,” *The Journal of Physiology*, vol. 468, pp. 693–710, 1993.

[178] A. Yakushenko, J. Schnitker, and B. Wolfrum, “Printed carbon microelectrodes for electrochemical detection of single vesicle release from PC12 cells.,” *Analytical chemistry*, vol. 84, no. 10, pp. 4613–7, May 2012.

[179] F. Albertorio, A. J. Diaz, T. Yang, V. a Chapa, S. Kataoka, E. T. Castellana, and P. S. Cremer, “Fluid and air-stable lipopolymer membranes for biosensor applications.,” *Langmuir : the ACS journal of surfaces and colloids*, vol. 21, no. 16, pp. 7476–82, Aug. 2005.

[180] F. Albertorio, V. A. Chapa, X. Chen, A. J. Diaz, and P. S. Cremer, “The alpha,alpha-(1-1) Linkage of Trehalose Is Key to Anhydrobiotic Preservation,” *J. AM. CHEM. SOC*, vol. 129, no. 12, pp. 10567–10574, 2007.

[181] V. Maybeck, “Tools for Non-Invasive Communication with Electrogenic Cells: Optogenetic Stimulation and Diamond Recording Devices,” RWTH Aachen, 2011.

[182] A. C. von Philipsborn, S. Lang, A. Bernard, J. Loeschinger, C. David, D. Lehnert, M. Bastmeyer, and F. Bonhoeffer, “Microcontact printing of axon guidance molecules for generation of graded patterns.,” *Nature protocols*, vol. 1, no. 3, pp. 1322–8, Jan. 2006.

Band / Volume 11
Correlation between Raman spectroscopy and electron microscopy on individual carbon nanotubes and peapods
C. Spudat (2010). xiv, 125 pp.
ISBN: 978-3-89336-648-4

Band / Volume 12
DC and RF Characterization of NiSi Schottky Barrier MOSFETs with Dopant Segregation
C. J. Urban (2010), iv, 151 pp.
ISBN: 978-3-89336-644-6

Band / Volume 13
Alternative Systems for Molecular Electronics: Functionalized Carboxylic Acids on Structured Surfaces
M. C. Lennartz (2010), 183 pp.
ISBN: 978-3-89336-667-5

Band / Volume 14
Highly conductive electrodes as diffusion barrier for high temperature applications
B. Mešić (2010), VII, 138 pp.
ISBN: 978-3-89336-670-5

Band / Volume 15
Modeling, Fabrication and Characterization of Silicon Tunnel Field-Effect Transistors
C. P. Sandow (2010), XIII, 112 pp.
ISBN: 978-3-89336-675-0

Band / Volume 16
Substituted Coronenes for Molecular Electronics: From Supramolecular Structures to Single Molecules
P. Kowalzik (2010), ix, 149 pp.
ISBN: 978-3-89336-679-8

Band / Volume 17
Resistive switching in TiO2 thin films
L. Yang (2011), VII, 117 pp.
ISBN: 978-3-89336-707-8

Band / Volume 18
Crystal- and Defect-Chemistry of Fine Grained Thermistor Ceramics on $BaTiO_3$ Basis with BaO-Excess
H. Katsu (2011), xxvii, 163 pp.
ISBN: 978-3-89336-741-2

Band / Volume 19
Flächenkontakte zu molekularen Schichten in der Bioelektronik
N. Sanetra (2012), XIII, 129 pp.
ISBN: 978-3-89336-776-4

Band / Volume 20
Stacked device structures for resistive memory and logic
R. D. Rosezin (2012), 137 pp.
ISBN: 978-3-89336-777-1

Band / Volume 21
Optical and electrical addressing in molecule-based logic circuits
M. Manheller (2012), XIV, 183 pp.
ISBN: 978-3-89336-810-5

Band / Volume 22
Fabrication of Nanogaps and Investigation of Molecular Junctions by Electrochemical Methods
Z. Yi (2012), 132 pp.
ISBN: 978-3-89336-812-9

Band / Volume 23
Thermal Diffusion in binary Surfactant Systems and Microemulsions
B. Arlt (2012), 159, xlvi pp.
ISBN: 978-3-89336-819-8

Band / Volume 24
Ultrathin Gold Nanowires - Chemistry, Electrical Characterization and Application to Sense Cellular Biology
A. Kisner (2012), 176 pp.
ISBN: 978-3-89336-824-2

Band / Volume 25
Interaction between Redox-Based Resistive Switching Mechanisms
C. R. Hermes (2012), iii, 134 pp.
ISBN: 978-3-89336-838-9

Band / Volume 26
Supported lipid bilayer as a biomimetic platform for neuronal cell culture
D. Afanasenkau (2013), xiv, 132 pp.
ISBN: 978-3-89336-863-1

Weitere ***Schriften des Verlags im Forschungszentrum Jülich*** unter
http://wwwzb1.fz-juelich.de/verlagextern1/index.asp

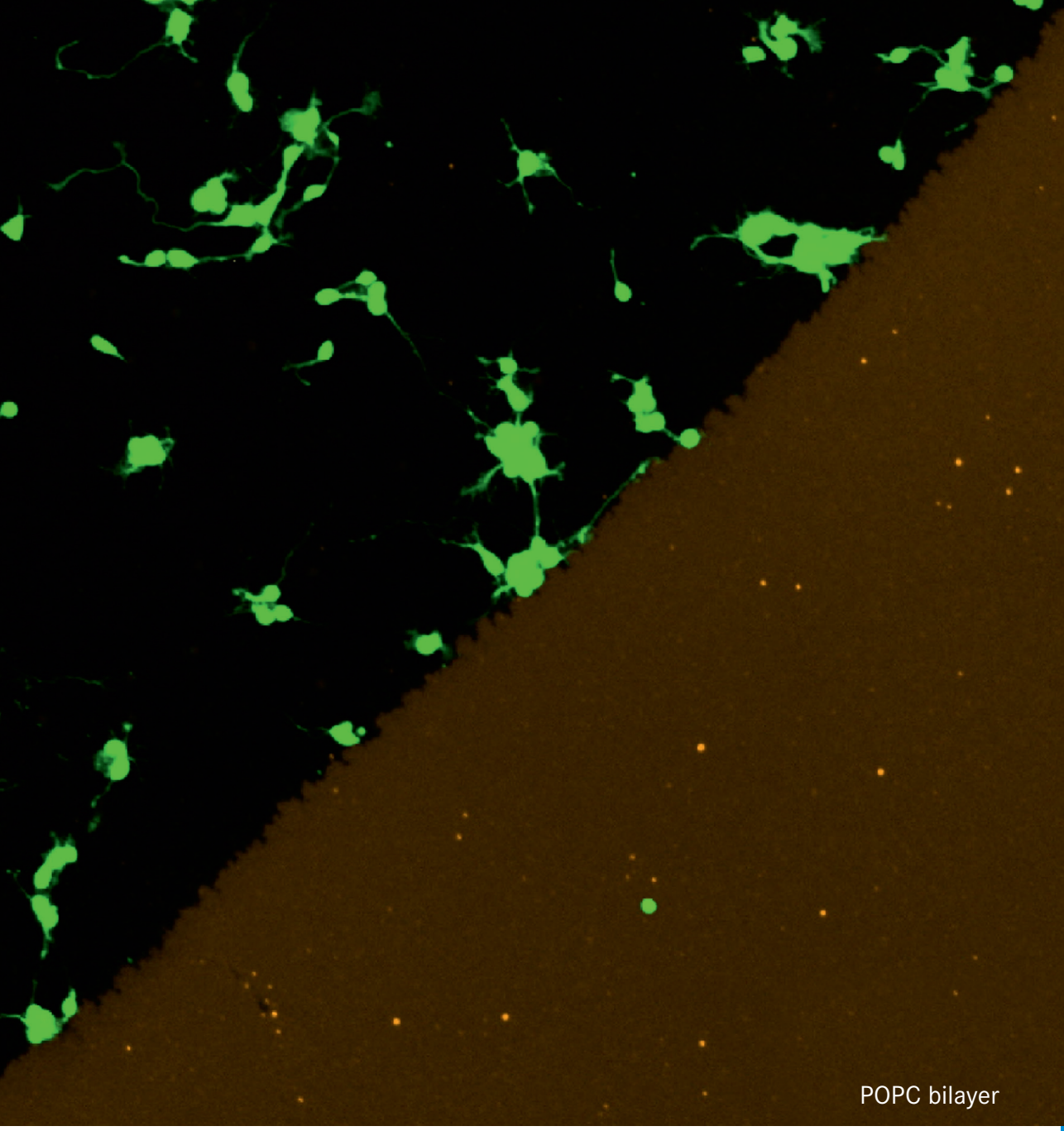

Information / Information
Band / Volume 26
ISBN 978-3-89336-863-1

JÜLICH
FORSCHUNGSZENTRUM